

HYDROGEOLOGIC APPROACH TO THE CHARACTERIZATION
OF AQUIFER CONTAMINATION AND RESTORATION
USING MATHEMATICAL MODELS

by

Douglas C. Kent, Principal Investigator
School of Geology
Oklahoma State University
Stillwater, Oklahoma 74078

Chi-Chung Chang and Lorraine LeMaster
School of Geology
Oklahoma State University
Stillwater, Oklahoma 74078

and

Jan Wagner, Principal Investigator
School of Chemical Engineering
Oklahoma State University
Stillwater, Oklahoma 74078

Supplement

to

FINAL REPORT

for

NATIONAL CENTER FOR GROUND WATER RESEARCH

Project Title: Scenarios of Ground-Water Impacts
from Hazardous Waste Disposal

U.S. Environmental Protection Agency
Cooperative Agreement No. CR811116-01-0

National Center for Ground Water Research
Subcontract No. 722-311-OSU-1

PREFACE

This report is a supplement to the final project report for "Scenarios of Ground-Water Impacts from Hazardous Waste Disposal", submitted to the E.P.A. by Jan Wagner and D. C. Kent in 1985. This project was subcontracted through the National Center for Ground Water Research to Oklahoma State University by the Rober S. Kerr Laboratory, Environmental Protection Agency in Ada, Oklahoma.

The potential for ground-water pollution from a hazardous waste is partly dependent on the characteristics of the waste or leachate, the hydrogeology of the site and the site management techniques. Waste disposal scenarios which include a range of management techniques and hydrogeological settings have been defined in cooperation with the U.S. Environmental Protection Agency. These contamination scenarios provide a basis for evaluation of hazardous waste management alternatives in terms of potential impacts on the ground-water quality based on predictions using existing mathematical models.

The severity of ground-water pollution is partly dependent on the characteristics of the waste or leachate, i.e. the volume, composition, concentration of various constituents, time rate of release of contaminant, the size of the area from which the contaminants are derived and the density fo the leachate, etc. Data describing these

parameters are difficult to obtain and often are lumped into the term "mass flow-rate". Once the leachate is formed, it begins to migrate slowly downward through the unsaturated zone where several physical, chemical, and biological forces act upon it. Eventually however, the leachate may reach saturated strata where it will then flow primarily in a horizontal direction as defined by the hydraulic gradient. From this point on, the concentration will decrease due to a number of phenomena including dilution, filtration, sorption, chemical processes, microbial degradation, and dispersion. All of these factors are dependent on the type of hydrogeologic regime in which a waste of leachate is introduced.

Because there are several types of hydrogeologic regimes that can characterize an aquifer, it is important that the diversity of hydrogeologic factors within a given geologic setting be considered in selecting scenarios for model applications. It is necessary to establish an approach to be used when applying chemical transport models to the proper hydrogeologic setting under various management constraints.

The objective of this project is to provide comparative contamination scenarios using combinations of existing models and site characteristics. These contamination scenarios would provide a basis for evaluation of hazardous waste management alternatives in terms of potential impacts on ground-water quality based on predictions using mathematical models.

The project was developed in three phases. Phase I included a review of a preliminary list of scenarios of ground-water impacts from hazardous waste disposal, and development of guidelines for the selection of a subset of scenarios for further evaluation. The selection was based, in part, upon the following; (a) waste characteristics, (b) site hydrogeology, (c) management techniques, and (d) extent of available data.

Following the initial selection of a subset of scenarios, Phase II was initiated which included evaluation of modeling alternatives and anticipated results based on existing mathematical models implemented on EPA computers. The guidelines developed in cooperation with EPA were used as the basis for the selection of a suite of specific scenarios. Each of the waste disposal scenarios were evaluated in light of predicted impact on ground-water quality by using available mathematical models.

Phase III of the project includes a "case history" type of approach developed for each waste management scenario in the final suite. Documentation includes a description of the problem and data, typical of a specific hydrogeologic regime, the rationale for the selection of the mathematical model(s), protocol for applying the model to the data, and an evaluation and discussion of predicted impacts on ground-water quality.

This report addresses Phase II and Phase III of the project with emphasis on the hydrogeologic aspects of the

study. This report is an adaptation of a thesis by Chang (1985).

In the past decade many mathematical models have been developed to simulate ground-water flow and solute transport. Most mathematical models were not fully tested for their capabilities and limitations; therefore, their applications were limited. In this study, an analytical model (Wilson and Miller) and a numerical model (modified NRC version of the USGS Solute Transport Model, Kent et al, 1986) were selected for saturated flow. The cross sectional perspective of the USGS Model was coupled with an unsaturated flow model (Phan Model), which was also implemented in their study and described in a separate report (Wagner and Kent, 1985). The model capabilities were also evaluated in reference to landfill studies and to the simulations of the aquifer restoration.

The accuracies of the models were tested before applying them to hypothetical and actual contaminated sites. The approach to the application of the models to the selected sites requires specifying the boundary and initial conditions of the hydrogeologic settings. These conditions are set by using input variables and matrices.

Eleven scenarios are used to simulate the cross-sectional view of possible geological variations of aquifers. Variations of scenarios include alternating high and low permeable layers as well as faults and dipping layers.

The Babylon landfill, located on Long Island, New York, is a well-studied contaminated site. From previous studies, there is sufficient hydrogeological information available for developing model simulations. The contamination source parameters, such as source injection rate and the time when the slugs entered the saturated zone were unknown. Both the planar and cross-sectional analyses using the modified NRC version of the USGS model (Konikow and Bredehoeft) (Kent et al, 1986) are applied to this site.

The analytical model can be effectively applied to contaminated sites that consist of homogeneous aquifers. A prediction for the development of the plume can be clearly illustrated by combining the planar and cross-sectional analyses. The simulation of the Babylon site offers a good example for the numerical model use; however, the assumptions and limitations of the analytical model restrict its wide application.

The numerical model was successfully applied to both the Babylon data and to the hypothetical cases (3W). The hypothetical cases provided evidence for some of the capabilities of the numerical model for handling geological variations of aquifers. In addition, the numerical model was successfully linked with the unsaturated model using one of the hypothetical cases (homogeneous 3W). The capability of the numerical model to simulate the aquifer restoration was demonstrated by applying the numerical model to the hypothetical cases and the Babylon case.

TABLE OF CONTENTS

Chapter	Page
I. INTRODUCTION.....	1
General.....	1
Objectives.....	2
Mathematical Models.....	2
Application Sites.....	3
Theoretical Scenarios (3W)	3
Locations.....	4
Previous Studies.....	4
Actual Site (Babylon landfill).....	4
Location.....	4
Previous Studies.....	7
II. COMPARISON OF THE KONIKOW MODEL AND THE PHAN MODEL.....	8
III. SELECTED MATHEMATICAL MODELS.....	10
The Analytical Model.....	10
General Concepts of The Model.....	10
Assumptions and Limitations.....	13
The Numerical Model.....	14
General Concepts of The Model.....	14
The Groundwater Flow Equation.....	14
The Solute Transport Equation.....	16
The Decay Equation.....	17
The Equilibrium Sorption.....	18
Assumptions and Limitations.....	18
IV. MODEL APPLICATION APPROACH.....	19
The Analytical Model.....	19
Boundary and Initial Conditions.....	21
Analytical Matrices and Input Data Set.	22
The Numerical Model.....	22
Boundary and Initial Conditions.....	22
Analytical Matrices and Input Data Set.	28
V. HYPOTHETICAL SCENARIO APPLICATIONS.....	34
3W Scenarios.....	34
Climate.....	36
Geology.....	36

Chapter	Page
Hydraulic Characteristics.....	42
Ground-Water Flow.....	42
Calibration of the Model.....	42
Analytical Model.....	42
Cross-sectional.....	44
Planar.....	45
Numerical Model.....	46
Cross-sectional.....	47
Planar.....	48
Results.....	50
Analytical.....	50
Numerical.....	53
Cleanup.....	70
 VI. EXISTING SITE APPLICATIONS.....	 75
Babylon Landfill.....	75
Climate.....	77
Land Use.....	77
Geology.....	77
General Geology.....	77
Aquifer Lithology.....	79
Hydraulic Characteristics.....	80
Ground water Table.....	80
Porosity and Velocity.....	80
Saturated Thickness.....	80
Hydraulic Conductivity and Transmissivity.....	80
Dispersion Coefficient.....	82
Ground Water Flow System.....	82
Native Ground-Water Quality.....	83
Calibration of the Model.....	83
Source Injection Rate Calibration.....	86
Plume Calibration.....	88
Analytical Model.....	90
Cross-sectional.....	90
Planar.....	90
Numerical Model.....	92
Cross-sectional.....	94
Planar.....	95
Results.....	97
Analytical Model.....	97
Numerical Model.....	97
Cleanup.....	101
 VII. CONCLUSION.....	 108
The Analytical Model.....	108
The Numerical Model.....	108
Summary.....	109

Chapter	Page
REFERENCES CITED.....	111
APPENDIXES.....	115
APPENDIX A - MODIFICATIONS AND EFFICIENCY TEST OF THE ANALYTICAL MODEL.....	116
APPENDIX B - MODIFICATIONS AND EFFICIENCY TEST OF THE NUMERICAL MODELS.....	124
APPENDIX C - COMPARISON OF MATRIX SIZES OF THE NUMERICAL MODEL.....	140
APPENDIX D - INPUT DATA SETS OF 3W CASES.....	145
APPENDIX E - THE INFLUENCES OF SURFACE RECHARGE....	156
APPENDIX F - INPUT DATA SETS OF THE BABYLON SITE...	160
APPENDIX G - COMPARISON OF THE KONIKOW MODEL AND THE PHAN MODEL: FIGURES.....	165
APPENDIX H - GRAPHICS PROGRAMS.....	171

LIST OF TABLES

Table	Page
I. Transmissivities, Hydraulic Gradients, and Aquifer Discharges at Six Flow Regions.....	6
II. Input Data for the Analytical Model.....	26
III. Input Data Set of the Analytical Model of 3W- 1A Scenario (Cross-Sectional).....	27
IV. Input Data Set of the Analytical Model of 3W- 1A Scenario (Planar).....	27
V. Input Parameters of the Numerical Model	33
VI. Range of Permeabilities for Earth Materials....	37
VII. Summary of Stratigraphy of the Babylon Area ...	78
VIII. Input Data Set of the Analytical Model of the Babylon Site (Planar).....	93
IX. Input Data Set of the Analytical Model of the Babylon Site (Cross-Sectional).....	93
X. Comparison Between the Simulated Results and Measured Data of the Babylon Site.....	100
XI. Summary of Sensitivity Test of the Analytical model.....	122
XII. Computational Efficiency for Tested Problems...	131
XIII. Model Parameters for Test Problem 1.....	133
XIV. Model Parameters for Test Problem 2 and 3	135
XV. Effect of NPTPND on Accuracy, Precision, and Efficiency of Solution to Test Problem 3	136
XVI. Effect of CELDIS on Accuracy, Precision, and Efficiency of Solution to Test Problem 3	136
XVII. Computational Efficiency for Transient Test Problem 1.....	139

Table		page
XVIII.	Computational Efficiency for Transient Test Problem 2	138
XIX.	Cross-Sectional Comparison of Different Matrices (Konikow Model).....	141
XX.	C.P.U. Time for Different Matrices Size.....	142
XXI.	Gound-Water Flow Velocity Distribution of Case 3W-1A.....	158
XXII.	Cross-Sectional Comparison of Konikow Model (50*50) with Phan Model.....	168

LIST OF FIGURES

Figure	Page
1. The terrain of 3W Scenarios and Ground-Water Flow Regions.....	5
2. Location of the Babylon Landfill.....	5
3. Differential Control Volume for Mass Balance.....	11
4. Plume With a Planar View.....	20
5. Plume With a Cross-Sectional View.....	20
6. Planar View of 3W Scenarios.....	23
7. Flux of 3W Scenarios With Cross-Sectional View.....	23
8. 10 by 10 Grid Map for the Analytical Model.....	24
9. Planar View of the Analytical Matrix for 3W Scenarios (Analytical Model).....	25
10. Cross-Sectional View of the Analytical Matrix for 3W Scenarios (Analytical Model).....	25
11. No-Flow boundary of an Analytical Grid Map (Top) and a Conceptual Scene (Bottom).....	29
12. Planar Matrix for 3W Scenarios (Numerical Model)...	30
13. Cross-Sectional Matrix for 3W Scenarios (Numerical Model).....	30
14. Case 3W-1A, Homogeneous Aquifer with Moderate Permeability.....	38
15. Case 3W-2A, Two Layered Scenario, with Low Permeability Top Layer.....	38
16. Case 3W-2B, Two Layered Aquifer with High Permeability Top Layer.....	40
17. Case 3W-2C, Two Layered Case with Fractures at the Top Low Permeable Layer.....	40

Figure	Page
18. Case 3W-3A, Three Layered Aquifer with High Permeability Layer in Between.....	41
19. Case 3W-3B, Three Layered Aquifer with Low Permeability Layer in Between.....	41
20. Case 3W-4A, A Incline High Permeability Layer.....	43
21. Case 3W-5A, A Normal Fault Scenario.....	43
22. The Conceptual Matrix of Injection Sources and Discharge Points with Cross-Sectional View.....	49
23. The Conceptual Matrix of Aquifer Restoration with Cross-Sectional View.....	49
24. The Conceptual Matrix of Injection Sources and Discharge Points with Planar View.....	51
25. The Conceptual Matrix of Aquifer Restoration with Planar View.....	51
26. Simulation of 3W-1A Case of Analytical Model (Cross-Sectional).....	52
27. Simulation of 3W-1A Case of Analytical Model (Planar).....	52
28. Simulation of 3W-1A Case of Numerical Model (Planar).....	54
29. The Ground-Water Table Map of 3W-1A Scenario.....	54
30. Simulated Plume of 3W-1A (50 Years).....	55
31. Simulated Plume of 3W-1A (100 Years).....	55
32. Simulated Plume of 3W-1A (200 Years).....	56
33. Simulated Plume of 3W-1A (300 Years).....	56
34. Simulated Plume of 3W-1A (400 Years).....	57
35. Distribution of Equal-Potential Lines of the 3W-1A Scenario.....	57
36. Color Ploted Plume of the 3W-1A Scenario (50 years).....	58
37. Color Ploted Plume of the 3W-1A Scenario (400 years).....	58

Figure	Page
38. Distribution of Equal-Potential Lines of 3W-1B.....	59
39. Plume of 3W-1B (300 Years).....	59
40. The Simulated Plume of 3W-1D (300 Years).....	61
41. The Simulated Plume of 3W-2A (300 Years).....	61
42. Distribution of Equal-Potential Lines of 3W-2B.....	62
43. The Simulated Plume of 3W-2B (50 Years).....	62
44. The Simulated Plume of 3W-2B (200 Years).....	63
45. The Simulated Plume of 3W-2C (200 Years).....	63
46. The Simulated Plume of 3W-2C (400 Years).....	65
47. Distribution of Equal-Potential Lines of 3W-3A.....	65
48. Distribution of Equal-Potential Lines of 3W-3B.....	66
49. The Simulated Plume of 3W-3B (200 Years).....	66
50. Distribution of Equal-Potential Lines of 3W-4A.....	67
51. The Simulated Plume of 3W-4A (200 Years).....	67
52. The Simulated Plume of 3W-5A (400 Years).....	68
53. Aquifer Restoration of 3W-1A with a Planar View (At Beginning).....	68
54. Aquifer Restoration of 3W-1A with a Planar View (10 Years).....	69
55. Aquifer Restoration of 3W-1A with a Planar View (20 Years).....	69
56. Aquifer Restoration of 3W-1A with a Cross-Sectional View (At Beginning).....	71
57. Aquifer Restoration of 3W-1A with a Cross-Sectional View (10 Years).....	71
58. Aquifer Restoration of 3W-1A with a Cross-Sectional View (30 Years).....	72
59. Aquifer Restoration of 3W-1A with Cross-Sectional View (50 Years).....	72

Figure	Page
60. Aquifer Restoration of 3W-1A with Cross-Sectional View by Pattern Plotting (At Beginning).....	73
61. Aquifer Restoration of 3W-1A with Cross-Sectional View by Pattern Plotting (50 Years).....	73
62. Distribution of Equal-Potential Lines of Aquifer Restoration of 3W-1A After 10 Years Operation....	74
63. Distribution of Equal-Potential Lines of Aquifer Restoration of 3W-1A After 50 Years Operation....	74
64. Location of Refuse Piles in the Babylon Site.....	76
65. Geological Feature of the Babylon Area (After Pluhowski, 1964).....	78
66. The Perspective View of the Babylon Landfill.....	81
67. Leachate Movement and Dispersion in Ground Water Beneath the Babylon Landfill.....	85
68. Two Designed Simulation Region for the Babylon Site.....	87
69. The Perspective View of the Babylon Plume in Three Layers.....	89
70. The Cross-Sectional View of the Babylon Plume.....	91
71. Conceptual Matrix for the Babylon Site Leachate Introducing Wells (Cross-Sectional).....	96
72. Conceptual Matrix for the Babylon Site Cleanup (Cross-Sectional).....	96
73. Nodeid Matrix of Injection Sources of the Babylon Site (Planar).....	98
74. Nodeid Matrix of Aquifer Restoration of the Babylon Site (Planar).....	98
75. The Simulated Plume of the Babylon Site with a Cross-Sectional View (by Analytical Model).....	99
76. The Simulated Plume of the Babylon Site with a Planar View (by Analytical Model).....	99
77. The Simulated Plume of the Babylon Site with a Cross-Sectional View (by Numerical Model).....	102

Figure	Page
78. The Simulated Plume of the Babylon Site with a Planar View (by Numerical Model).....	102
79. Distribution of Equal-Potential Lines of the Babylon Site.....	103
80. The Simulated Aquifer Restoration of the Babylon Site with Cross-Sectional View (At Beginning)....	104
81. The Simulated Aquifer Restoration of the Babylon Site with Cross-Sectional View (10 Years).....	104
82. The Simulated Aquifer Restoration of the Babylon Site with Cross-Sectional View (20 Years).....	105
83. The Simulated Aquifer Restoration of the Babylon Site with Planar View (At Beginning).....	105
84. The Simulated Aquifer Restoration of the Babylon Site with Planar View (10 Years).....	106
85. The Simulated Aquifer Restoration of the Babylon Site with Planar View (20 Years).....	106
86. The Simulated Aquifer Restoration of the Babylon Site with Planar View (30 Years).....	107
87. The Simulated Aquifer Restoration of the Babylon Site with Planar View (40 Years).....	107
88. Concentration as a Function of Velocity.....	120
89. Concentration as a Function of Dispersion.....	120
90. Concentration as a Function of Mass Rate.....	121
91. Mass Balance errors for Test Problem 1.....	133
92. Mass Balance errors for Test Problem 2.....	135
93. Effect of NPTPND on Mass Balance Errors for Test Problem 3; CELDIS=0.5 (After Konikow, 1978).....	136
94. Effect of CELDIS on Mass Balance Errors for Test Problem 3; NPTPND=9 (After Konikow, 1978).....	137
95. Equalpotential Lines of Case 3W-1A (with Surface Recharge).....	158
96. Equalpotential Lines of Case 3W-1A (without Surface Recharge).....	158

Figure	Page
97. 10 by 10 Grid Map for the Konikow Model.....	166
98. Grid Configuration for the Phan Model.....	167
99. The Concentration Comparison of the Konikow Model with Phan Model (at River).....	169
100. The Concentration Comparison of the Konikow Model with Phan Model (400 ft from River).....	169
101. The Comparison of the Change of Concentration with Time (Depth=20 ft).....	170
102. The Comparison of the Change of Concentration with Time (Depth=220 ft).....	170

CHAPTER I

INTRODUCTION

General

Because of increasing water usage and future water requirements in many areas, ground water is becoming a major source of supply, especially for drinking water. In the past decade, many aquifers have been contaminated by leachates from solid-waste landfills or chemical-waste disposal lagoons. Hence, polluted ground water, which threatens our health, has become a general problem.

To study the contamination, many mathematical models have been developed to simulate ground-water flow and solute transports. Ground-water researchers are not only concerned with the simulation and prediction of the development of plumes but also the way to solve the problem of contamination.

To help accomplish these goals, two mathematical models have been selected and their capabilities evaluated in reference to landfill studies and cleanup of contaminated aquifer. A user-friendly preprocessor for the numerical model and a computer graphics package, Statistical Analysis System (SAS) graphics, are also used in this study. The

graphics serve as visual aids to let users easily understand the results.

Objectives

The main objectives of this research are :

1. Evaluate the capabilities of the models.
2. Apply the models to an actual landfill as well as hypothetical situations and predict the trend of plume development for various hydrological scenarios.
3. Solve the contamination problem by using model simulations using injection and pumping wells to restore the aquifer.

Mathematical Models

There are three types of mathematical models for ground-water simulation: analog, analytical, and numerical. In this research two mathematical models, one analytical (Wilson and Miller) and one numerical (Konikow and Bredehoeft), were selected to accomplish the goals.

The Wilson model is an analytical mass transport differential equation (Wilson and Miller, 1978). The model was converted to computer programs by Kent, Pettyjohn, Prickett, and Witz (1982) and Pettyjohn, Kent, Prickett, and Witz (1982). A new FORTRAN version with steady-state time calculation has been developed (Kent, Wagner, and Witz, 1984).

The Konikow model is a numerical model originally developed by Konikow and Bredehoeft (1978). It was then modified by Tracy (1982) to add the decay and adsorption function to the model. In 1984 a Strongly Implicit Procedure and other options were added (Kent et al, 1986) to increase the efficiency and flexibility of this model. A new preprocessor for the Konikow model was to facilitate data input. The preprocessor is described in a final report for U.S. Environmental Protection Agency by Kent et al, (1986).

These new updated versions were applied to several theoretical and actual sites of ground-water pollution.

Application sites

Infiltration of precipitation causes leachate to seep from a landfill to subsurface ground water, transporting a high dissolved-solids concentration and also injurious substances into the aquifer. Thus, the areas of greatest concern are in humid regions.

Theoretical Scenarios (3W)

The "3W" group, defined by Geraghty and Miller (1983), is the third group of the seven scenarios which were set to classify the scenarios of the flow systems of the United States. It also reflects the climatic settings of the scenarios (W=humid region). The characteristics of this scenario are identified as: 1) a humid climate setting (precipitation greater than 20 in/year), 2) the contaminated

facility (source) is located in the recharge area of the flow system, and 3) overall flow system dimensions are 1000 ft in thickness and 1000 ft in length (Geraghty and Miller, 1983).

In this study a modified version of the 3W conditions was used by assuming geological scenarios where hydrogeological properties are not as rigidly defined as by Geraghty and Miller (1983), and also by assuming that the aquifer is heterogenous.

Locations. 3W cases are set for the humid regions where the mean annual precipitation is greater than 20 inches. It includes the area from the Atlantic coast to the Mississippi Valley and most parts of the Pacific Northwest coast (Figure 1). The areas also include the ground-water flow regions of the glacial central, non-glacial central, Atlantic and Gulf Coastal Plain, Southeast Coastal Plain, and alluvial basins as defined by Heath (1982).

Previous Studies. The ground-water flow regions were studied and defined by Meinzer in 1923. Heath (1982) redefined the regions based on new data. Pertinent hydrogeological data for these regions has been summarized by Fetter (1981), Naymik (1979) and by a number of others listed in Table I.

Actual Site (Babylon landfill)

Location. The Babylon landfill is located in the south central part of Long Island, New York (Figure 2). It

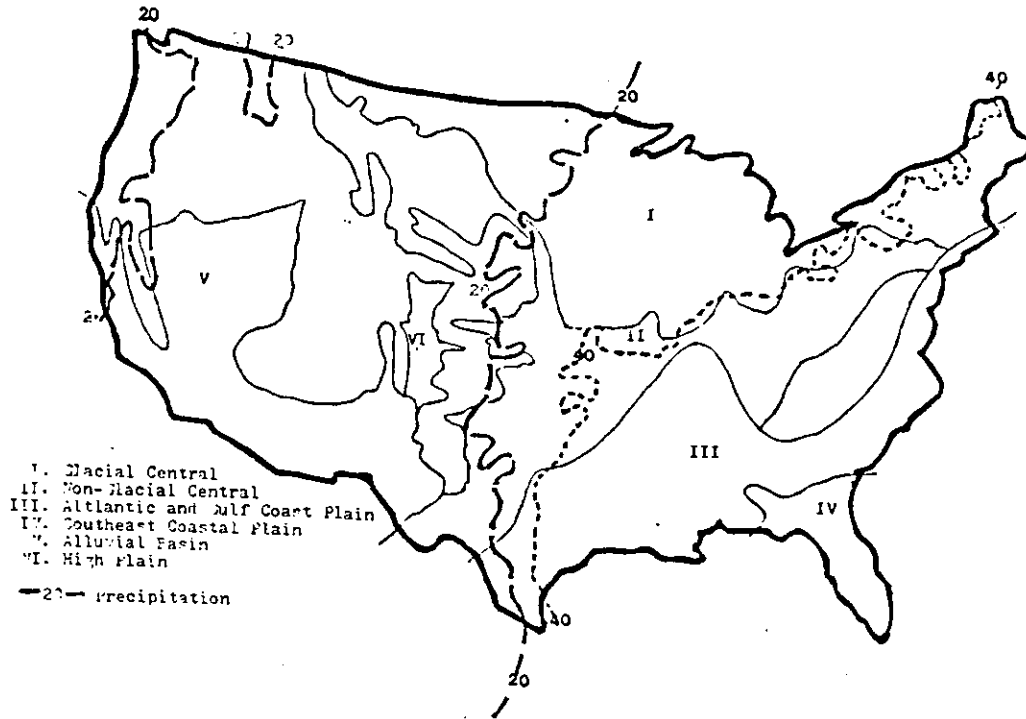


Figure 1. The Terrain of 3W Scenarios and Ground-Water Flow Regions

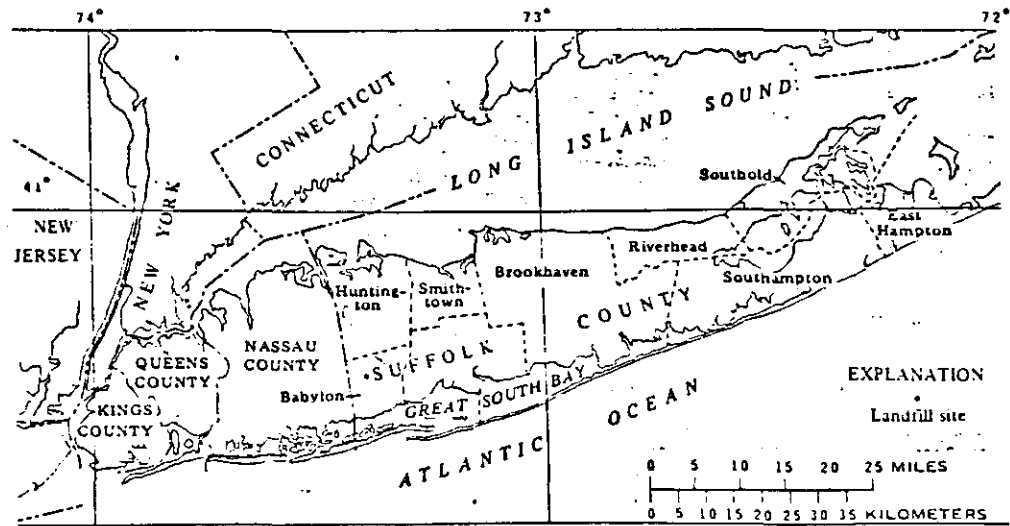


Figure 2. Location of the Babylon Landfill
 (After Kimmel 1980)

TABLE I
TRANSMISSIVITIES, HYDRAULIC GRADIENTS, AND AQUIFER DISCHARGES AT SIX FLOW REGION.

Site	ISOS Region	State Location	Aquifer Name/type	Aquifer Transmissivity (gal/day/ft)	Hydraulic Gradient (ft/mi)	Aquifer Discharge (lqrd/mi)	Method Used*	Source of Data
1	Glaciated Central	Wisconsin	Sandst. Bedrock	5,000-25,000	16-29	0.15-0.4	2	Fetter, 1981
2	Glaciated Central	Ohio	Limest. & Sandst. Bedrock	35,000	5-50	0.10-1.8	3	Rajurk, 1972
3	Glaciated Central	Indiana	Glacial Sand/Gravel	75,000-450,000	3-20	1.4-1.5	2	Lebrigiotta and others, 1981
4	Glaciated Central	New York	Glacial Sand/Gravel	140,000	8-12	1.1-1.7	3	Kennel and others, 1979
5	Atlantic and Gulf Coastal Plain	Texas	Fluvial/Deltaic Sands	100,000-300,000	7.5-10	0.75-3.0	1	Kennel and others, 1979
6	Atlantic and Gulf Coastal Plain	Mississippi	Miss. River Alluvium	97,000-590,000	1.1-2.0	0.19-0.65	2	Dalsin, 1978
7	Atlantic and Gulf Coastal Plain	Maryland	Patuxent Fm. Sandst.	600-80,000	9.2-60	0.04-0.74	2	Hack, 1962
8	Atlantic and Gulf Coastal Plain	Maryland	Patapsco Fm. Sandst.	1,300-52,000	6.6-40	0.05-0.34	2	Hack, 1962
9	Southeast Coastal Plain	Florida	Floridan Limest.	2,200-200,000	2.3-6.7	0.01-0.46	2	Trapp and others, 1977
10	Southeast Coastal Plain	Florida	Floridan Limest.	3,000,000	0.56-8.3	1.7-25.	3	Tibbels and others, 1977
11	Southeast Coastal Plain	Florida	Floridan Limest.	300,000-900,000	5.0-6.7	2.0-4.5	2	Robertson and Hallory, 1977
12	Non-Glaciated Central	West Virginia	Sandst./Limest. Bedrock	350-7,000	27	0.01-0.19	4	Bain and Friel, 1972
13	Non-Glaciated Central	Colorado	Fluvial Sand	7,500	30	0.23	1	Konikow, 1975
14	Non-Glaciated Central	Wyoming	Madison Limest.	15,000-21,000	7-46	0.15-0.69	1	Konikow, 1976
15	Non-Glaciated Central	Texas	Hosston/Hensel Fm. Sandst.	3,200-48,000	5-20	0.06-0.24	2	Hall and Turk, 1975
16	Alluvial Valleys	Illinois	Glacial/Fluvial Sand	50,000-300,000	2.5-10	0.13-3.0	1	Walton, 1970
17	Alluvial Valleys	Kentucky	Glacial Sand/Gravel	20,000-100,000	6.3-20	0.40-2.0	2	Rumrbaugh and others, 1953

*Method of selecting transmissivity (T) and gradient (I) for computing aquifer discharge with the Darcy equation:

- 1 - Overlay maps of T and I
- 2 - Map of I with range of T
- 3 - Map of I with average T or single value of T in known area
- 4 - Range of or average T and I

(After Geraghty and Miller, 1983)

consists of a plain mantled by outwash deposits and is between the ground-water flow region of the glacial central region and the region of Atlantic and Gulf Coastal Plains (Heath, 1982). This site is a typical case of ground water contaminated by solid waste.

Previous Studies. The geological and hydrological characteristics of the Babylon landfill have been well documented since 1914 when Fuller (1914) prepared a summary of previous work. The report written by Pluhowski and Kantrowitz (1964) offered most of the hydrological information at this site. In 1972, McClymonds and Franke (1972) published calculations of the hydraulic conductivity of the site and summarized the work done at this site prior to 1972. The leachate plume was reported in 1975 by Kimmel and Braids (1975), and the physical and chemical properties of the aquifer and the plume was described by them in 1980 (Kimmel and Braids, 1980). Braids discussed that the plume reached a steady-state condition in 1982 (Geraghty and Miller, 1982).

CHAPTER II

COMPARISON OF THE KONIKOW MODEL AND THE PHAN MODEL

Since the applications of the Konikow model are limited to the saturated zone of aquifers, some contaminated sites with unsaturated zones may not be applicable. A comparison was made for evaluating the limitation of the Konikow model in a cross-sectional perspective by simulating a selected scenario site with the Konikow model and the Phan model.

The Phan model is a cross-sectional mathematical model for two-dimensional pollutant transport. It was developed by Wagner and others in the report titled "Computer Models for Two Dimensional Subterranean Flows and Pollutant Transport" for the E.P.A. (Wagner, et al, 1983). This model is applicable to both the unsaturated and saturated zones of the aquifers; the numerical method of finite elements is used.

The scenario of case 3W-2B with a 10 ft unsaturated zone was selected for this study. It was applied to the Phan model by Wagner and others (1983). In applying it to the Konikow model, the initial and boundary conditions were set by transferring to the results at the water table from the simulation of the Phan model. The initial time for the

Konikow model was set to the break through time at the water table based on the Phan model. The sources for the Konikow model were located where the contaminants entered the saturated zone at the break through time using the Phan model.

The analytical matrices that were used for the Konikow model and the Phan Model are different (Appendix G, Figure 97, Figure 98). The matrix of the Konikow model is designed with an equal interval for each grid with depth, while the matrix intervals of the Phan model increase with depth. Therefore, the comparison between these two models is based upon the average values over a specified interval of depth at two selected locations (Appendix G, Table XXII).

The simulated results are not quite the same because the mathematical equation for the Phan model lacks the dispersion term and the numerical methods are different. Therefore, the decreasing rate of the concentrations with depth are different during the same simulated time. The differences between the selected points are within 0.4 mg/l (Appendix G, Table XXII).

The decreasing rate of the simulated concentrations of the Phan model at the discharge point dropped rapidly within a depth of 80 ft. There were no significant changes for the depths greater than 80 ft (Appendix G, Figure 99). The simulated concentrations of the Konikow model at the discharge point decreased gradually with increasing depth (Appendix G, Figure 99). The results at the points which

were located 400 ft from the facility are similar to those points which are located at the discharge points (Appendix G, Figure 100).

Although the decreasing rates with depth during one simulated time period are different, the developmental trend of the plumes with increasing time in the saturated zone are the same for both models (Appendix G, Figure 101, Figure 102). The simulated concentrations increased gradually with time up to 150 years, then reached a steady state after 150 years for every case. The only exception was in the Konikow model at a distance of 400 ft from the facility and at a depth of 220 ft where the concentration increased at a rate slightly higher than the others after 150 years (Appendix G, Figure 102). This comparison implies that the Konikow model is verified using the Phan model and applicable to sites with a relatively shallow unsaturated zone. Further more, it has been shown that the Konikow model can be used in conjunction with cross-sectional unsaturated models to characterize contaminant movement in both the unsaturated and saturated zones.

CHAPTER III

SELECTED MATHEMATICAL MODELS

The Analytical Model

General Concepts of the Model

The analytical model used in this research is based primarily upon the paper published by Wilson and Miller (1978). Basically, the concept of this model can be described as (Figure 3):

$$\begin{aligned} \text{|RATE OF MASS ACCUMALATION|} &= \text{|RATE OF MASS IN|} \\ &- \text{|RATE OF MASS OUT| (+-) |RATE OF MASS GENERATION|} \end{aligned}$$

This physical phenomena is expressed in a mathematical model by Wilson and Miller (1978) as:

$$Rd \frac{\partial C}{\partial t} = D_x \frac{\partial^2 C}{\partial x^2} + D_y \frac{\partial^2 C}{\partial y^2} + D_z \frac{\partial^2 C}{\partial z^2} - V \frac{\partial C}{\partial x} - \lambda Rd C \quad (\text{III-1})$$

in which

Rd = retardation factor (linear adsorption) (*)

C = concentration of the substance in
solution (M/L³)

t = the time (T)

D_x = longitudinal dispersion coefficient (L²/T)

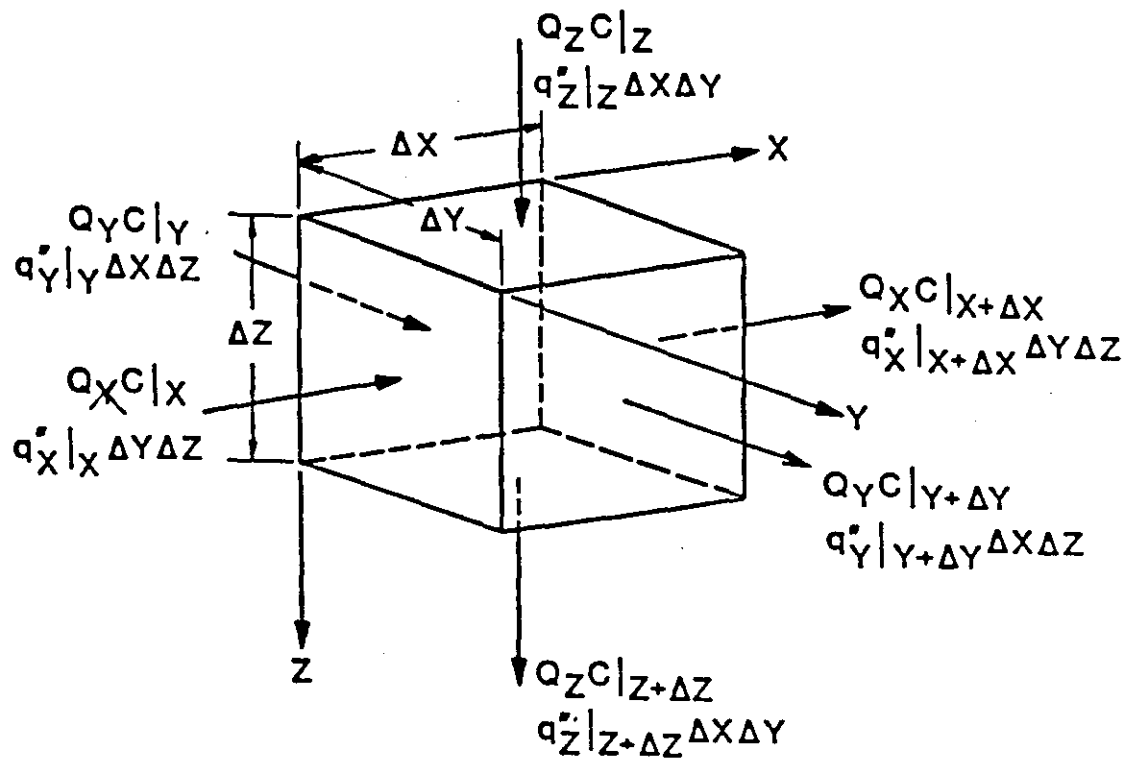


Figure 3. Differential Control Volume for Mass Balance
(After Wagner, 1984)

D_y, D_z = transverse dispersion coefficient (L²/T)

V = seepage velocity in the flow direction
along the x-axis (L/T)

λ = radioactive decay constant (T)

x, y, z = Cartesian coordinates. (L)

The "*" indicates a dimensionless factor.

The retardation factor slows the movement of the dissolved species due to adsorption. In a two-dimensional analysis, the "D_y" term is used for planar (x-y plane) cases and the "D_z" term is used for cross-sectional (x-z plane) cases.

The molecular diffusion can be ignored in most applied problems and the dispersion coefficient can be approximated as :

$$D_i = \alpha_i V_i \quad i=x, y, z \quad (\text{III-1.1})$$

in which the α (L) value is the dispersivity.

The concentration in the differential equation (a planar view) is described mathematically by

$$C = \frac{f'_m \exp\left(-\frac{x}{B}\right)}{4\pi n(D_x D_y)^{1/2}} W\left(u, \frac{r}{B}\right) \quad (\text{III-2})$$

and the cross-sectional (x-z plane) solution is

$$C = \frac{f'_m \exp\left(-\frac{x}{B}\right)}{4\pi n(D_x D_z)^{1/2}} W\left(u, \frac{r}{B}\right) \quad (\text{III-3})$$

in which

- $f'm$ = a continuous injection of mass per
 unit length (m/LT)
- n = the effective porosity (*)
- $W(u, r/B)$ = the well function. (*)
- $B = 2Dx/V$ (L)

The premise of this solution is the existence of an infinite two-dimensional porous medium in the x, y plane (x, z for cross section) with mass injected instantaneously along the z -axis (y -axis for cross section).

Assumptions and Limitations

Due to the boundary conditions for this differential equation, the analytical model is restricted by the following assumptions and limitations:

1. Darcy's law is applicable.
2. The ground-water flow regime is saturated.
3. The aquifer is infinite in areal extent.
4. The aquifer is homogeneous.
5. Aquifer thickness is a constant.
6. The ground-water flow is continuous and uniform in direction and velocity.
7. The leachate is evenly distributed over the saturated zone.
8. The leachate source supplies a constant mass flow rate.

The modifications and the sensitivity analysis of the analytical model are described in Appendix A.

in which

K_x, K_y, K_z = permeability	(L/T)
h = water head	(L)
H_s = hydraulic head from the source	(L)
x, y, z = Cartesian coordinates	(L)
S_s = specific storage	(*)
t = time	(T)
W = volume flux (positive for pumping out and negative for injection into the element)	(L ³ /T)
Q = rate of withdraw or recharge	(L/T)
M = thickness of the confined layer.	(L)

The "(*)" indicates a dimensionless factor.

In a two-dimensional planar view, the equation becomes

$$\frac{\partial}{\partial x} \left(K_x \frac{\partial h}{\partial x} \right) + \frac{\partial}{\partial y} \left(K_y \frac{\partial h}{\partial y} \right) = S_s \frac{\partial h}{\partial t} + W_p \quad (\text{III-5})$$

For a cross-sectional view, the equation becomes

$$\frac{\partial}{\partial x} \left(K_x \frac{\partial h}{\partial x} \right) + \frac{\partial}{\partial z} \left(K_z \frac{\partial h}{\partial z} \right) = S_s \frac{\partial h}{\partial t} + W_c \quad (\text{III-6})$$

in which

W_p, W_c = volume flux per unit area (positive for
out, negative for in the element). (L²/T)

Since

$$S = S_s M, \quad (\text{III-7})$$

The Numerical Model

General Concepts of the Model

The selected numerical model includes the ground-water flow equation, the solute-transport equation and the adsorption-decay modification equation. This combination is applicable to a wide range of problem types, such as one- or two-dimensional problems that involve steady state or transient flow with adsorption and decay. The ground-water flow and solute-transport equations are from the paper published by Konikow and Bredehoeft (1978), and the adsorption-decay modification equation was developed by Tracy in 1982 (Appendix B).

Ground-Water Flow Equation

The phenomena of groundwater flow can be described as:

$$\begin{aligned} & \{ \text{WATER MASS WITHIN ELEMENT} \} = \{ \text{CHANGE OF STORAGE} \} (+) - \\ & \{ \text{WATER MASS OUT OR IN} \} \end{aligned}$$

For a transient saturated flow in a three dimensional anisotropic aquifer, the mathematical equation is

$$\frac{\partial}{\partial x} \left(K_x \frac{\partial h}{\partial x} \right) + \frac{\partial}{\partial y} \left(K_y \frac{\partial h}{\partial y} \right) + \frac{\partial}{\partial z} \left(K_z \frac{\partial h}{\partial z} \right) = S_s \frac{\partial h}{\partial t} + W \quad (\text{III-4})$$

$$W = Q - \frac{K_z}{M} (H_s - h) \quad (\text{III-4.1})$$

and

$$T_i = K_i M \quad (i=x,y,z) \quad (\text{III-8})$$

where S is the storativity (L), T is the transmissivity (L²/T) and M is saturated thickness (L), equations III-7 and III-8 can be substituted into equations III-5 and III-6 and the transient flow equation becomes

$$\frac{\partial}{\partial x} \left(T_x \frac{\partial h}{\partial x} \right) + \frac{\partial}{\partial y} \left(T_y \frac{\partial h}{\partial y} \right) = S \frac{\partial h}{\partial t} + W \quad (\text{III-9})$$

for planar, and

$$\frac{\partial}{\partial x} \left(T_x \frac{\partial h}{\partial x} \right) + \frac{\partial}{\partial z} \left(T_z \frac{\partial h}{\partial z} \right) = S \frac{\partial h}{\partial t} + W \quad (\text{III-10})$$

for cross-sectional.

The Solute Transport Equation

The phenomenon of a nonreactive dissolved chemical species in ground water can be described as:

$$\begin{aligned} & \text{|CHEMICAL MASS WITHIN ELEMENT|} = \\ & \text{|CHANGE IN CONCENTRATION DUE TO HYDRODYNAMIC DISPERSION|} \\ & - \text{|THE EFFECT OF CONVECTION TRANSPORT|} - \text{|A FLUID SOURCE} \\ & \text{OR SINK|} \end{aligned}$$

Expressed in mathematical terms, the equation is

$$\frac{\partial (CM)}{\partial t} = \frac{\partial}{\partial x} \left(M \frac{\partial C}{\partial x} \right) + \frac{\partial}{\partial y} \left(M \frac{\partial C}{\partial y} \right) + \frac{\partial}{\partial z} \left(M \frac{\partial C}{\partial z} \right) - \frac{\partial}{\partial x} (MCVx) - \frac{C'W}{n} \quad (\text{III-11})$$

in which

C = concentration of the dissolved chemical species (M/L³)

M = saturated thickness of the aquifer (L)

Dx, Dy, Dz = dispersion coefficient (L²/T)

C' = the concentration of the dissolved chemical in a source or sink fluid (M/L³)

n = effective porosity of the aquifer (*)

W = volume flux per unit area. (L/T)

For a two-dimensional situation, the following expression was derived by Sunada (1970) as:

$$\frac{\partial (CM)}{\partial t} = \frac{\partial}{\partial x} \left(M \frac{\partial C}{\partial x} \right) + \frac{\partial}{\partial y} \left(M \frac{\partial C}{\partial y} \right) - \frac{\partial}{\partial x} (MCVx) - \frac{C'W}{n} \quad (\text{III-12})$$

for planar, and

$$\frac{\partial (CM)}{\partial t} = \frac{\partial}{\partial x} \left(M \frac{\partial C}{\partial x} \right) + \frac{\partial}{\partial z} \left(M \frac{\partial C}{\partial z} \right) - \frac{\partial}{\partial x} (MCVx) - \frac{C'W}{n} \quad (\text{III-13})$$

for cross section.

The Decay Equation

The radioactive materials in ground water will change their concentration over a period of time. This is called decay of material. A rate of decay is directly proportional to the quantity of material (Appendix B).

Equilibrium Sorption.

There are three processes that affect the adsorption of the dissolved constituent on the solid components of the aquifer. These are: 1) the exchange of constituent material with the dissolved, solute state; 2) the storage of constituent on the solid components of the aquifer; and 3) if the element being adsorbed is radioactive, the decay of the adsorption constituent (Tracy, 1982). The mathematical expression that describes sorption is in Appendix B.

Assumptions and Limitations

The assumptions for Konikow's model are listed as :

- 1) Darcy's law is valid and hydraulic-head gradient is the only significant driving mechanism for fluid flow.
- 2) No chemical reactions occur that affect the fluid properties or the aquifer properties.
- 3) The boundary conditions will isolate the plume flow system.
- 4) For adsorption of the Langmuir Isotherm, free energy and probability of occupancy are equal for all sites.

The modifications and the efficiency test of the numerical model are represented in Appendix B.

CHAPTER IV

MODEL APPLICATION APPROACH

After the characteristics of the selected models have been introduced, the application of these models to the chosen study sites is discussed in this chapter.

To obtain a solution, for either an analytical or a numerical model that includes the ground-water flow and solute transport equations, requires the specification of initial and boundary conditions for the terrain of the problem. Once the required conditions for the region of contaminated site have been set, the geological and hydraulic parameters within the area should be decided for the calculation of these models.

For studying a landfill site in two dimensions, the combination of planar and cross-sectional views will help the user to gain a better perspective vision of the plume. Two conceptual diagrams show the basic concept of the domain setting in two dimensions. A planar view is represented in Figure 4 and a cross-sectional view is shown in Figure 5. In setting up the input data set, the boundary conditions and initial conditions are different for the analytical model and numerical model.

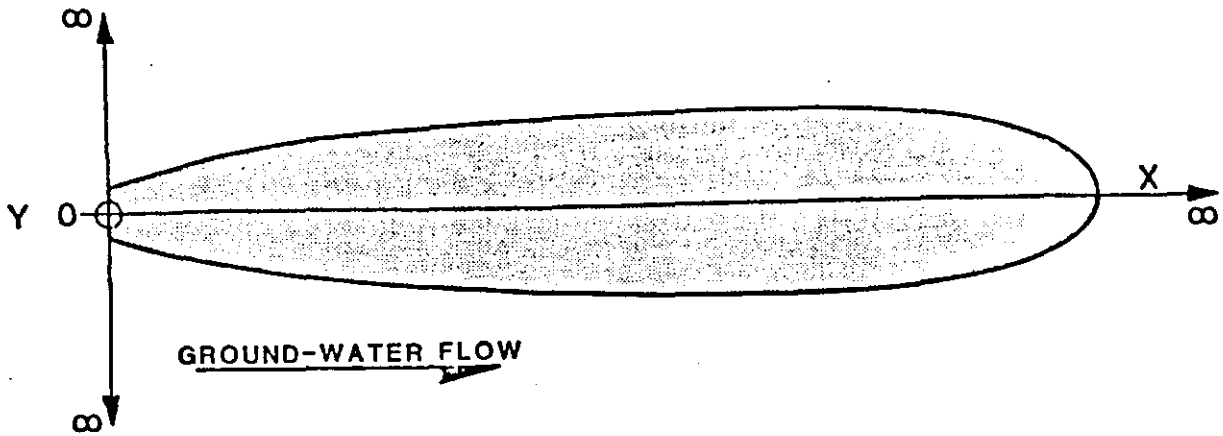


Figure 4. The Plume with a Planar View

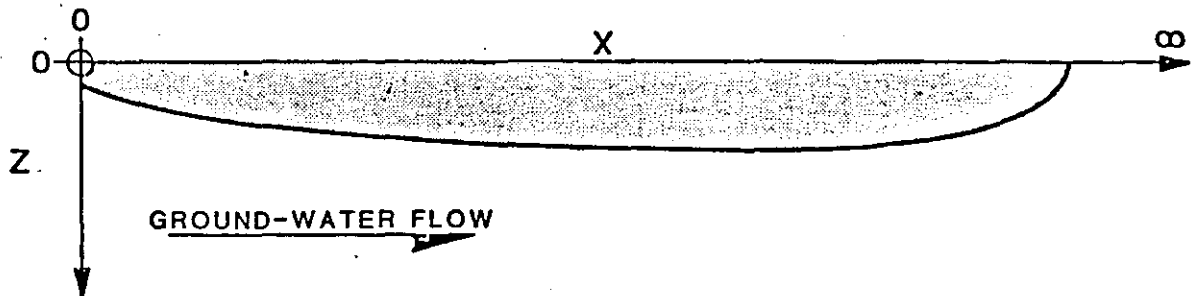


Figure 5. The Plume with a Cross-sectional View
(After Wagner, 1984)

Analytical Model

Boundary and Initial Conditions

For a planar view (Wagner and Kent, 1984), the appropriate boundary and initial conditions for solving the selected analytical model can be written as:

$$\begin{aligned} C(x, y, 0) &= 0 \\ C(x, \pm\infty, t) &= 0 \\ C(\pm\infty, y, t) &= 0 \end{aligned} \tag{IV-1}$$

in which

$$\begin{aligned} C &= \text{concentration, which is a function of } x\text{-}y \\ &\quad \text{domain and time} && (M/L^3) \\ x &= \text{Cartesian coordinate, which extends infinitely } (L) \\ y &= \text{Cartesian coordinate, which extends infinitely } (L) \\ t &= \text{time.} && (T) \end{aligned}$$

For a cross-sectional view (Wagner and Kent, 1984), the boundary condition can be described as :

$$\begin{aligned} C(x, z, 0) &= 0 \\ C(\pm\infty, z, t) &= 0 \\ C(x, \pm\infty, t) &= 0 \end{aligned} \tag{IV-2}$$

in which

$$\begin{aligned} C &= \text{concentration, which is a function of } x\text{-}z \\ &\quad \text{domain and time} && (M/L^3) \\ x &= \text{Cartesian coordinate, which extends infinitely } (L) \\ z &= \text{Cartesian coordinate, which is a finite depth } (L) \\ t &= \text{time.} && (T) \end{aligned}$$

To meet these boundary and initial conditions, the

grid matrices and mass injection of different time steps are used.

Analytical Matrices and Input Data Set

Analytical Matrices. Two simplified planar and cross-sectional schemes of the study site 3W are shown in Figure 6 and Figure 7. A simple grid map (ie. 10 * 10) which represents the boundaries in the area using a scale of 100 ft/grid is shown in Figure 8. The grid map can be superimposed on the maps shown in Figure 6 and Figure 7 to get the analytical matrices using Cartesian coordinates in planar and cross-sectional views (Figure 9, Figure 10). The selection of matrix size is described in Appendix C.

The relative positions of contaminate source and discharge area (river) were located by Cartesian coordinates which represent the distance or depth. For instance, in Figure 9 the contaminate source is in the region of $x=150$ to 550 feet and $y=550$ to 650 feet. These analytical matrices help to simulate the plume more conveniently.

Input Data Set. The parameters of the analytical model are listed in Table II. Two sets of the analytical input data of study site 3W, a planar and a cross-sectional, are shown in Table III and Table IV.

The Numerical Model

Boundary and Initial Condition

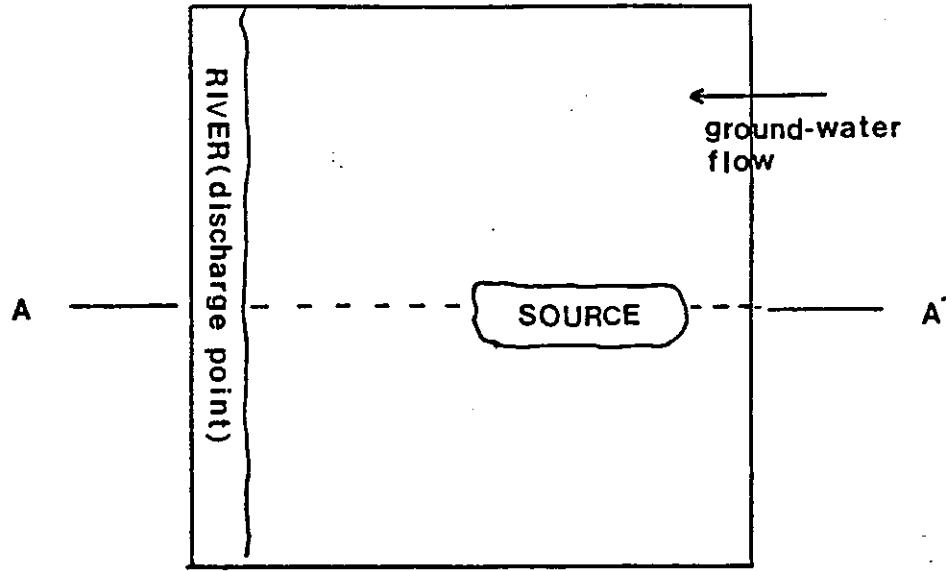


Figure 6. Planar View of the 3W Scenarios.

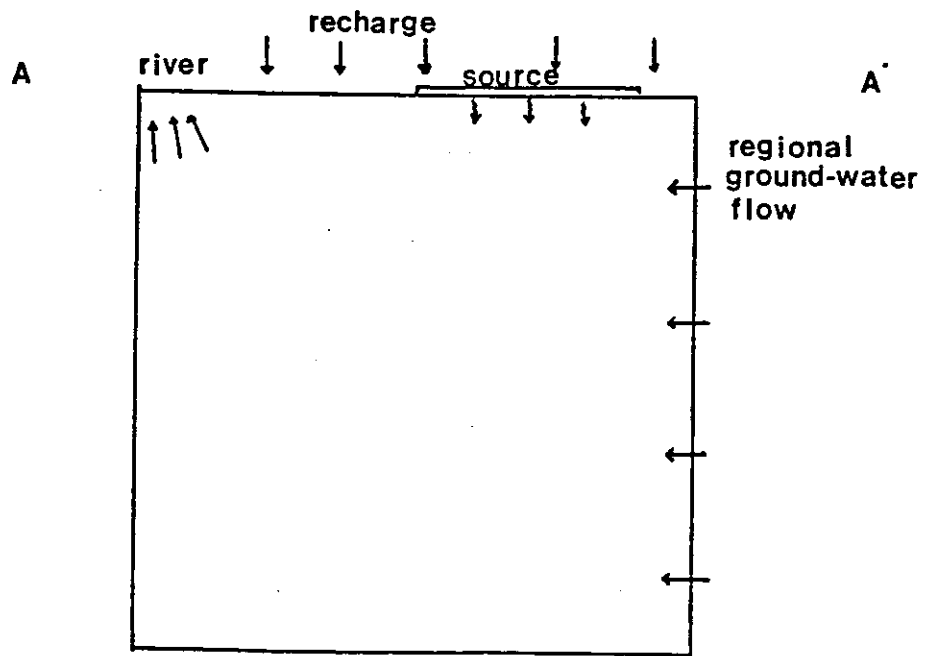


Figure 7. Flux of the 3W Scenarios with Cross-sectional View

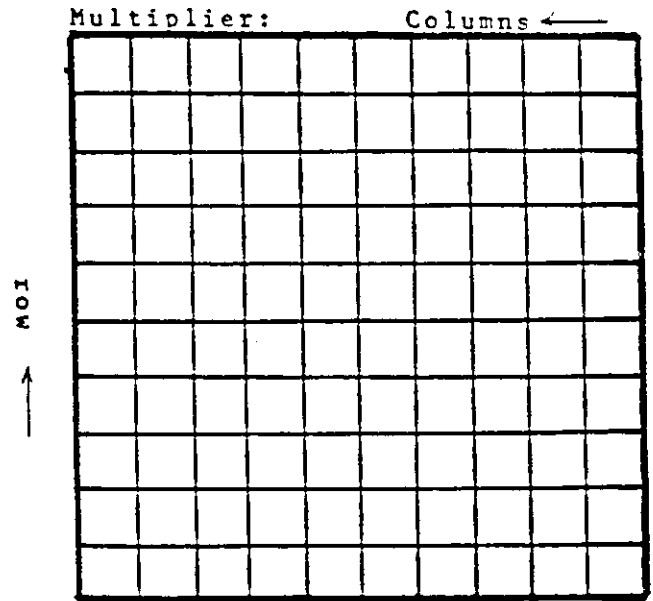


Figure 8. The 10 by 10 Grid Map for the Matrices

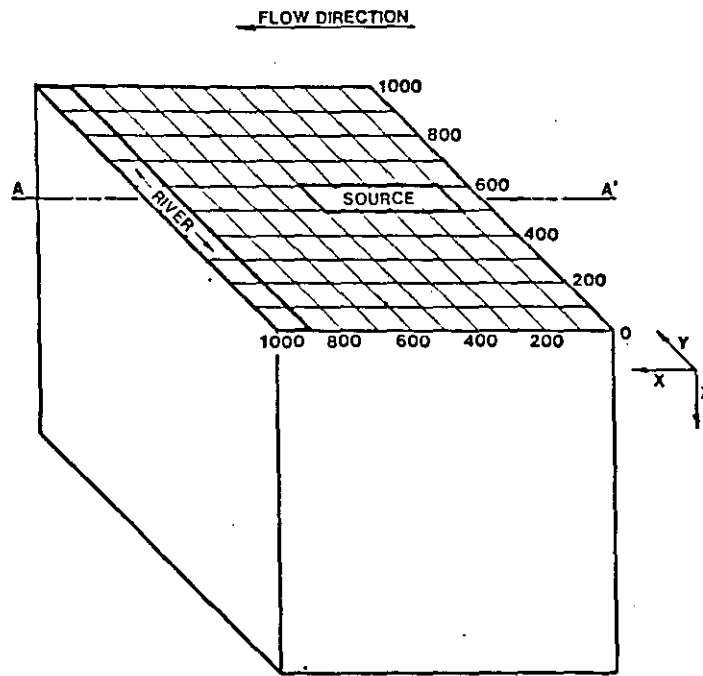


Figure 9. The Planar View of the Analytical Matrix for 3W Scenarios (Analytical Model)

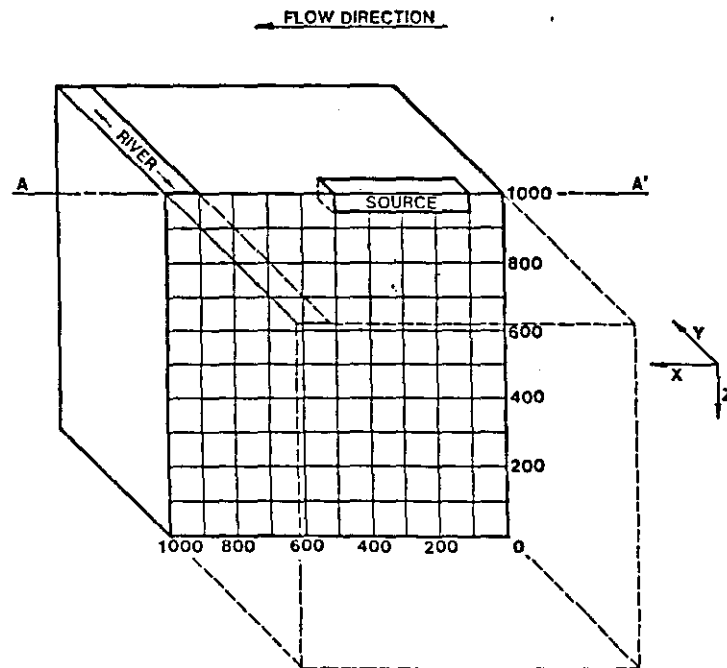


Figure 10. The Cross-sectional View of the Analytical Matrix for 3W Scenarios (Analytical Model)

TABLE II
INPUT DATA FOR THE ANALYTICAL MODEL

THE PARAMETERS	UNIT
Title Line	*
Aquifer Thickness	ft
Porosity	*
Seepage Velocity	ft/d
Grid Map Domain	
x-direction	ft
y(z)-direction	ft
Location of the Leachate Source(s)	ft
Time Increments of the Contaminant	day
Mass Flow Rate	lb/day (cf/d)(mg/l)
Sampling Time	day
Retardation	*
Decay	*
Dispersion Coefficient	ft ² /day

TABLE III

INPUT DATA SET OF THE ANALYTICAL MODEL OF
3W-1A SCENARIO (CROSS-SECTIONAL)

**** TSO FOREGROUND HARDCOPY ****
DSNAME=U11834C.X3W1ACR.DATA

THE 3W-1A CASE FOR THE ANALYTICAL MODEL
THE INPUT DATA SET
CROSS-SECTIONAL VIEW

THICKNESS = 1.00000 FT
POROSITY = 0.300000
VELOCITY = 0.350000E-01 FT/D

X DISPERSION = 2.64000 FT²/D
Y DISPERSION = 1.32000 FT²/D

RETARDATION = 1.00000
DECAY GAMMA = 1.00000

X LOCATION (FT)	Y LOCATION (FT)	AREA (FT ²)	START TIME (DAYS)	VOLUME FLOW RATE (FT ³ /D)	SOURCE CONCENTR. (MG/L)
150.000	901.000	39600.0	0.000000E+00	1.24000	100.000
550.000	1000.00				
150.000	901.000	39600.0	36500.0	1.24000	100.000
150.000	901.000	39600.0	73000.0	1.24000	100.000

TABLE IV

INPUT DATA SET OF THE ANALYTICAL MODEL OF
3W-1A SCENARIO (PLANAR)

**** TSO FOREGROUND HARDCOPY ****
DSNAME=U11834C.X3W1APL.DATA

3W-1A CASE FOR THE ANALYTICAL MODEL
THE INPUT DATA SET
PLANAR VIEW

THICKNESS = 100.000 FT
POROSITY = 0.300000
VELOCITY = 0.350000E-01 FT/D

X DISPERSION = 2.64000 FT²/D
Y DISPERSION = 1.32000 FT²/D

RETARDATION = 1.00000
DECAY GAMMA = 1.00000

X LOCATION (FT)	Y LOCATION (FT)	AREA (FT ²)	START TIME (DAYS)	VOLUME FLOW RATE (FT ³ /D)	SOURCE CONCENTR. (MG/L)
150.000	550.000	40000.0	0.000000E+00	124.000	100.000
550.000	650.000				
150.000	550.000	40000.0	36500.0	124.000	100.000
150.000	550.000	40000.0	73000.0	124.000	100.000

The numerical model uses a finite-difference method for solving the flow and the transport equations; therefore, the hydrogeological parameters defined in each node will control the solution. Each node area in the grid map should therefore have a complete set of these parameters specified for it.

For the initial condition, the solute transport equation directly depends on hydraulic and concentration gradients; Thus, the head and concentration in the ground-water flow system at the start of the simulation step must be specified. These initial conditions can be determined from field data or from previous simulations.

Basically, there are two general types of boundary conditions incorporated in the numerical model. These are constant-flux and constant-head conditions, which can be applied to represent the real boundaries of a ground-water flow system and the artificial boundaries required to fulfill the assumptions for the model.

Analytical Matrices and Input Data Set

Analytical Matrices. First, the procedure used in this numerical model requires that the terrain of interest should be isolated from the surrounding areas by a no-flow boundary (Figure 11). No-flow boundaries are designated by setting the transmissivity equal to zero at appropriate nodes, thereby precluding the flow of water or dissolved chemicals across the boundaries of the cell containing that

	1	2	3	4	5	6	7	8	9	10	11	12		
1	O	O	O	O	O	O	O	O	O	O	O	O	O	FLOW
2	O												O	
3	O												O	
4	O												O	
5	O												O	
6	O												O	
7	O												O	
8	O												O	
9	O												O	
10	O												O	
11	O												O	
12	O	O	O	O	O	O	O	O	O	O	O	O	O	

column

Figure 11. No-Flow Boundary of an Analytical Grid Map

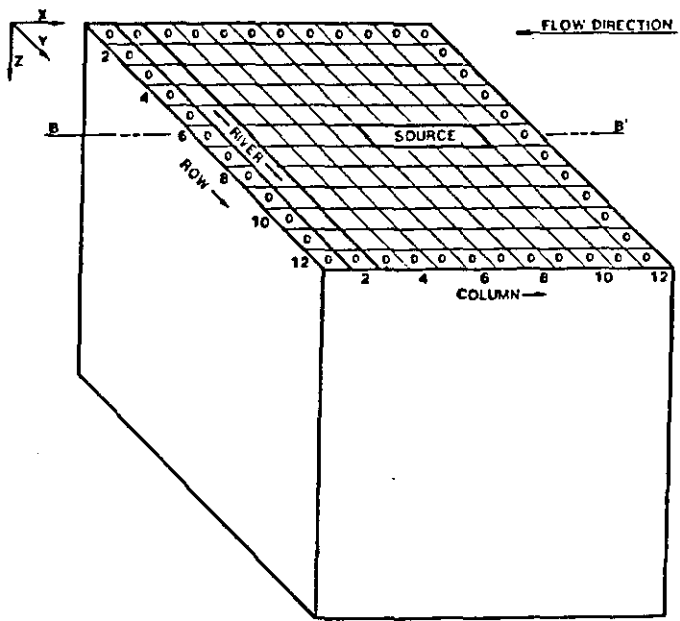


Figure 12. The Planar Matrix for 3W Scenarios (Numerical Model)

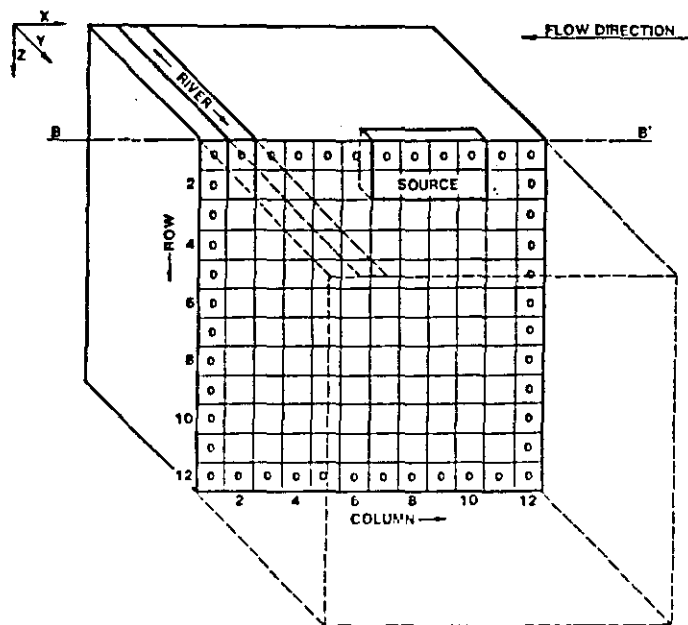


Figure 13. The Cross-sectional Matrix for 3W Scenarios (Numerical Model)

node is similar to setting the analytical matrices and is shown in Figure 12 and Figure 13.

A finite flux is designated by specifying the flux rate of discharge (pumping wells, a gaining stream, etc.) or injection rate (an injection well, precipitation, etc.) for the appropriate nodes (Figure 7).

"A constant-head boundary in the model can represent parts of the aquifer where the head will not change with time, such as recharge boundaries or area beyond the influence of hydraulic stresses. In this model, constant-head boundaries are simulated by adjusting the leakage term (the last term on the right side of equation III-4.1) at the appropriate nodes. This is accomplished by setting the leakance coefficient (K/M) to a sufficient high value such as 0.1), so as to allow the head in the aquifer at a node to be implicitly computed as a value that is essentially equal to the value of H_s , which in this case would be specified as the desired constant-head altitude" (After Konikow and Bredhoeft, 1978).

If a constant-flux or constant-head boundary represents a fluid source, then the chemical concentration in the source fluid (C) must also be specified. If the boundary represents a fluid sink, then the concentration of the produced fluid will equal the concentration in the aquifer at the location of the sink.

The matrices include transmissivity, permeability, node ID and potentiometric distribution in this model.

Input Data Set. The parameters of the numerical model are shown in Table V. A preprocessor was designated for the input of data and the matrices (Kent, et al, 1986).

TABLE V
INPUT PARAMETERS OF THE NUMERICAL MODEL

LONPLAN CASE

INPUT DATA

GRID DESCRIPTORS

NX (NUMBER OF COLUMNS) =
 NY (NUMBER OF ROWS) =
 XDEL (X-DISTANCE IN FEET) =
 YDEL (Y-DISTANCE IN FEET) =

TIME PARAMETERS

NTIM (MAX. NO. OF TIME STEPS) =
 NPMP (NO. OF PUMPING PERIODS) =
 PINT (PUMPING PERIOD IN YEARS) =
 TIMX (TIME INCREMENT MULTIPLIER) =
 TINIT (INITIAL TIME STEP IN SEC.) =

HYDROLOGIC AND CHEMICAL PARAMETERS

S (STORAGE COEFFICIENT) =
 POROS (EFFECTIVE POROSITY) =
 BETA (CHARACTERISTIC LENGTH) =
 DLTRAT (RATIO OF TRANSVERSE TO
 LONGITUDINAL DISPERSIVITY) =
 ANFCTR (RATIO OF T-YY TO T-XX) =

NON-DECAYING SPECIES

ROCK DENSITY (GRM/CM**3) = 1.000E+00BULK DENSITY/POROSITY =

LINEAR SORPTION DISTRIBUTION CONSTANT (KD) =

SIP USED

UNCONFINED AQUIFER

EXECUTION PARAMETERS

NITP (NO. OF ITERATION PARAMETERS) =
 TOL (CONVERGENCE CRITERIA - ADIP) =
 ITMAX (MAX. NO. OF ITERATIONS - ADIP) =
 CELDIS (MAX. CELL DISTANCE PER MOVE
 OF PARTICLES - M.O.C.) =
 NPMAX (MAX. NO. OF PARTICLES) =
 NPTPND (NO. PARTICLES PER NODE) =

PROGRAM OPTIONS

NPNT (TIME STEP INTERVAL FOR
 COMPLETE PRINTOUT) =
 NPNTMV (MOVE INTERVAL FOR CHEM.
 CONCENTRATION PRINTOUT) =
 NPNTVL (PRINT OPTION-VELOCITY
 0=NO; 1=FIRST TIME STEP;
 2=ALL TIME STEPS) =
 NPNTD (PRINT OPTION-DISP. COEF.
 0=NO; 1=FIRST TIME STEP;
 2=ALL TIME STEPS) =
 NUMOBS (NO. OF OBSERVATION WELLS
 FOR HYDROGRAPH PRINTOUT) =
 NREC (NO. OF PUMPING WELLS) =
 NCODES (FOR NODE IDENT.) =
 NPNCHV (PUNCH VELOCITIES) =
 NPDEL (PRINT OPT.-CONC. CHANGE) =

CHAPTER V

HYPOTHETICAL SCENARIO APPLICATIONS

3W Scenarios

Due to the adverse health effects of many water supplies, ground water and surface water contaminated by leachate from solid-waste landfills has become a problem of public concern. Geraghty and Miller, Inc. made a survey titled "Geologic and Hydrologic Locational Factors for Controlling Land Disposal Facility Siting" for the U.S. Environmental Protection Agency (Geraghty and Miller, 1983) and made several conclusions :

- "In humid regions, where leachate releases are greater and water tables are typically shallow, the travel time advantage of an unsaturated zone is small or non-existent."

- "In recharge areas of the flow system, plume growth is enhanced by downward components of groundwater flow, whereas in discharge areas, plume growth is restricted vertically by upward components of flow."

In referring to the site group "3W", they outline the unfavorable hydrogeologic conditions for setting up disposal waste facilities as:

- "Shallow water table"
- "Humid climate setting"
- "Moderate-K bedrock".

For ground-water contamination analysis, the greatest concern is the worst contaminated area which would probably occur in a humid region that has highly permeable aquifers. To study this pollution, selected models have been applied to simulate the plume, predict the development of the plume and to simulate cleanup. The 3W cases are designed for this purpose, and show the capabilities of the selected models.

The geological and hydrological factors of 3W cases in this research were obtained from the report of Geraghty and Miller, in 1983. The range of geological variations has been broadened in order to properly characterize the diversity of sites to be analyzed.

Climate

3W cases occur the humid regions of the country where the mean annual precipitation is greater than 20 inches (Geraghty and Miller, 1983). Areas where the mean annual precipitation is greater than 20 inches are largely from the East Coast to the Mississippi Valley, the Southeast, and most parts of the Pacific Northeast coast (Figure 1).

Geology

Eleven cases are used to represent varied geological

situations in the subsurface. Various combinations of low, moderate and high permeability layers are used. Values of Permeability used for each layer can be noted in Table VI.

Case 3W-1A

A homogeneous aquifer with medium permeability ($9.6 * 10^{-5}$ (ft/sec)), possibly fractured igneous rocks, permeable basalt or silty sand (Figure 14).

Case 3W-1B

A homogeneous aquifer with low permeability ($3.2 * 10^{-7}$ (ft/sec)) which could be carbonate, metamorphic rock or silt.

Case 3W-1C

This case is for cleanup of a plume. The geological conditions are the same as in case 3W-1A.

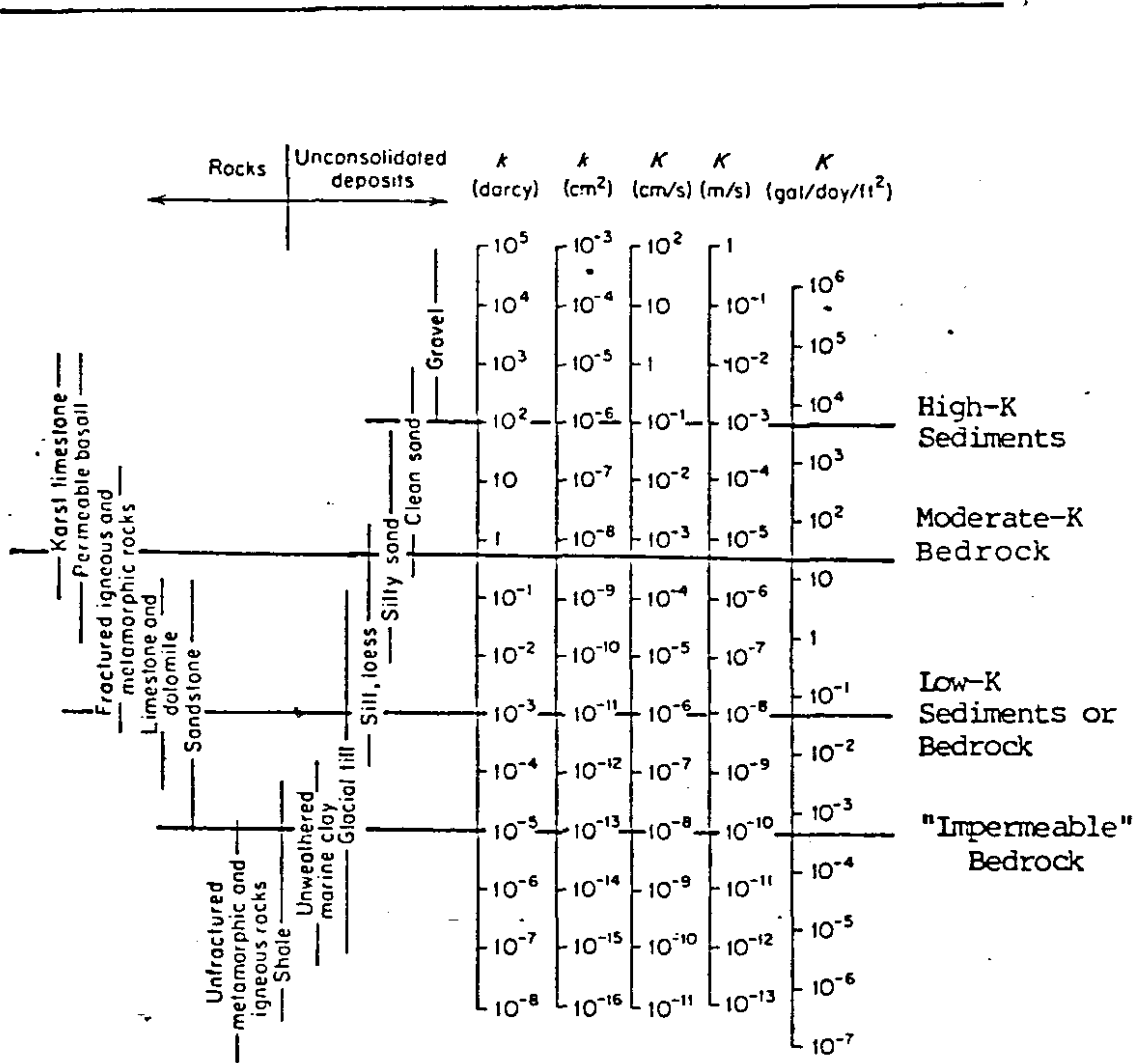
Case 3W-1D

This case is for different ratio of T_z/T_x from 3W-1A; the other geological conditions are the same as in case 3W-1A. The different ratio would represent difference in preferred orientation of bedding planes.

Case 3W-2A

This case delineates a two-layered aquifer which is overlain by a layer of low permeability such as silt or

TABLE VI
RANGE OF PERMEABILITIES FOR EARTH MATERIALS



(After Freeze and Cherry, 1979)

Multiplier: 1.E -5 (FT/S)

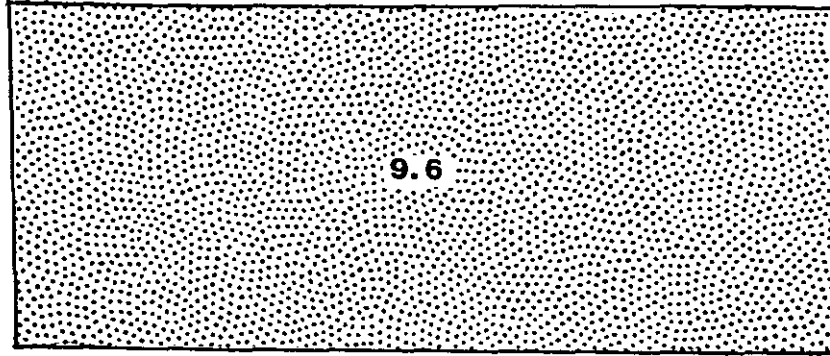


Figure 14. Case 3W-1A, Homogeneous Aquifer with Moderate Permeability

1.E -5 (FT/S)

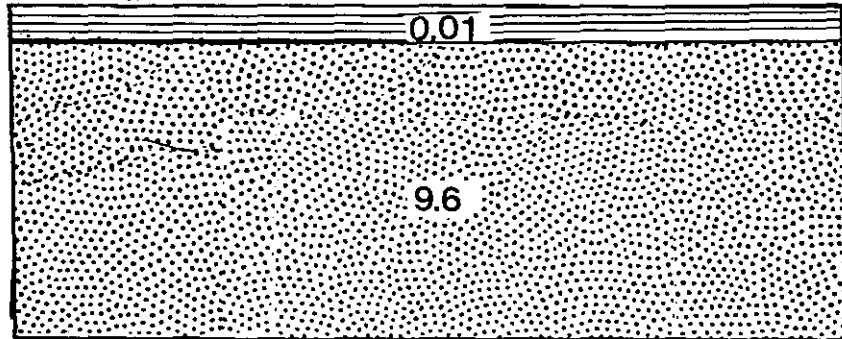


Figure 15. Case 3W-2A, Two-Layered Scenario with Low Permeable Top Layer

loess with clean sand below (Figure 15).

Case 3W-2B

A two-layered aquifer is represented; a highly permeable layer is underlain by a moderately permeable layer, such as an alluvial or glacial outwash bed overlying a sandstone bedrock (Figure 16).

Case 3W-2C

This is the case for a two-layered aquifer similar to case 3W-2A but with fractures beneath the contaminant sources in the upper impermeable layer (Figure 17).

Case 3W-3A

This is a three-layered aquifer with a highly permeable layer between two relatively impermeable layers, which could represent buried stream channel or glacial outwash deposits (Figure 18).

Case 3W-3B

This is a three-layered aquifer with a low permeability layer between two relatively highly permeable layers. It simulates a surficial aquifer and a confined aquifer, such as one clay layer between two high-permeability sandstone layers (Figure 19).

Case 3W-4A

$1.E-5$ (FT / S)

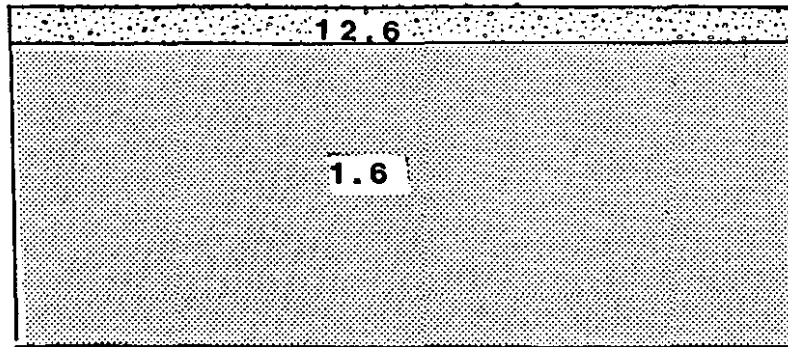


Figure 16. Case 3W-2B, Two-Layered Aquifer with a High Permeable Layer at Top

$1.E-5$ (FT / T)

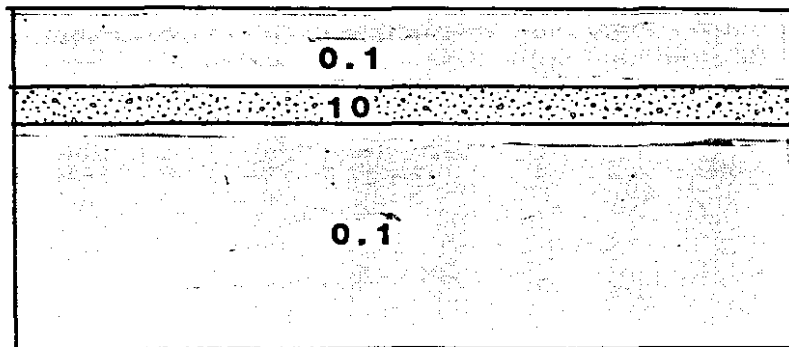


Figure 17. Case 3W-3A, Three-Layered Aquifer with a High Permeability Layer in Between

1.E-5 (FT/S)

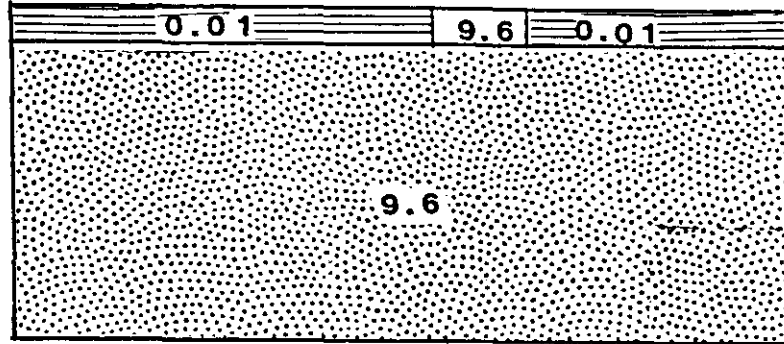


Figure 18. Case 3W-2C, Two-Layered Case with Fractures in the Top Low Permeable Layer

1.E-5 (FT/S)

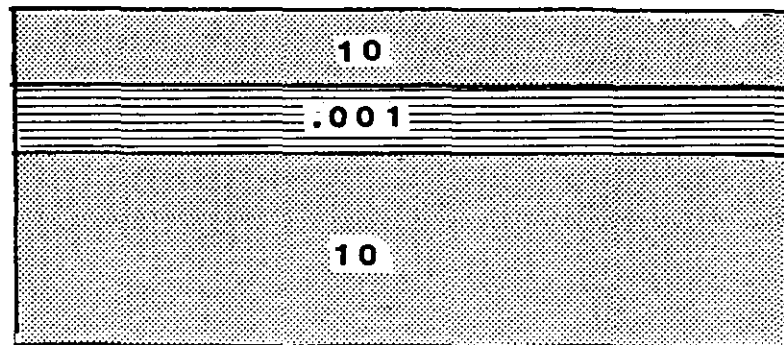


Figure 19. Case 3W-3B, Three-Layered Aquifer with a Low Permeability Layer in Between

An inclined high-permeability aquifer is studied. It could be one limb of an anticline or syncline of highly permeable sandstone (Figure 20).

Case 3W-5A

This represents a situation such as a high-permeability aquifer truncated by a normal fault (Figure 21).

Hydraulic Characteristics

The effective porosity for 3W cases is 0.3 (30%), the dispersivity is 75 (ft²/sec), the storage coefficient is 0.015 for transient simulation and 0.0 for steady-state. The permeability is different for each case depending on geological variations (Figures 14 to 21).

Ground-water Flow

The ground-water flow system for all 3W cases is the same. The system is described as a local flow system that is recharged by precipitation with a rate of 13.3 inches per year and discharged into a river. The flow direction is from constant head to the river with a gradient of 0.0125. The conceptual diagram is shown in Figure 15.

Calibration of the Model

Analytical Model

The case 3W-1A is applied to the analytical model for both planar and cross-sectional simulations. A two-hundred

1.E-4 (FT/S)

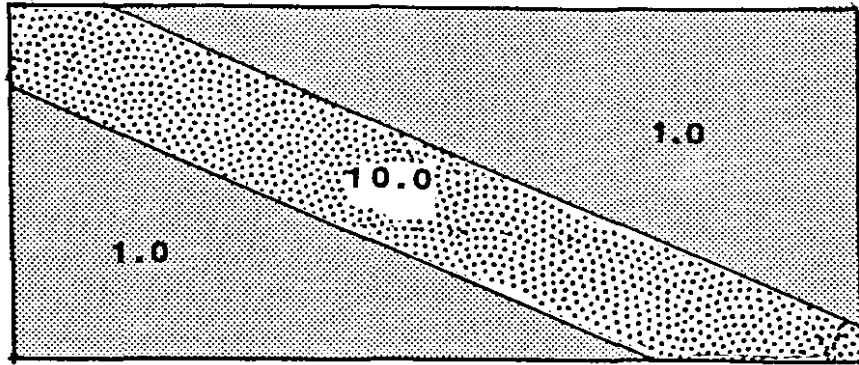


Figure 20. Case 3W-4A, An Incline High Permeability Aquifer

1.E-4 (FT/S)

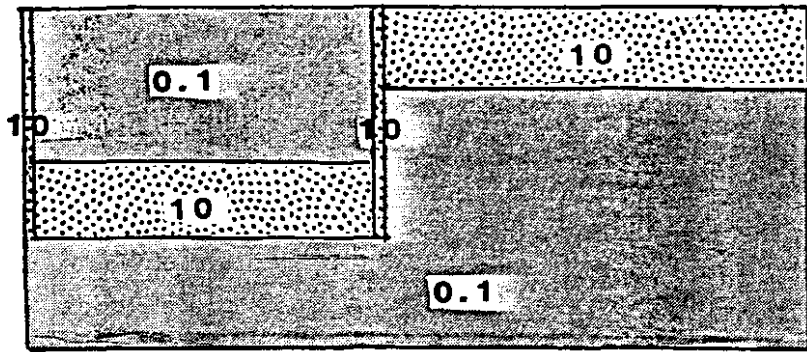


Figure 21. Case 3W-5A, A Normal Fault Scenario

year period is used for the analytical simulations. The ground water flows with a gradient of 0.00125. The mass recharge rate and the time steps were designed for a non-point contaminated source introducing leachate into the aquifer at a constant rate (Figure 9, 10).

The value for the initial concentration (C_0) is assumed to be 100 mg/l. Thus, all concentrations can be interpreted as relative concentrations (C/C_0) with a fractional percentage. Because of the limitations of the model, the discharge area (the river) can not be simulated.

Cross-sectional. This cross-sectional simulation is for the x-z plane, a 10 by 10 grid map (100 ft/node), with a unit width being the central part of the plume (Figure 10). The source is located at x = 150 feet to 550 feet, z = 901 feet to 1000 feet and the depth, 1000 feet, is treated being as infinite.

The mass flow rate is

$$\begin{aligned}
 QCo &= Q \quad Co && (V-1) \\
 &= Pi \quad A \quad Co \\
 &= (13.6 \text{ in/year})(400 \text{ ft}^2)(100 \text{ mg/l}) \\
 &= (1.24 \text{ ft}^3/\text{day})(100 \text{ mg/l}) \\
 &= 0.0074 \text{ (lb/day)},
 \end{aligned}$$

and the seepage velocity is

$$V_s = \frac{K \quad I}{n} \quad (V-2)$$

$$\begin{aligned}
 &= (.000096 \text{ ft/sec})(0.00125)/(0.3) \\
 &= 0.035 \text{ (ft/day)}
 \end{aligned}$$

in which

$$QCo = \text{mass flow rate} \quad (M/T)$$

$$Q = \text{volume flow rate} \quad (L^3/T)$$

$$Co = \text{source concentration} \quad (M/L^3)$$

$$Pi = \text{infiltration rate} \quad (L/T)$$

$$K = \text{permeability} \quad (L^2/T)$$

$$I = \text{gradient of ground water flow} \quad (*)$$

$$\begin{aligned}
 A = \text{cross sectional area (perpendicular to ground} \\
 \text{water flow direction)} \quad (L^2)
 \end{aligned}$$

$$Vs = \text{seepage velocity} \quad (L/T)$$

$$n = \text{effect porosity} \quad (*)$$

The input data set is listed in Table III.

Planar. The simulation for planar case is a 1000 feet by 1000 feet area subdivided by 100 nodes (Figure 8) and the source is located at the region $x = 150$ feet to 550 feet, $y = 550$ feet to 650 feet (Figure 9). The aquifer thickness is assumed to be 100 feet. The mass flow rate (QCo) is calculated as:

$$\begin{aligned}
 Q &= Pi A \\
 &= (13.6 \text{ in/year})(40000 \text{ ft}^2) \\
 &= 124 \text{ (ft}^3/\text{day)}
 \end{aligned}$$

$$\begin{aligned}
 QCo &= Q Co \\
 &= (124 \text{ ft}^3/\text{day})(100 \text{ mg/l})(0.0000022 \text{ lb/mg})(28.2 \text{ l/ft}^3) \\
 &= .7741(\text{lb/day}),
 \end{aligned}$$

and the seepage velocity (Equation V-2) is

$$V_s = \frac{K I}{n}$$

$$= (.000096 \text{ ft/sec})(0.00125)/(0.3)$$

$$= 0.035 \text{ (ft/day)}$$

in which

QCo	= mass flow rate	(M/T)
Q	= volume flow rate	(L ³ /T)
Co	= source concentration	(M/L ³)
K	= permeability	(L ² /T)
I	= gradient of ground water flow	(*)
A	= cross-sectional area (perpendicular to the ground water flow direction)	(L ²)
Vs	= seepage velocity	(L/T)
n	= effective porosity	(*)

Table IV is the input data set.

Numerical Model

For the numerical simulations, one planar case and twelve cross-sectional cases are applied. The basic boundary conditions are shown in Figure 7. A four-hundred year period is used for four pumping periods, one hundred years each, to simulate possible happenings. All cases were run using the options for head only and solute transport. The initial concentration of injection wells is assumed to be 1 mg/l in order to interpret the concentrations of the plume as

relative concentrations with fractional percentage.

The convergence criterion (TOL) for the calculation is set as 0.01 and a conservative chemical element ($K_d = 0.2$) is assumed as an indicator. The ground-water table of the region is from 10.00 feet to 11.25 feet with a gradient of 0.00125.

All the 3W cases are assumed to be saturated aquifers due to the limitation of the Konikow model (Chapter III). One scenario case was simulated cross-sectionally by using both the Konikow model and the Phan model. The simulated results from the Konikow model are sufficiently close to the simulated results from the saturated portion of the Phan model (Chapter II) so as to verify the use of the Konikow model for cross-sectional simulations.

Cross-sectional. From the cross-sectional view, the simulated plane is the profile of the central line of the plume with a 1000 feet by 1000 feet region (Figure 19). The grid map is 12 by 12 (includes a no-flow boundary) with unit thickness. The leachate is introduced into the ground water by assuming four injection wells (Figure 22). The infiltration rate is assumed to be 13.6 in/year. The recharge rate is calculated as:

$$\begin{aligned} Q_i &= P_i A && (V-1) \\ &= (13.6)(\text{in/year})(100)(\text{ft}^2) \\ &= 3.6e-6(\text{ft}^3/\text{sec}) \end{aligned}$$

in which

Q = injection rate (L³/T)

P_i = precipitation (L/T)

A = source area (L²)

The recharge rate will be adjusted when there is a low permeability layer at the top of the aquifer, such as case 3W-2A (Figure 21). The ratio for anisotropic transmissivity will affect the shape of the plume. Thus, it is a factor for simulating the shape of plume. Case 3w-1D was designed for this purpose. After the plume development had been simulated, the cleanup simulations were considered, as in case 3W-1C (Figure 23). Eight more wells were designed to accomplish this goal; at the same time, the sources of contamination were terminated. The rates for injection and pumping were calculated to obtain the water mass balance. All input data sets and the permeability matrices for different geological variations are listed in Appendix D.

Planar. The 3w-1A (Figure 18) case is applied to this simulation. The simulated region is specified by a 12 by 12 (100 ft/grid) grid map which includes no-flow boundary, and the aquifer thickness is assumed to be 500 feet. The leachate is introduced by four injection wells which are shown in Figure 24. The recharge rate $3.6 * 10^{-4}$ is from the calculation shown as:

$$\begin{aligned} Q_i &= P_i A \\ &= (13.6) (\text{in/year}) (10000) (\text{ft}^2) \\ &= 3.6\text{E-}4 (\text{ft}^3/\text{sec}) \end{aligned}$$

	1	2	3	4	5	6	7	8	9	10	11	12		
1	O	O	O	O	O	O	O	O	O	O	O	O	O	ROW
2	O	D					L	L	L	L		O		
3	O											O		
4	O											O		
5	O											O		
6	O											O		
7	O											O		
8	O											O		
9	O											O		
10	O											O		
11	O											O		
12	O	O	O	O	O	O	O	O	O	O	O	O		

column

Figure 22. The Conceptual Matrix of Injection Sources and Discharge Points (Cross-sectional View)

	1	2	3	4	5	6	7	8	9	10	11	12	
1	O	O	O	O	O	O	O	O	O	O	O	O	ROW
2	O	D	D				L	L	L	L	I	O	
3	O		D								I	O	
4	O		D								I	O	
5	O		D								I	O	
6	O											O	
7	O											O	
8	O											O	
9	O											O	
10	O											O	
11	O											O	
12	O	O	O	O	O	O	O	O	O	O	O	O	

column

Figure 23. The Conceptual Matrix of Aquifer Restoration (Cross-sectional View)

in which

Q_i = recharge rate	(L ³ /T)
P = precipitation	(L/T)
A = source area.	(L ²)

As to the cleanup simulation, eight more wells were installed to inject fresh (recycled) water in and pump contaminated water out; at the same time, the sources of contamination were terminated (Figure 25). The rate for injection and pumping were designed by calculating the water mass balance of the flow system.

The input data set is listed in Appendix D.

Results

Analytical

A cross-sectional view of the plume for case 3W-1A is shown in Figure 26. The shape of the plume and the distribution of concentration are clearly displayed. The plume elongated downgradient and the 15 percent concentration boundaries reached the 320 ft depth level.

A planar view for the plume of 3W-1A (Figure 27) shows its downgradient development and its sides spreading out. The 15 percent concentration boundary dispersed about 150 feet from the central line at the discharge edge of the map. The results of the analytical simulations present a general view of the development of the plume in a 3W region (with a moderate permeability and homogeneous aquifer) after a

	1	2	3	4	5	6	7	8	9	10	11	12		
1	O	O	O	O	O	O	O	O	O	O	O	O	O	ROW
2	O	D											O	
3	O	D											O	
4	O	D											O	
5	O	D											O	
6	O	D					L	L	L	L			O	
7	O	D											O	
8	O	D											O	
9	O	D											O	
10	O	D											O	
11	O	D											O	
12	O	O	O	O	O	O	O	O	O	O	O	O	O	
	column													

Figure 24. The Matrix of Injection Sources and Discharge Points (Planar View)

	1	2	3	4	5	6	7	8	9	10	11	12		
1	O	O	O	O	O	O	O	O	O	O	O	O	O	ROW
2	O	D											O	
3	O	D											O	
4	O	D	P								I	O	O	
5	O	D	P								I	O	O	
6	O	D	P				L	L	L	L	I	O	O	
7	O	D	P								I	O	O	
8	O	D											O	
9	O	D											O	
10	O	D											O	
11	O	D											O	
12	O	O	O	O	O	O	O	O	O	O	O	O	O	
	column													

Figure 25. The Matrix of Aquifer Restoration (Planar)

THE LEACHATE FATE AND TRANSPORT FROM CASE 3W-1A

THE ANALYTICAL SIMULATION
THE CROSS-SECTIONAL VIEW
AT 200 YEARS

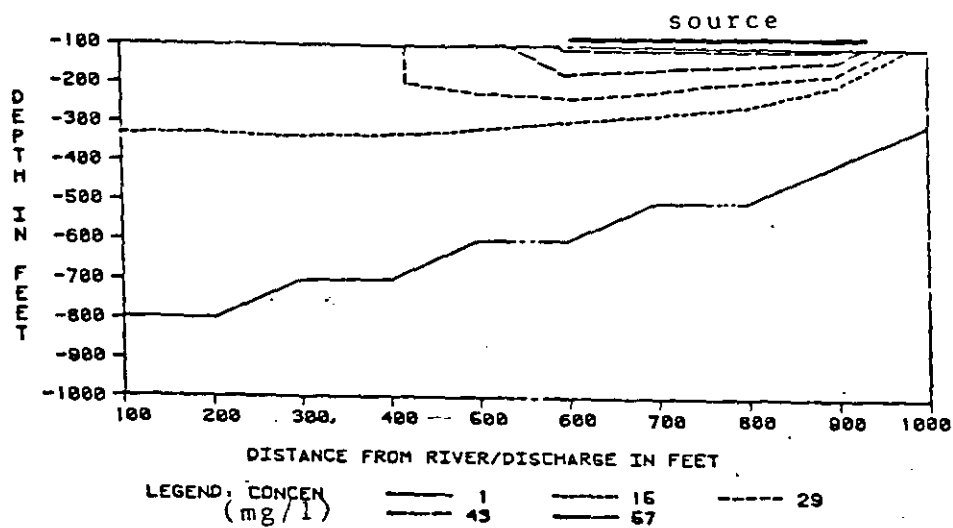


Figure 26. The Simulation of 3W-1A of the Analytical Model (Cross-sectional View)

THE LEACHATE FATE AND TRANSPORT FROM CASE 3W-1A

THE ANALYTICAL SIMULATION
THE PLANAR VIEW
AT 200 YEARS

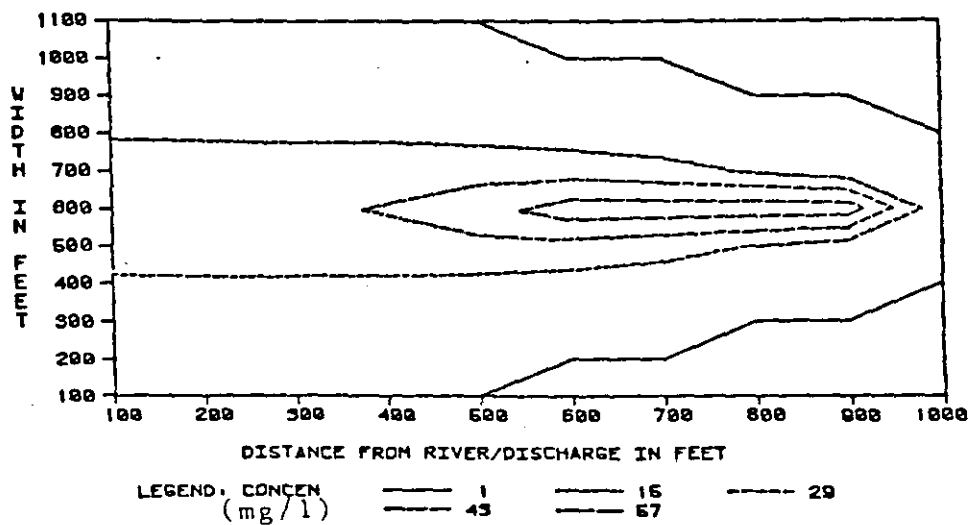


Figure 27. The Simulation of 3W-1A Scenario of the Analytical Model (Planar View)

certain period of contamination.

Numerical Model

3W-1A. The numerical simulation for 3W-1A with a planar view resulted in the trend of contamination shown in Figure 28. A map of the ground-water equalpotential lines, Figure 29, shows the ground-water flow from the recharge side to the discharge side (river). As to the cross-sectional simulation, the results more closely matched the results of the analytical simulation (Figure 26). The development of the plume during a four-hundred year period is presented by a series of figures (Figure 30 to Figure 34). The distribution of equalpotential lines is shown in Figure 35 with a cross-sectional view. Due to the surface recharge, the equal-potential lines bent slightly downgradient at the upper part (Figure 35). This is further discussed in Appendix E. Figure 36 and Figure 37 are the results of the simulated plume at 50 years and 400 years. These two figures are presented by the pattern plotting method which plotted in colors to enhance the vision of resolution. The surface recharge resulted in the upper gradient migration of the plume (Appendix E).

3W-1B. This is the cross-sectional case for a homogeneous aquifer with low permeability. There was very little water was that discharged or recharged in the low permeability aquifer. Thus, the ground-water head was not influenced (Figure 38) and no leachate infiltrated into the

LEACHATE FATE AND TRANSPORT FROM WASTE FACILITY 3W-1A

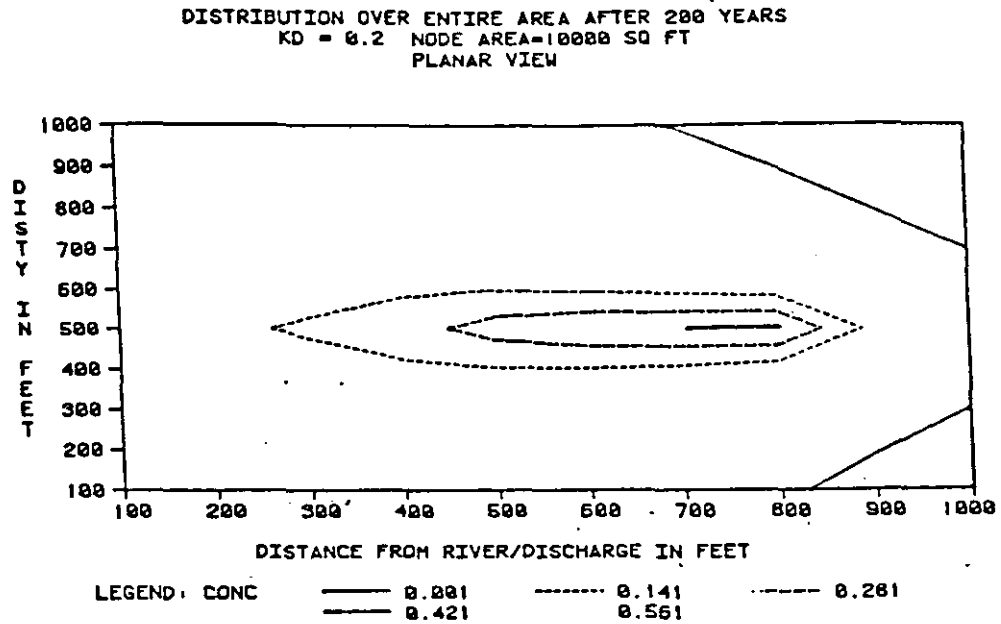


Figure 28. The Simulation of 3W-1A Case of the Numerical Model with a Planar View

LEACHATE FATE AND TRANSPORT FROM WASTE FACILITY 3W-1A

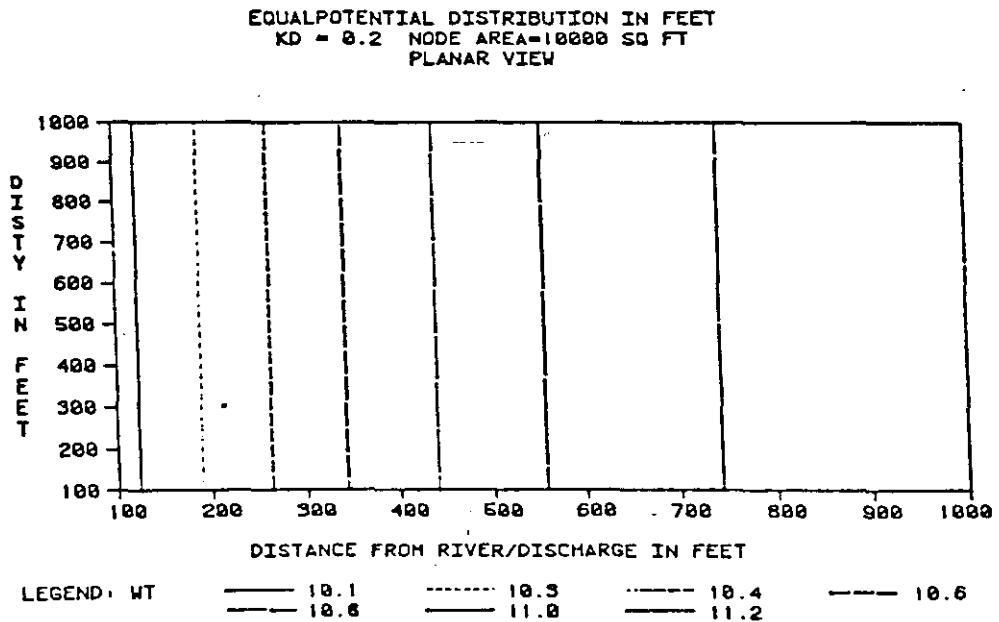


Figure 29. The Equal-potential Lines of the 3W-1A Case (Planar View)

LEACHATE FATE AND TRANSPORT FROM WASTE FACILITY 3W-1A

DISTRIBUTION OVER ENTIRE AREA AFTER 50 YEARS
 KD = 0.2 NODE AREA=10000 SQ FT

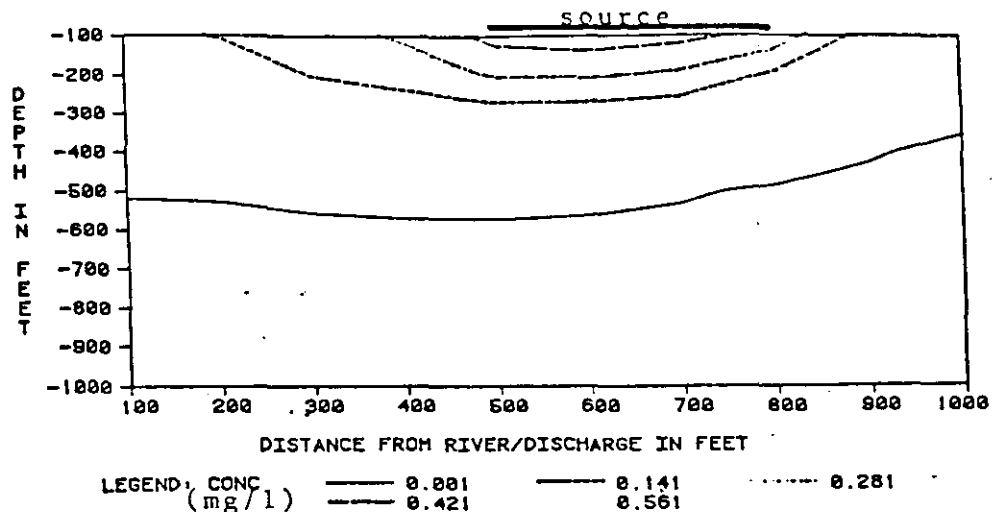


Figure 30. The Plume of Case 3W-1A After 50 Years Simulation

LEACHATE FATE AND TRANSPORT FROM WASTE FACILITY 3W-1A

DISTRIBUTION OVER ENTIRE AREA AFTER 100 YEARS
 KD = 0.2 NODE AREA=10000 SQ FT

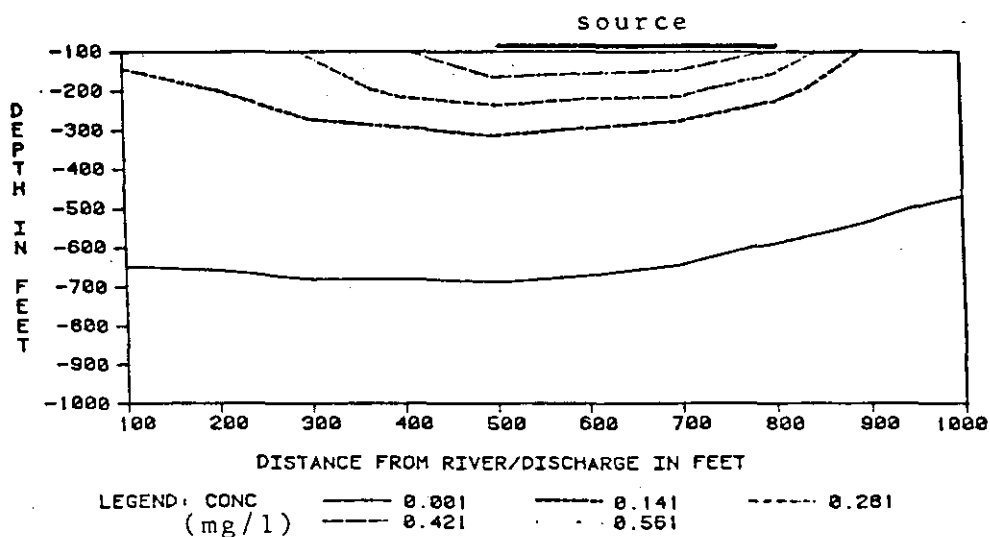


Figure 31. The Plume of Case 3W-1A After 100 Years Simulation

LEACHATE FATE AND TRANSPORT FROM WASTE FACILITY 3W-1A

DISTRIBUTION OVER ENTIRE AREA AFTER 200 YEARS
 KD = 0.2 NODE AREA=10000 SQ FT.

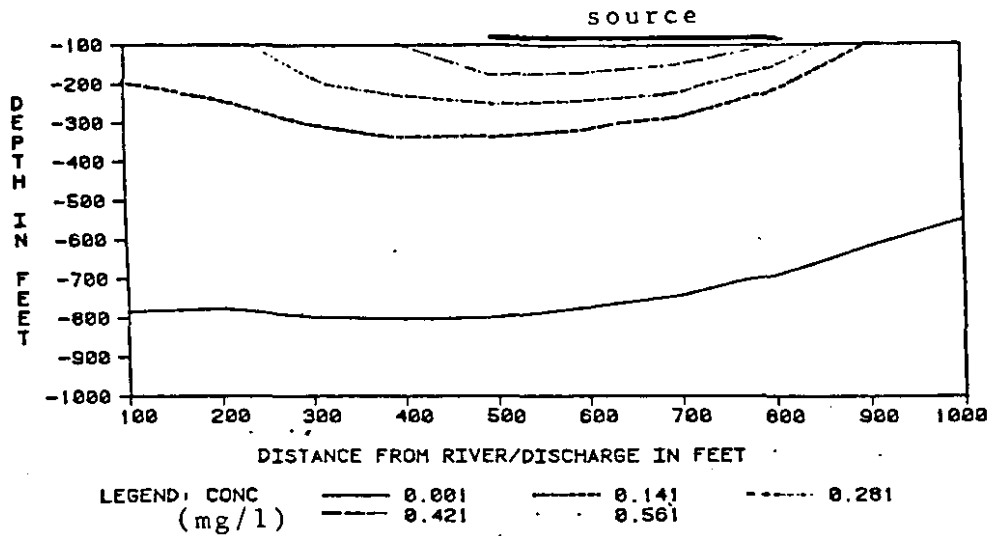


Figure 32. The Plume of Case 3W-1A After 200 Years Simulation

LEACHATE FATE AND TRANSPORT FROM WASTE FACILITY 3W-1A

DISTRIBUTION OVER ENTIRE AREA AFTER 300 YEARS
 KD = 0.2 NODE AREA=10000 SQ FT.

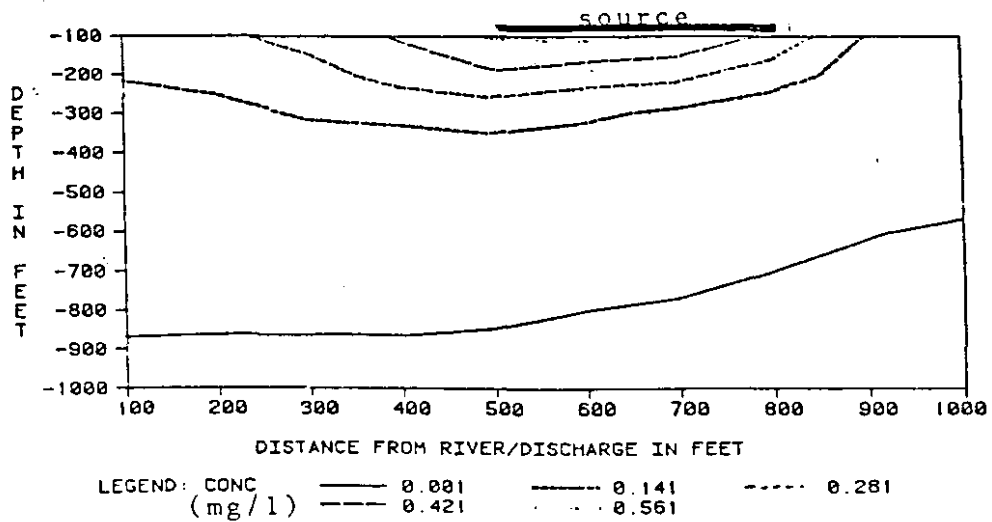


Figure 33. The Plume of Case 3W-1A After 300 Years Simulation

LEACHATE FATE AND TRANSPORT FROM WASTE FACILITY 3W-1A

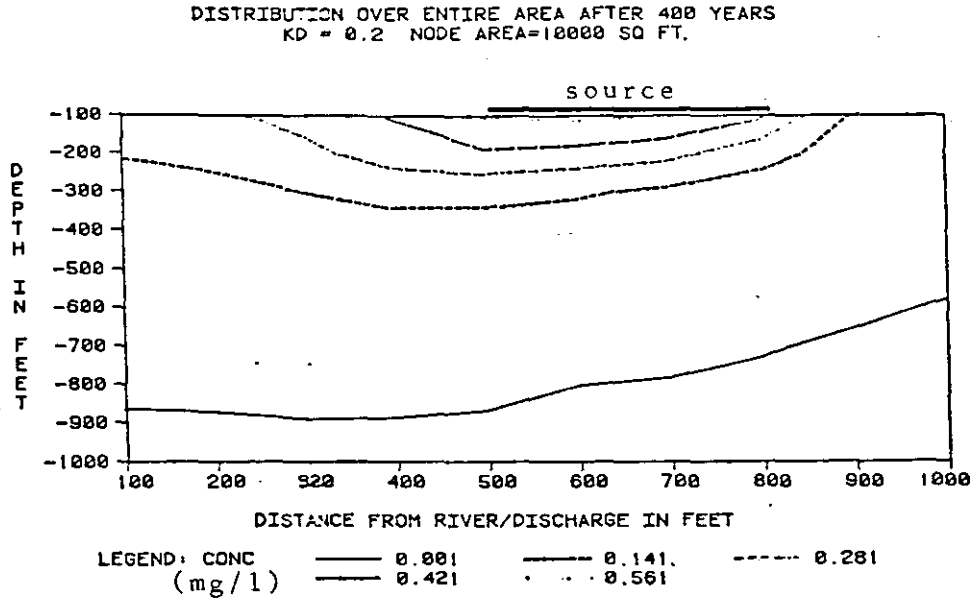


Figure 34. The Plume of Case 3W-1A After 400 Years Simulation

LEACHATE FATE AND TRANSPORT FROM WASTE FACILITY 3W-1A

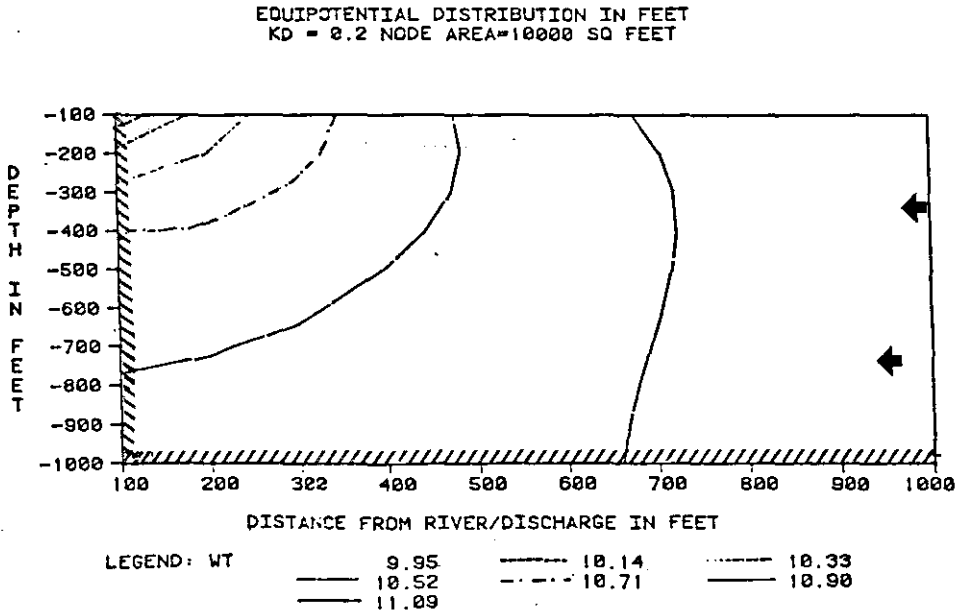


Figure 35. The Distribution of Equal-Potential Lines of the 3W-1A Scenario

LEACHATE FATE AND TRANSPORT FROM WASTE FACILITY 3W-1A

DISTRIBUTION OVER ENTIRE AREA AFTER 50 YEARS
 KD = 0.2 NODE AREA=10000 SQUARE FEET

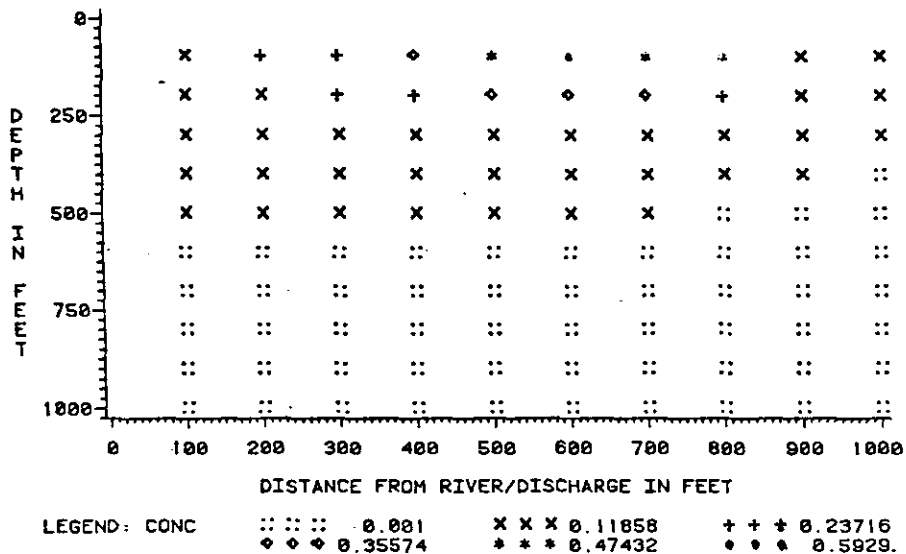


Figure 36. Pattern Plot of Case 3W-1A (50 Years)

LEACHATE FATE AND TRANSPORT FROM WASTE FACILITY 3W-1A

DISTRIBUTION OVER ENTIRE AREA AFTER 400 YEARS
 KD = 0.2 NODE AREA=10000 SQUARE FEET

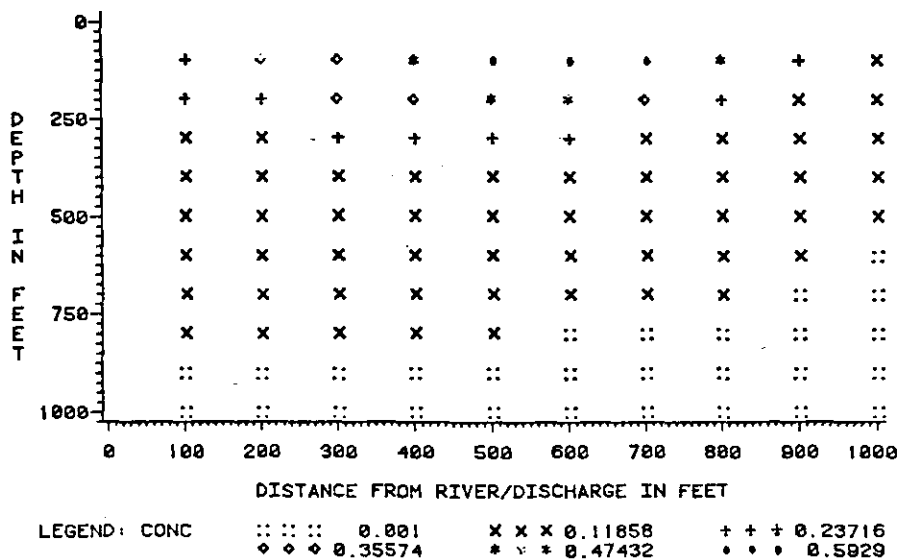


Figure 37. Pattern Plot of Case 3W-1A (400 Years Simulation)

LEACHATE FATE AND TRANSPORT FROM WASTE FACILITY 3W-1B

EQUIPOTENTIAL DISTRIBUTION IN FEET
 KD = 0.2 NODE AREA = 10000 SQ FT
 AT 200 YEARS

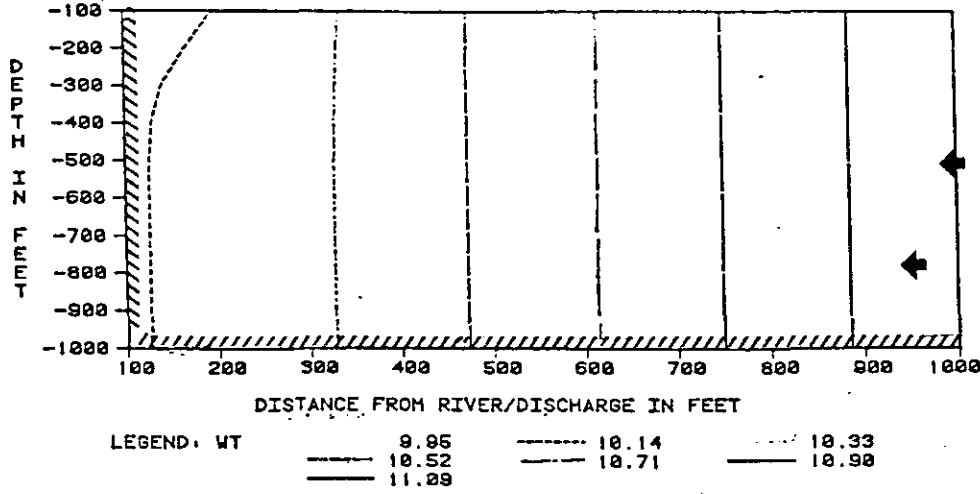


Figure 38. The Distribution of Equal-Potential Lines of the 3W-1B Scenario

LEACHATE FATE AND TRANSPORT FROM WASTE FACILITY 3W-1B

DISTRIBUTION OVER ENTIRE AREA AFTER 300 YEARS
 KD = 0.2 NODE AREA = 10000 SQUARE FEET

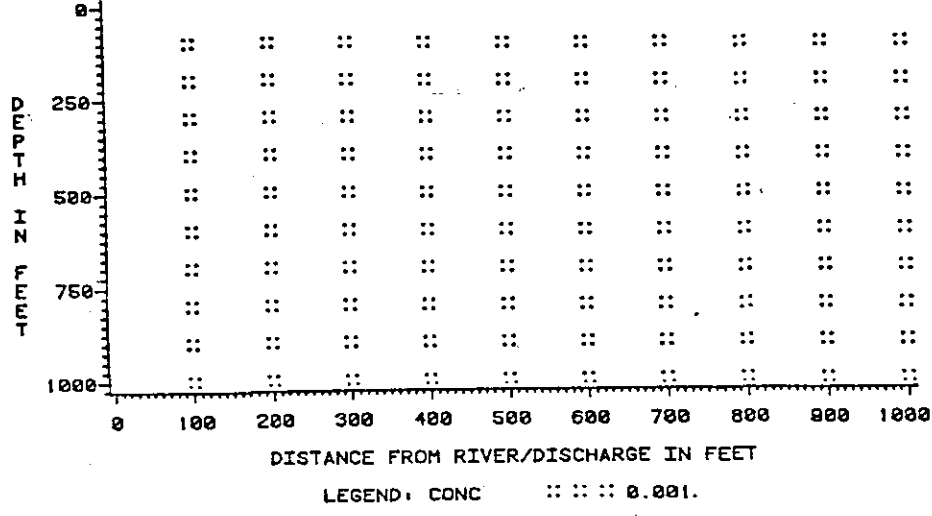


Figure 39. The Plume of Case 3W-1B After 300 Years Simulation

ground water system (Figure 39).

3W-1D. The simulated cross-sectional plume of case 3W-1D at 300 years (Figure 40) is shallower than the 3W-1A case at 300 years due to the lower T_z/T_x ratio, which hinders downward movement of the contaminants. This result effectively presents the characteristic of the orientation of deposits of aquifers.

3W-2A. The cross-sectional map of the two layered scenario shows that the low permeability top layer prevented the solute from leaking into the ground-water system even after a three-hundred year simulation (Figure 41). This result provides the information necessary for planning a possible location for landfill that will be on an impermeable layer.

3W-2B. The head distribution of ground water for the case 3W-2B is shown in Figure 42. It is interpreted that the top high permeability layer caused a fast ground water flow movement and resulted in the equipotential lines to bend downgradient. The distributions of concentration are shown in Figure 43 and Figure 44. These results represent the plumes which might occur in most alluvial deposits.

3W-2C. The fractures beneath the source of contamination allowed the leachate to go through the low permeability layer. The development of the plume is presented in Figure 45 and 46.

LEACHATE FATE AND TRANSPORT FROM WASTE FACILITY 3W-1D

DISTRIBUTION OVER ENTIRE AREA AFTER 300 YEARS
 KD = 0.2 NODE AREA=10000 SQ FT.

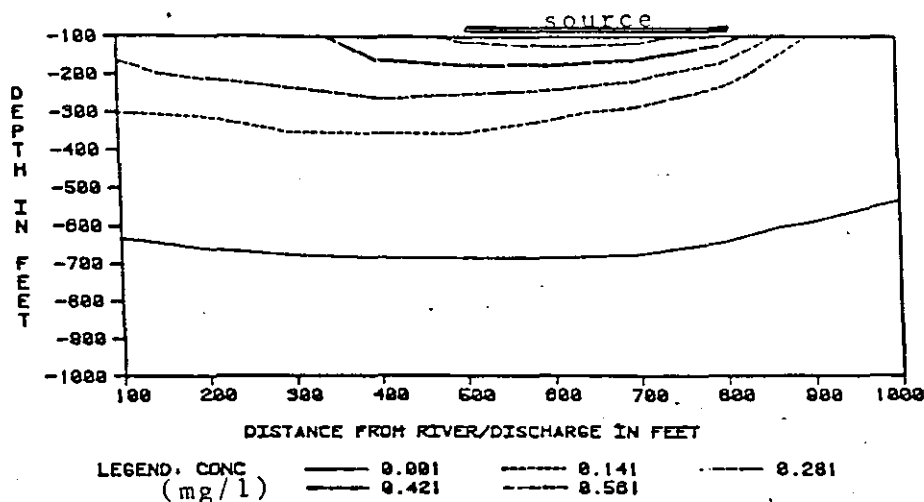


Figure 40. The Plume of the Case 3W-1D After 300 Years Simulation

LEACHATE FATE AND TRANSPORT FROM WASTE FACILITY 3W-2A

DISTRIBUTION OVER ENTIRE AREA AFTER 300 YEARS
 KD = 0.2 NODE AREA=10000 SQUARE FEET

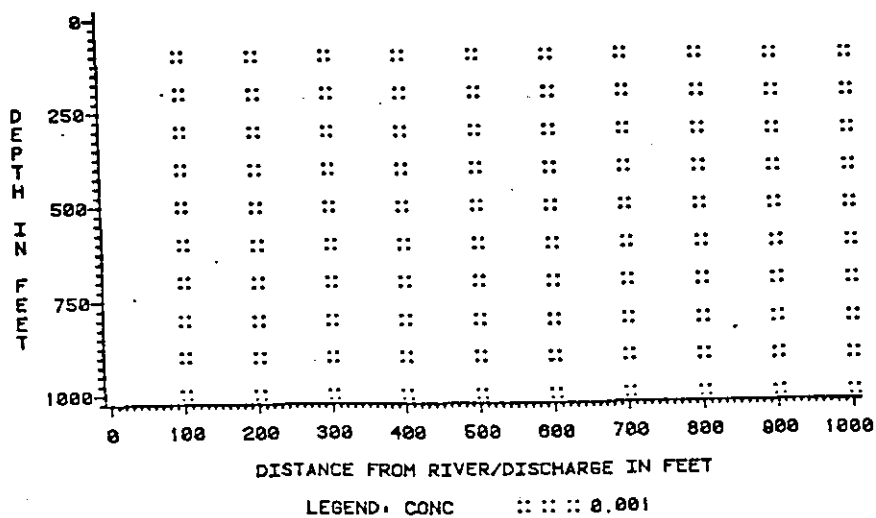


Figure 41. The Plume of the Case 3W-2A After 300 Years Simulation

LEACHATE FATE AND TRANSPORT FROM WASTE FACILITY 3W-2B

EQUIPOTENTIAL DISTRIBUTION IN FEET
 KD = 0.2 NODE AREA=10000 SQ FEET

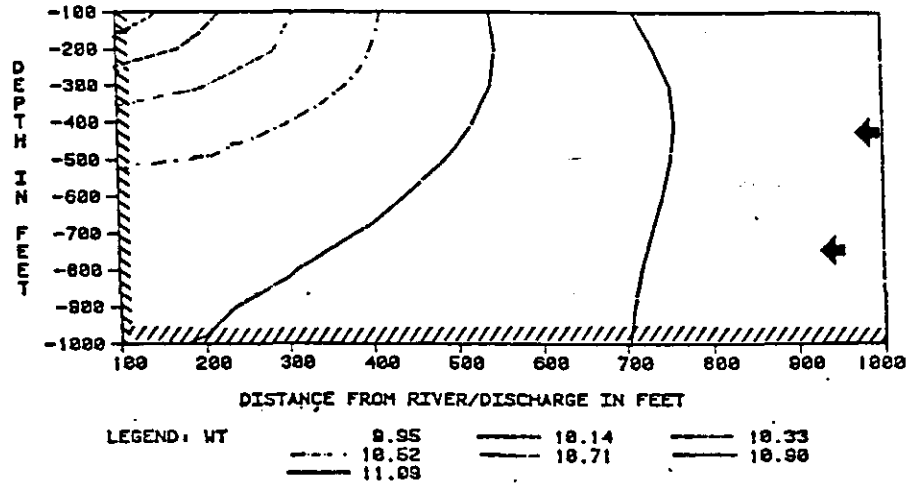


Figure 42. The Distribution of Equal-Potential Lines of 3W-2B Scenario

LEACHATE FATE AND TRANSPORT FROM WASTE FACILITY 3W-2B

DISTRIBUTION OVER ENTIRE AREA AFTER 50 YEARS
 KD = 0.2 NODE AREA=10000 SQ FEET

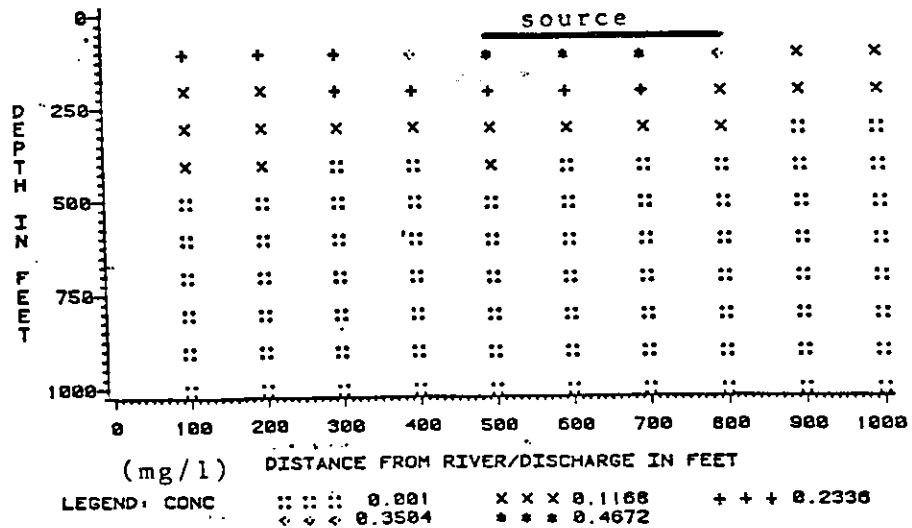


Figure 43. The Plume of Case 3W-2B After 50 Years Simulation

LEACHATE FATE AND TRANSPORT FROM WASTE FACILITY 3W-2B

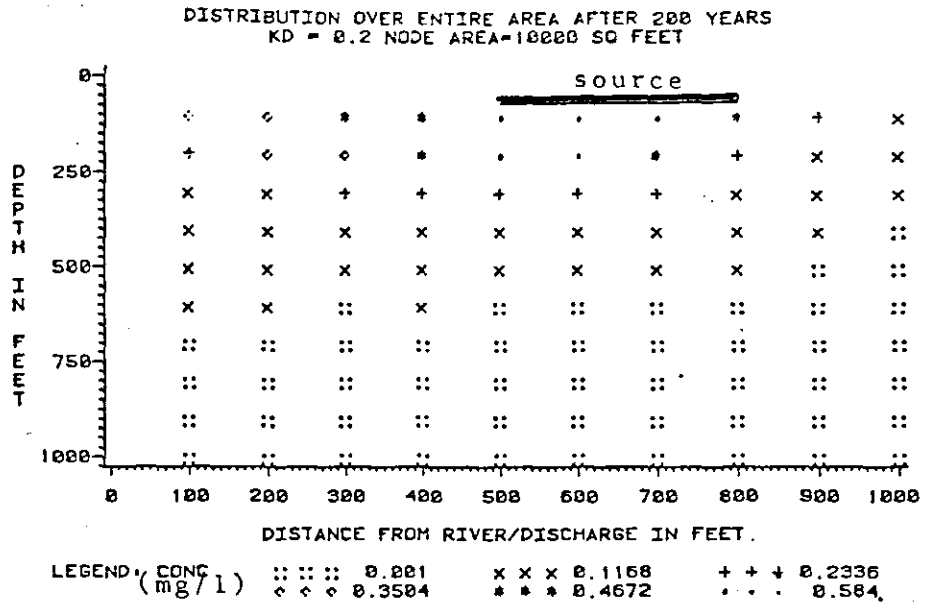


Figure 44. The Plume of Case 3W-2B After 200 Years Simulation

LEACHATE FATE AND TRANSPORT FROM WASTE FACILITY 3W-2C

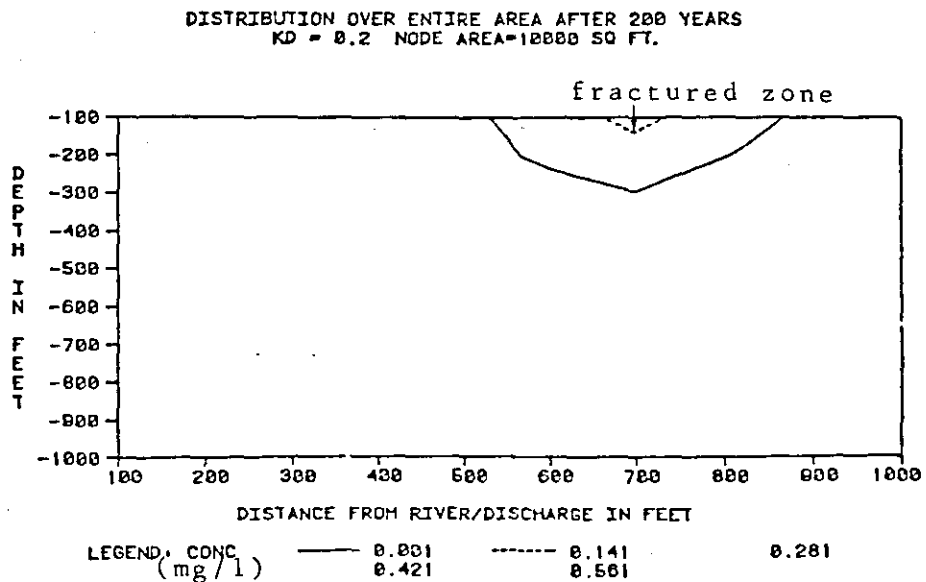


Figure 45. The Distribution of Equal-Potential Lines of 3W-3A Scenario

3W-3A. This is the result for the cross-sectional simulation of a three-layered aquifer. The highly permeable layer, which is located between two relatively low-permeability layers, is like a conduit to allow water to flow fast through it. Figure 47 shows the flow trend of ground water by drawing the equalpotential line.

3W-3B. These results present the three-layered case which the impermeable layer is located between two relatively high-permeability layers. The low-permeability layer stopped the ground-water flow (Figure 48) and leachate (Figure 49) downward at the middle of the aquifer. In other words, an aquitard between the two highly permeable layers is able to restrain the contaminants to the upper portion of the aquifer.

3W-4A. The ground water flow was faster in the inclined high-permeability aquifer than in the surrounding materials. This caused the equalpotential lines to bend toward the discharge point (Figure 50) and guide the contaminants to flow along this high permeability bed (Figure 51).

3W-5A. The high-permeability aquifer and the fault acted as the zone of high flow speed and caused the contaminants to leak into the aquifer. The plume developed along the fault zone with a downward movement (Figure 52).

LEACHATE FATE AND TRANSPORT FROM WASTE FACILITY 3W-2C

DISTRIBUTION OVER ENTIRE AREA AFTER 400 YEARS
 KD = 0.2 NODE AREA=10000 SQ FT

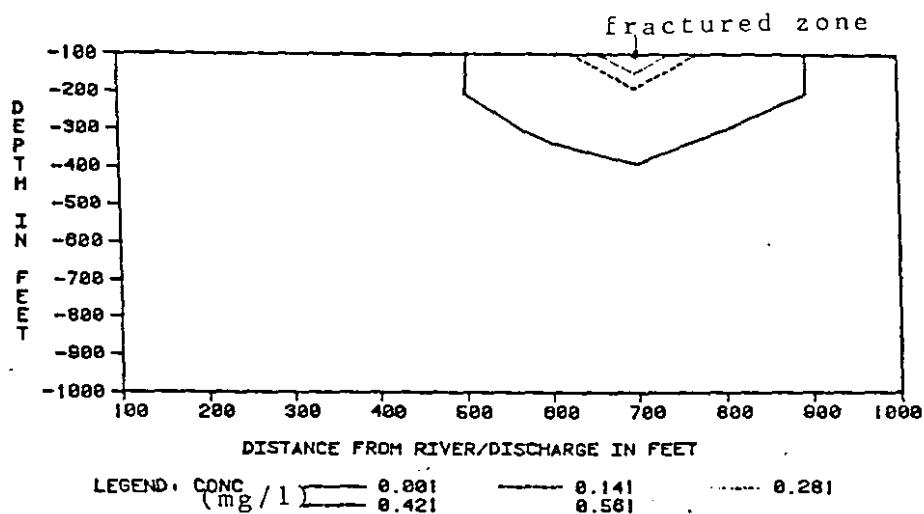


Figure 46. The Plume of Case 3W-2C After 200 Years Simulation

LEACHATE FATE AND TRANSPORT FROM WASTE FACILITY 3W-3A

EQUIPOTENTIAL DISTRIBUTION IN FEET
 KD = 0.2 NODE AREA = 10000 SQ FT
 AT 80 YEARS

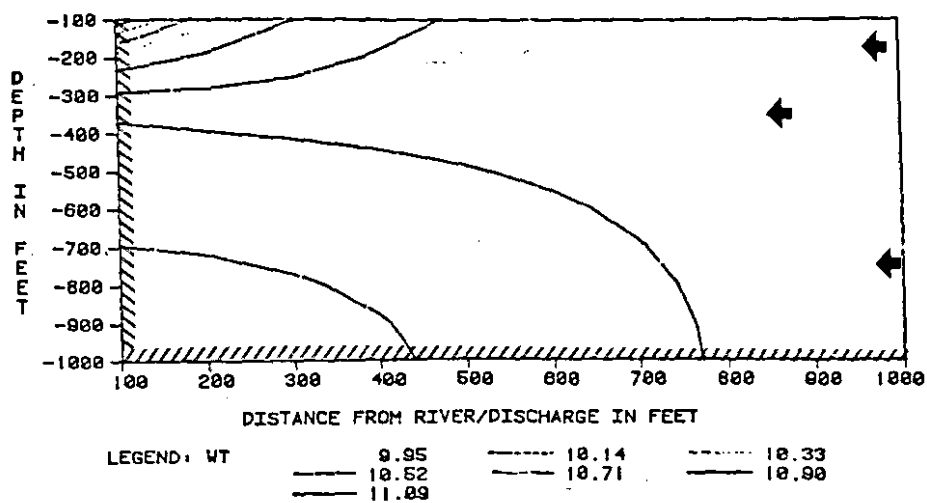


Figure 47. The Plume of Case 3W-2C After 400 Years

LEACHATE FATE AND TRANSPORT FROM WASTE FACILITY 3W-3B

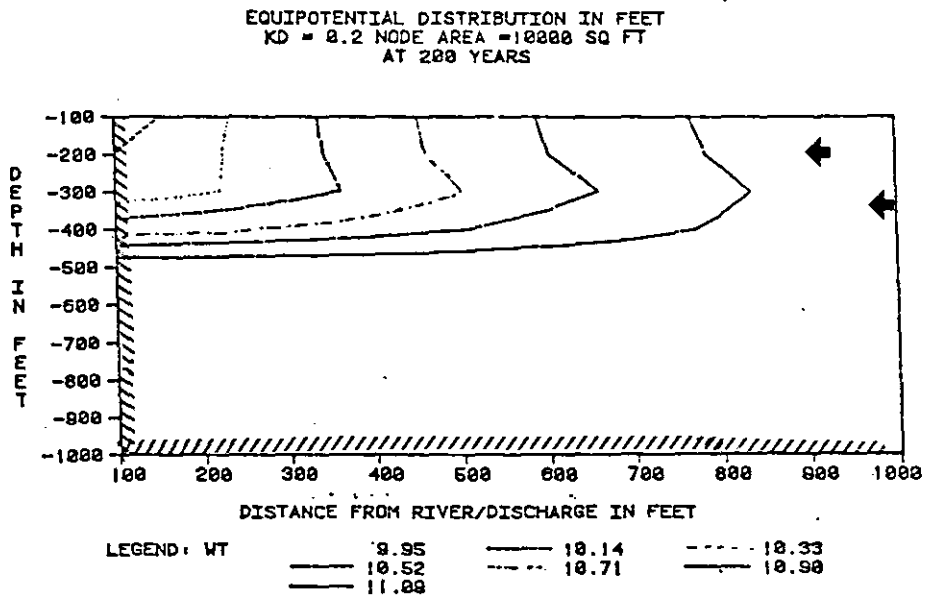


Figure 48. The Distribution of Equal-Potential Lines of Case 3W-3B

LEACHATE FATE AND TRANSPORT FROM WASTE FACILITY 3W-3B

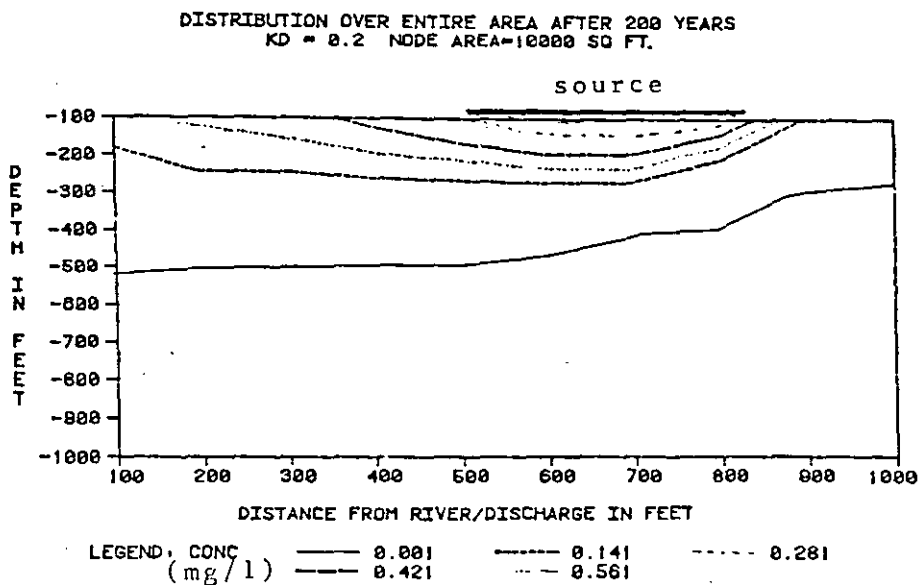


Figure 49. The Plume of Case 3W-3B After 200 Years

LEACHATE FATE AND TRANSPORT FROM WASTE FACILITY 3W-4A

EQUIPOTENTIAL DISTRIBUTION IN FEET
 KD = 0.2 NODE AREA = 10000 SQ FT

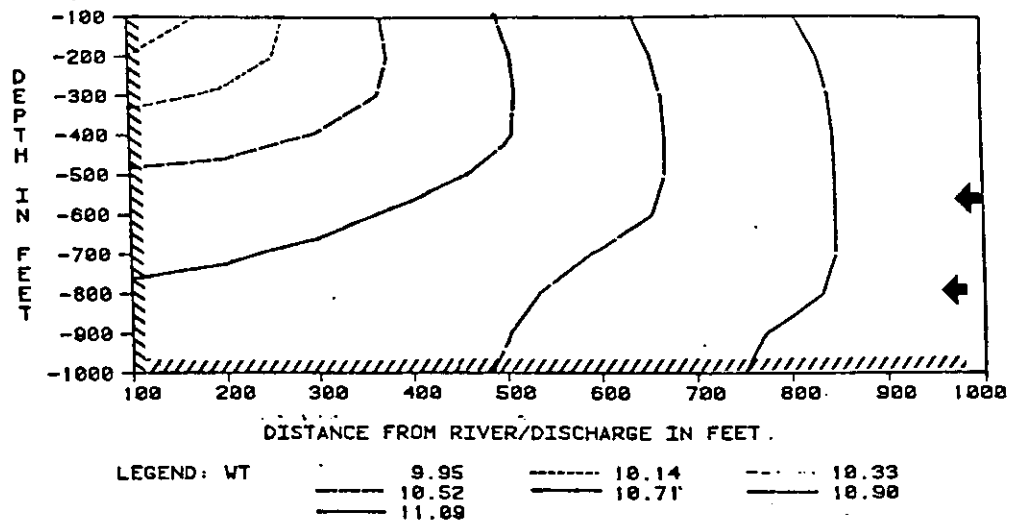


Figure 50. The Distribution of Equal-Potential Lines of Case 3W-4A

LEACHATE FATE AND TRANSPORT FROM WASTE FACILITY 3W-4A

DISTRIBUTION OVER ENTIRE AREA AFTER 200 YEARS
 KD = 0.2 NODE AREA = 10000 SQ FT.

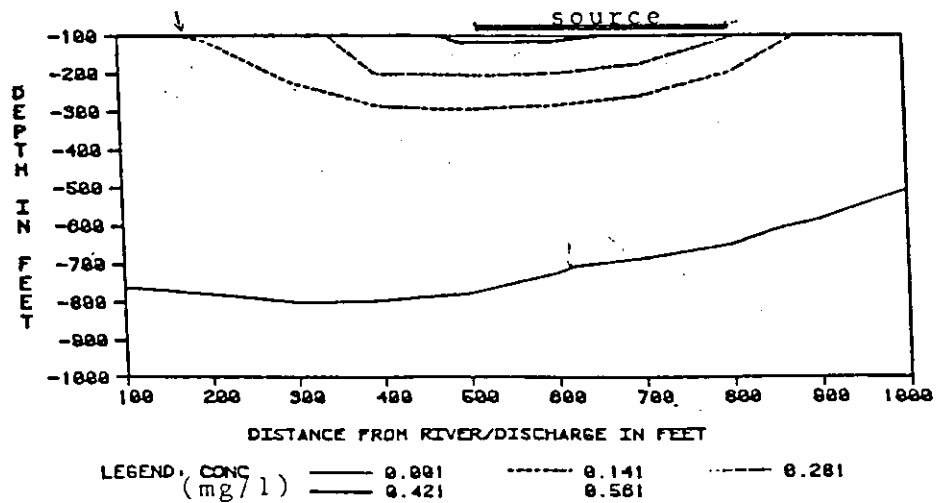


Figure 51. The Simulated Plume of Case 3W-4A (200 Years)

LEACHATE FATE AND TRANSPORT FROM WASTE FACILITY 3W-5A

DISTRIBUTION OVER ENTIRE AREA AFTER 400 YEARS
 KD = 0.2 NODE AREA=10000 SQ FT

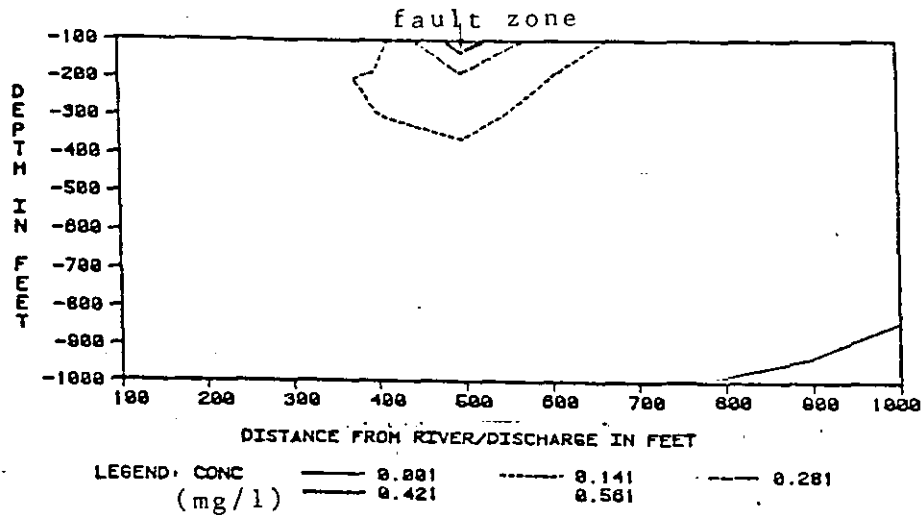


Figure 52. The Simulated Plume of Case 3W-5A (400 Years)

LEACHATE FATE AND TRANSPORT FROM WASTE FACILITY 3W-1C

DISTRIBUTION OVER ENTIRE AREA AFTER 300 YEARS
 KD = 0.2 NODE AREA=10000 SQ FT
 PLANAR VIEW

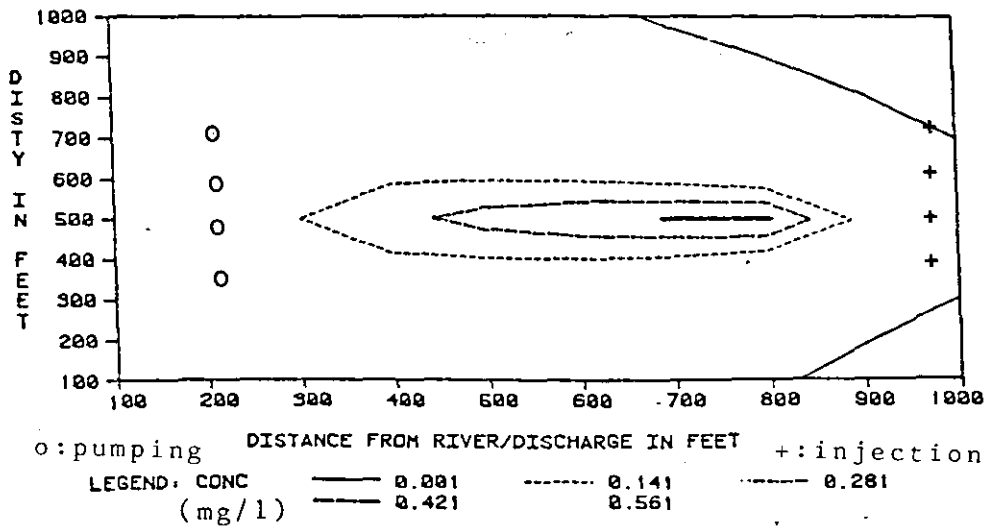


Figure 53. The Plume of Case 3W-1A with a Planar View at the Beginning of Aquifer Restoration

LEACHATE FATE AND TRANSPORT FROM WASTE FACILITY 3W-1C

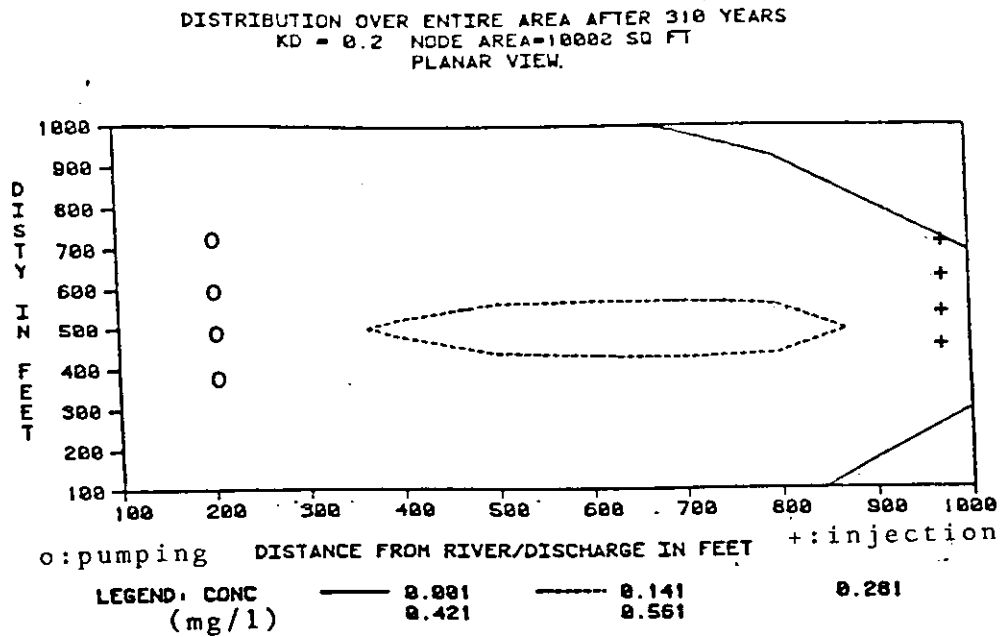


Figure 54. The Aquifer Restoration of Case 3W-1A After 10 Years Processing

LEACHATE FATE AND TRANSPORT FROM WASTE FACILITY 3W-1C

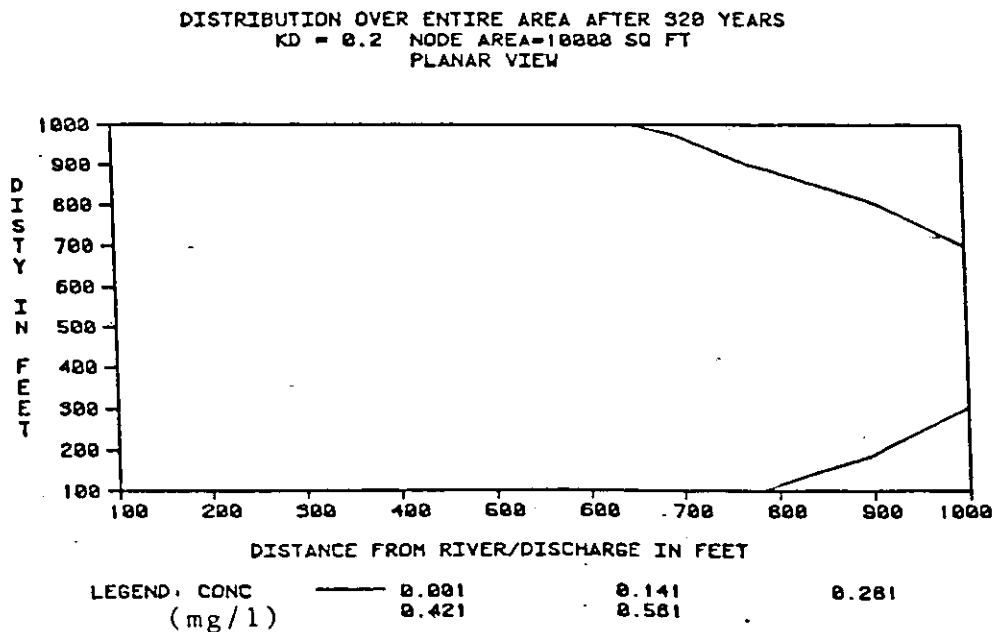


Figure 55. The Simulated Aquifer Restoration of Case 3W-1A After 20 Years Processing (Planar)

Cleanup

The cleanup case 3W-1C, which was run for a fifty year period in both the planar view (Figure 53 to Figure 55) and the cross-sectional view (Figure 56 to Figure 61), implies that the suggested cleanup method could possibly apply to the real world. The influences of equalpotential lines by the pumping and injection wells, during the cleanup period, are shown in Figure 62 and Figure 63.

LEACHATE FATE AND TRANSPORT FROM WASTE FACILITY 3W-1C

DISTRIBUTION OVER ENTIRE AREA AFTER 300 YEARS
 KD = 0.2 NODE AREA=10000 SQ FT.

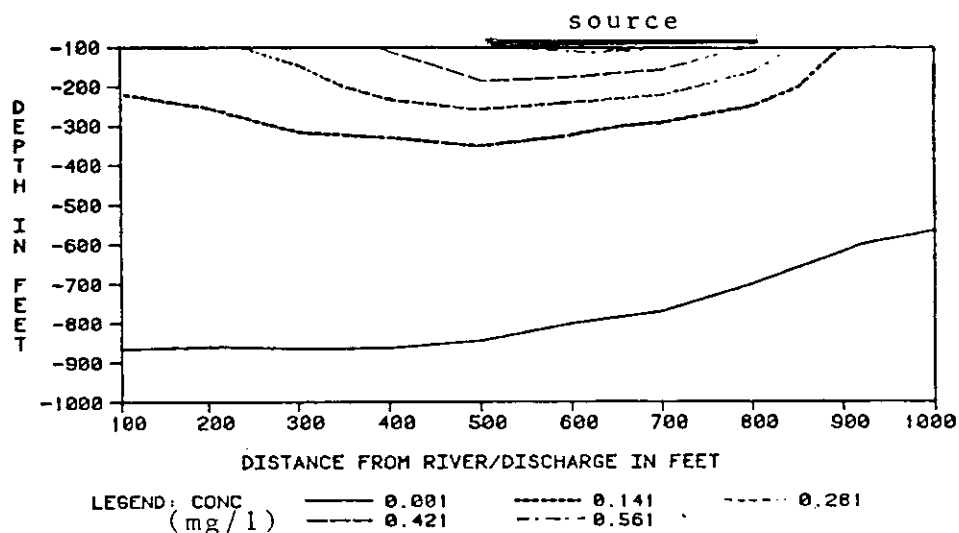


Figure 56. The Plume of Case 3W-1A at the Beginning of Aquifer Restoration (Cross-sectional View)

LEACHATE FATE AND TRANSPORT FROM WASTE FACILITY 3W-1C

DISTRIBUTION OVER ENTIRE AREA AFTER 310 YEARS
 KD = 0.2 NODE AREA=10000 SQ FT

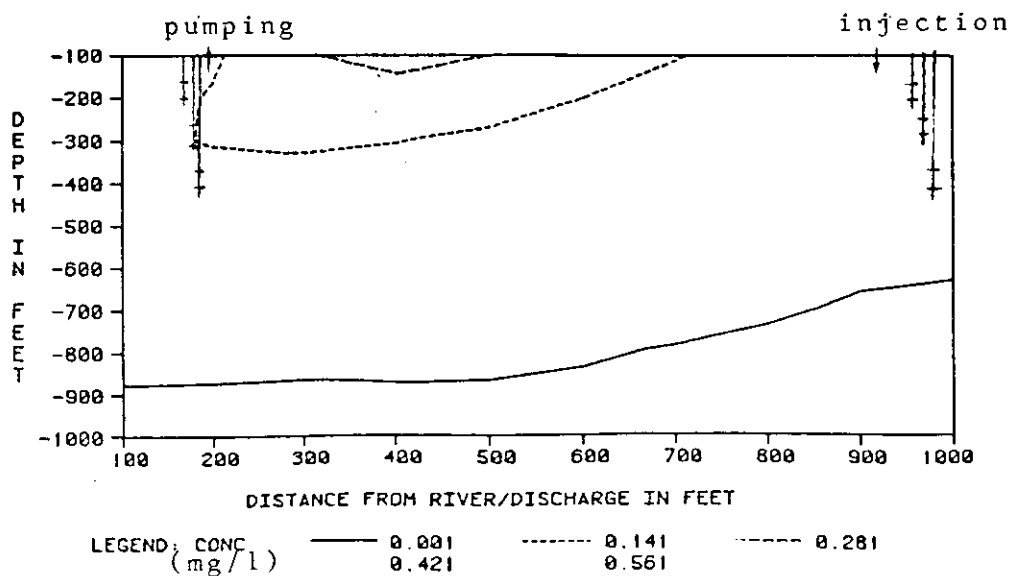


Figure 57. The Simulated Aquifer Restoration of Case 3W-1A with a Cross-sectional View (10 Years)

LEACHATE FATE AND TRANSPORT FROM WASTE FACILITY 3W-1C

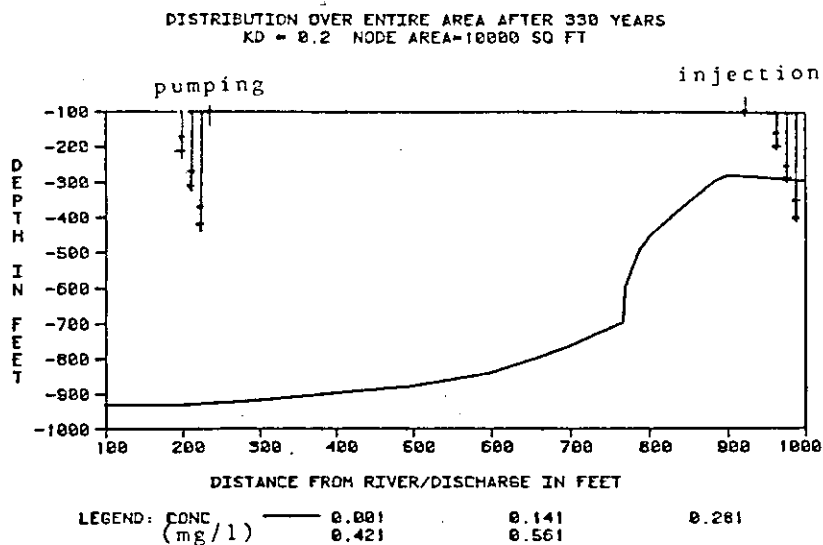


Figure 58. The Simulated Aquifer Restoration of Case 3W-1A With Cross-sectional View (30 Years)

LEACHATE FATE AND TRANSPORT FROM WASTE FACILITY 3W-1C

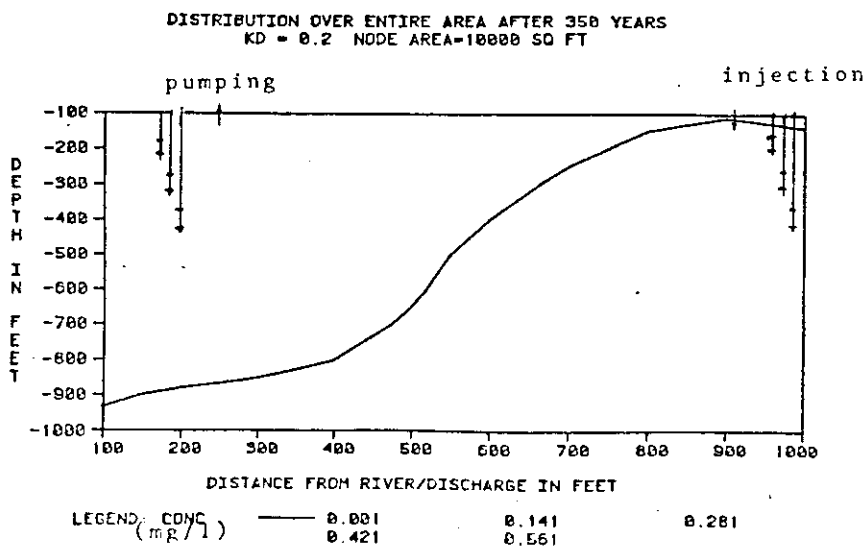


Figure 59. The Simulated Aquifer Restoration of Case 3W-1A with Cross-sectional View (50 Years)

LEACHATE FATE AND TRANSPORT FROM WASTE FACILITY 3W-1C

DISTRIBUTION OVER ENTIRE AREA AFTER 300 YEARS
 KD = 0.2 NODE AREA=10000 SQUARE FEET

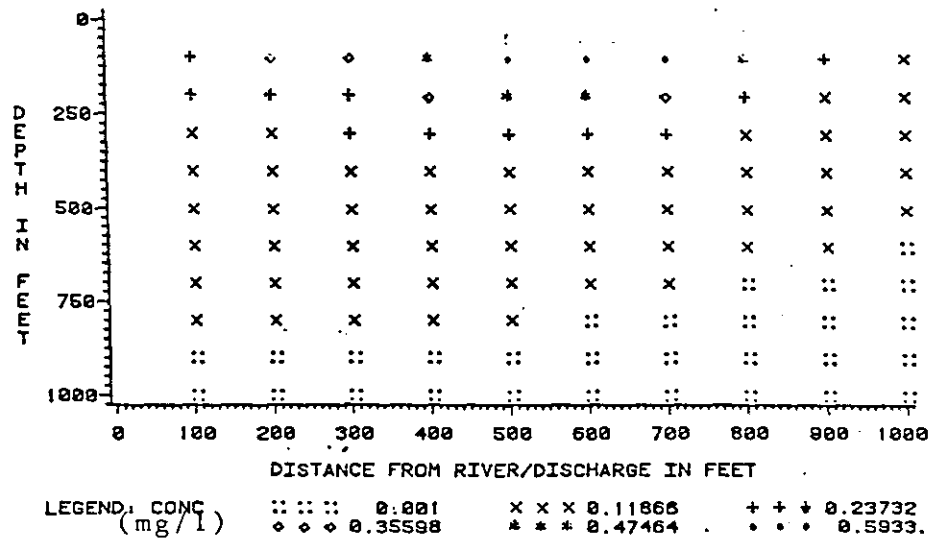


Figure 60. The Simulated Aquifer Restoration of Case 3W-1A with Pattern Plot (at Beginning)

LEACHATE FATE AND TRANSPORT FROM WASTE FACILITY 3W-1C

DISTRIBUTION OVER ENTIRE AREA AFTER 350 YEARS
 KD = 0.2 NODE AREA=10000 SQUARE FEET

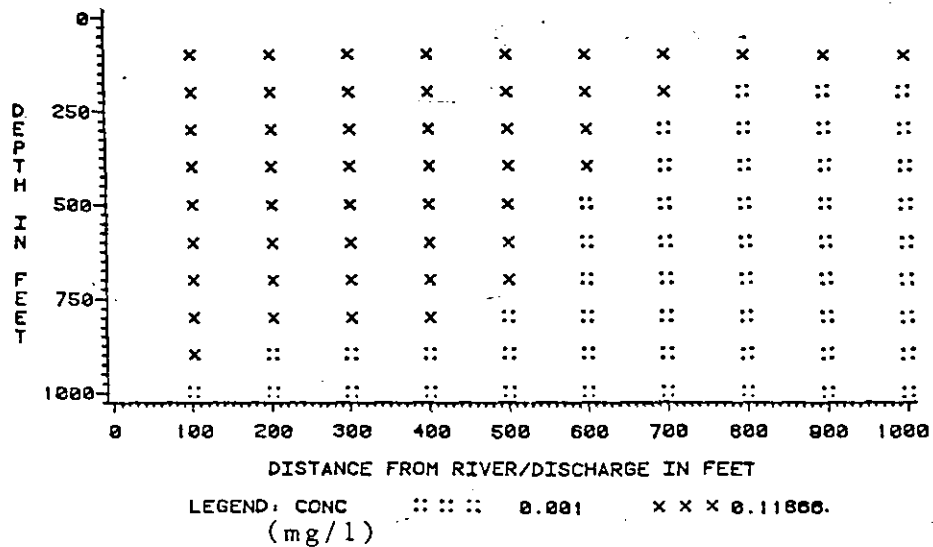


Figure 61. The Simulated Aquifer Restoration of Case 3W-1A with Pattern Plot (After 50 Years Process)

LEACHATE FATE AND TRANSPORT FROM WASTE FACILITY 3W-1C

EQUIPOTENTIAL DISTRIBUTION IN FEET
 KD = 0.2 NODE AREA = 10000 SQ FT
 AT 310 YEARS

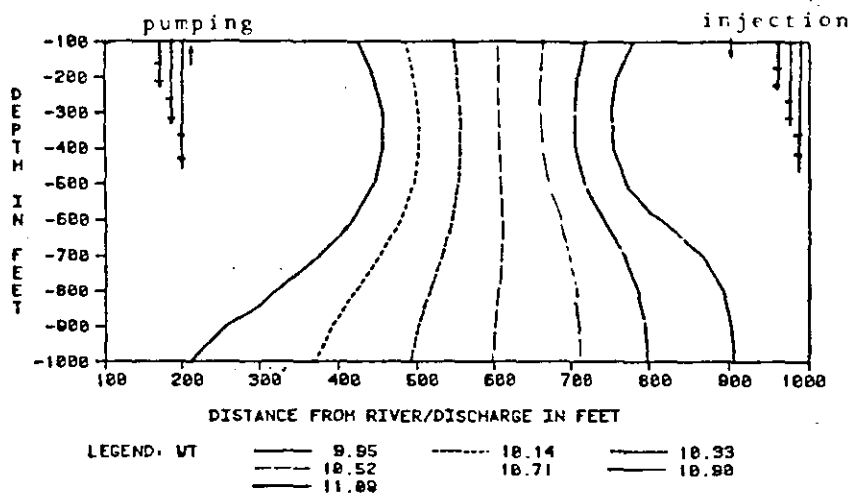


Figure 62. The Distribution of Equal-Potential Lines for Aquifer Restoration of Case 3W-1A

LEACHATE FATE AND TRANSPORT FROM WASTE FACILITY 3W-1C

EQUIPOTENTIAL DISTRIBUTION IN FEET
 KD = 0.2 NODE AREA = 10000 SQ FT
 AT 350 YEARS

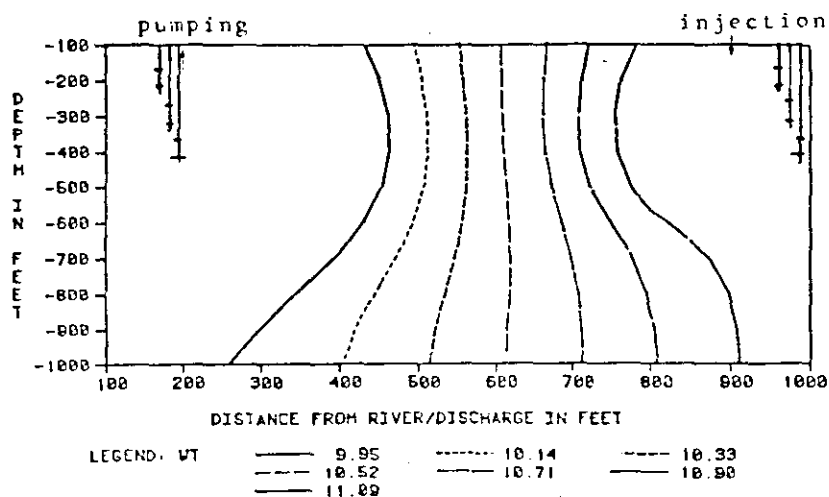


Figure 63. The Distribution of Equal-Potential Lines for Case 3W-1A (After 50 Years Restoration)

CHAPTER VI

EXISTING SITE APPLICATIONS

Babylon Landfill

The Babylon landfill site is located in the southern part of Long Island (Figure 2), and consists of a plain mantled by outwash deposits that are associated with the terminus of a Wisconsin glacial advance. The outwash plain has a porosity about 0.25, and averages about 90 feet in thickness. It is underlain by stratified sand containing some gravel. The ground-water flow rate was calculated at a velocity of 4 ft/day. The value of longitudinal dispersion of the Babylon plume is about 60 square feet/day by applying a dispersion model (Kimmel & Braids, 1980).

There are three refuse piles located on the Babylon site (Figure 64). These contain urban refuse, incinerated garbage, scavenger waste and some industrial refuse. The first pile was started in the early 1940's and since that time chemical substances have leached into the high permeability upper glacial aquifer.

The mean annual precipitation is 46 in/year; the recharge rate is estimated at 23 in/year. The downward migration of the leachate enriched water is retarded by an underlying aquitard. The width of the plume is 1900 feet at

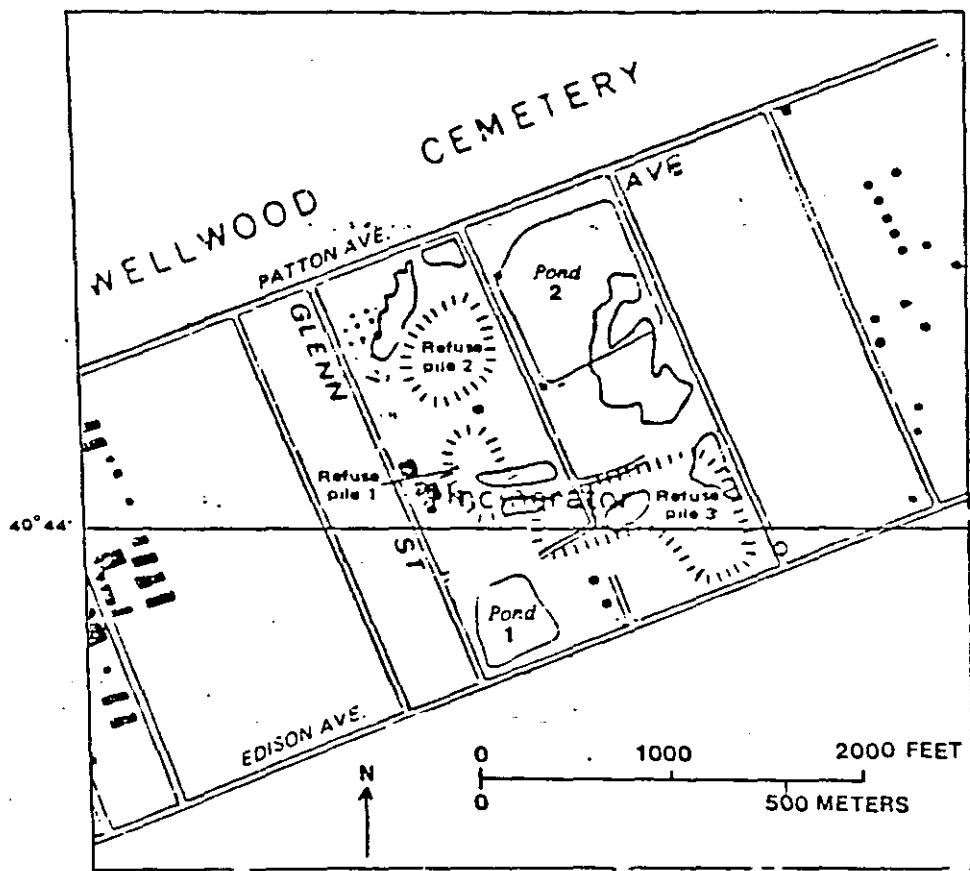


Figure 64. Location of Refuse Piles of the Babylon Site

the landfill, but narrows to 700 feet near its terminus which is 2 miles south of the landfill.

Climate

The Babylon landfill is in a continental, modified maritime climate. The mean annual temperature is 50 F inland, 52 F along the southern shore (Pluhowski and Kanthrowitz, 1964).

Land use

The landfill is surrounded by a light industrial park on the east and west sides and by a cemetery on the south side.

Geology

The Babylon landfill is located in the glacial region of the Atlantic Coastal Plain physiographic province (Figure 65 and Table VII).

General Geology

The formations are composed of a sequence of flat lying unconsolidated glacial materials that rest unconformably on consolidated strata that dip about 80 feet per mile to the southeast (Kimmel and Braids, 1980).

The bedrock underlying the Lloyd aquifer is schist and gneiss with granitic intrusions of Precambrian or early Paleozoic (?) age (Pluhowski and Kantrowitz, 1964).

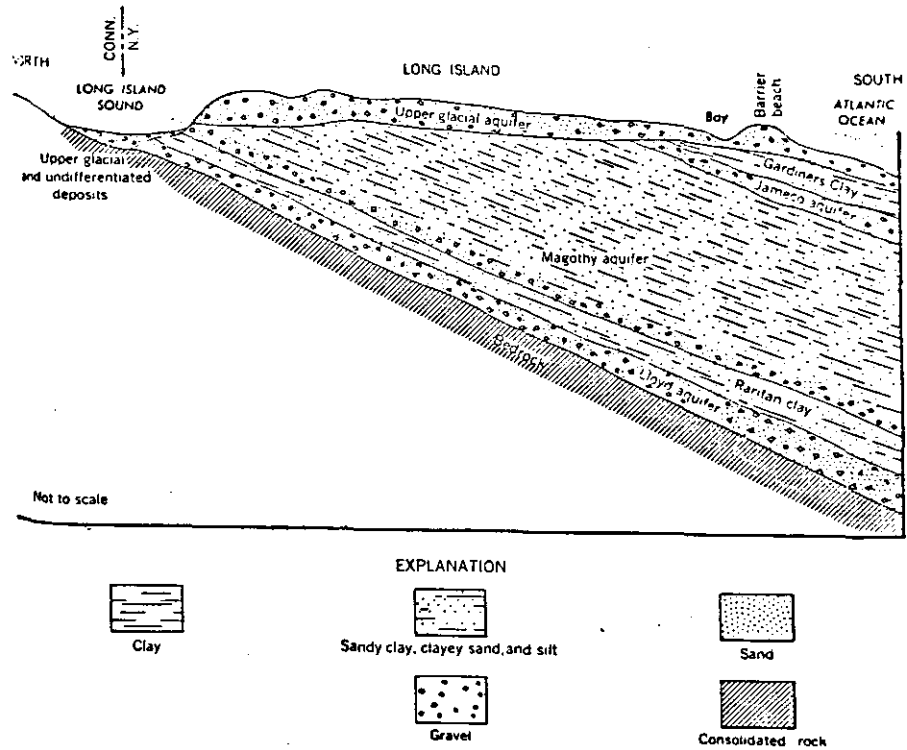


Figure 65. Geological Features of the Babylon Field
(After Pluhowski, 1964)

TABLE VII
SUMMARY OF STRATIGRAPHY OF THE BABYLON AREA

Era	Period	Epoch	Geologic unit	Remarks	
Cenozoic	Quaternary	Recent	Recent deposits	Stream, beach, and marsh deposits; small areal extent.	
		Pleistocene	Upper Pleistocene deposits	Till and outwash deposits of the Wisconsin Glaciation.	
			Gardiners Clay	Fossiliferous marine clay of probable Sangamon age.	
	Tertiary(?)	Pliocene(?)	Mannetto Gravel	Formerly believed to be an outwash deposit but now regarded as a stream-terrace deposit; small areal extent.	
Mesozoic	Cretaceous	Late Cretaceous	Magothy(?) Formation	Interbedded sand, silt, and clay.	
			Raritan Formation	Clay member	Dominantly clay but may contain some silty and sandy zones locally.
				Lloyd Sand Member	Sand, gravel, and interbedded clay and silt.
Precambrian and early Paleozoic(?)			Bedrock	Schist and gneiss containing some granitic intrusions.	

Aquifer Lithology

Raritan Formation. This formation includes two units, the lower Lloyd Sand member, which is predominantly light-colored sand, gravel, and interbedded clay and silt, and an upper multi-colored clay and silt member. The Lloyd sand ranges from 150 to 300 feet in thickness, which the upper member ranges from 170 to 300 feet in thickness (Pluhowski and Kantrowitz, 1964).

Magothy Formation. The Magothy consists of non-marine marine deposits of Cretaceous age. The lower part of this formation is composed of non-fossiliferous beds with lenses of gray and white fine sands, silty and clayey sands, and clay. The upper part of the formation consists of fossiliferous glauconitic clay with layers of lignite, pyrite, and iron concretions. It is about 800 to 1000 feet thick as shown in Figure 65 (Perlmutter and Geraghty, 1963).

Manetto Gravel. The Manetto Gravel is a stratified, crossbedded gravel that lays unconformably on the Magothy formation, Tertiary system. It is 90 feet thick and believed to be terrace deposits (Pluhowski and Kantrowitz, 1964).

Glacial Deposits. This is an aquifer about 90 feet thick which is the outwash deposits of stratified sands and gravel, terminal moraines and till lying unconformably on the Gardiners clay which is an under-lying aquitard

(Pluhowski and Kantrowitz, 1964).

This glacial deposit is the contaminated aquifer at the Babylon site (Figure 66). Thus, we used this formation to simulate the plume in this research.

Hydraulic Characteristics

Ground-water Table

The ground-water table is the upper boundary of the upper glacial aquifer, and it fluctuates throughout the year from 12 to 18 feet below the land surface. The gradient of the water table is about 0.0021 (Kimmel and Braids, 1980).

Porosity and Ground-water Velocity

Based on the material in the glacial aquifer, the effective porosity is assumed to be 0.25. The ground-water flow rate is calculated to be 4 ft/day (Kimmel and Braids, 1980).

Saturated Thickness

The glacial outwash deposits is about 90 feet thick, and about 75 feet is saturated (Figure 66).

Hydraulic Conductivity and Transmissivity

The studies of transmissivity at the Babylon site have been done by many investigators and the results are quite different. For instant, McClymonds and Frank (1972) calculated an average transmissivity value for upper glacial

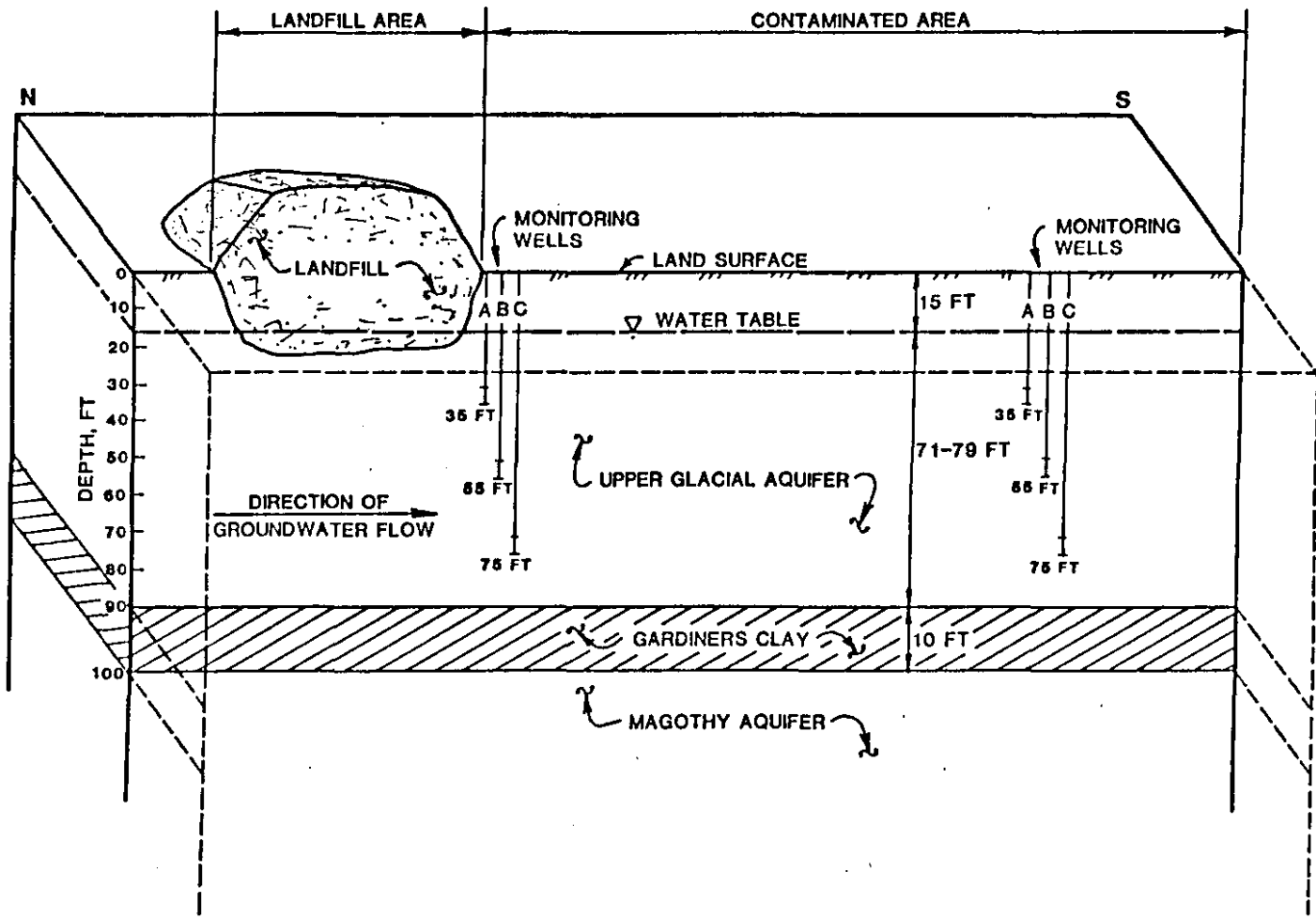


Figure 66. The Perspective View Of the Babylon Landfill

aquifer as 190,000 gpd/ft with a thickness of 100 feet of aquifer; using a thickness of 75 feet, the transmissivity at the site is computed to be 142,500 gpd/ft. This value was disputed by Kimmel and Braids (1980) who considered it to be too small and remarked that it could be reflecting screen losses or other losses due to variations in well construction.

The value of transmissivity used in this research is 280,500 gpd/ft (permeability = 500 ft/day) and is based on the aquifer tests by Kimmel and Braids (1980).

Dispersion Coefficient

The dispersion coefficient at the Babylon site was determined by applying the chloride concentration values in the deeper part of plume to the dispersion model. An initial chloride concentration of 200 mg/L was used, and an average dispersion coefficient of about 60 square feet/day is indicated (Ogata and Banks, 1961; Kimmel and Braids, 1980). This is the input dispersion coefficient value used for the selected models. It is close to the value of 100 square feet/day that was used (Pinder, 1973) for a contamination study in a nearby area.

Ground-Water Flow System

The aquifers described above, provide an extensive fresh ground-water reservoir and form a regional ground-water flow system. The upper glacial aquifer is recharged by

precipitation with a rate of 23 inches per year. Most of the recharge occurs during the cool and rainy season, February to June, when the evapotranspiration is not so large.

A small amount of shallow ground water discharges into a nearby stream, Santipoque Creek, which is about two miles south of the landfill. Most of the ground water in the upper glacial aquifer flow directly into the Great South Bay.

Native Ground-Water Quality

The native, fresh-uncontaminated, ground-water quality of the aquifer is good, with dissolved solids reported around 51 mg/L. The major cations are very low with their concentrations being about 10 mg/L (Kimmel and Braids, 1980).

The values for contained chemical species in unpolluted ground water in this area were useful for analyzing the plume. The contaminant plume in the study area is easily distinguished from the native ground water because the plume contains leachate which is high in total dissolved solids (TDS) and specific conductance.

Calibration of the Model

From the previous studies, there are two possible reasons for the highest leachate enrichment to have accumulated at the bottom of the aquifer beneath the Babylon landfill. The main probable reason is that the heavier, leachate-rich water sinks by gravity as it moves out of the

refuse. The other probable reason is that the landfill surfaces are more permeable than the surrounding area; the recharge rate at the landfill is probably greater than the annual average of 23 inches in the surrounding region (Kimmel and Braids, 1980).

Even though the infiltration of precipitation downgradient from the landfill is sufficient, the water-table contours give no evidence that the regional flow is disturbed by the inflow of leachate at the landfill. Thus, based on the fact that water with a high dissolved-solids content is more dense than water of the same temperature with a low dissolved-solids concentration (De Laguna, 1966), and based on a comparison of the physical characteristics of leachate-enriched ground water with those of ambient water, it seems likely that the downward movement of leachate results due to its greater density.

It is assumed that the leachate flows out of the landfill as pulsations of high-density fluid after periods of recharge, and moves diagonally as pockets or slugs, downward to the bottom of the aquifer (Figure 67). The vertical movement is more rapid than the horizontal flow due to the density of the plume; otherwise, the slugs would not reach the bottom of the aquifer beneath the landfill and would be strung out downgradient from it (Kimmel and Braids, 1980). This downward movement is also likely to be enhanced by surface recharge down gradient from the site.

The leachate-rich water sinks to the bottom of the

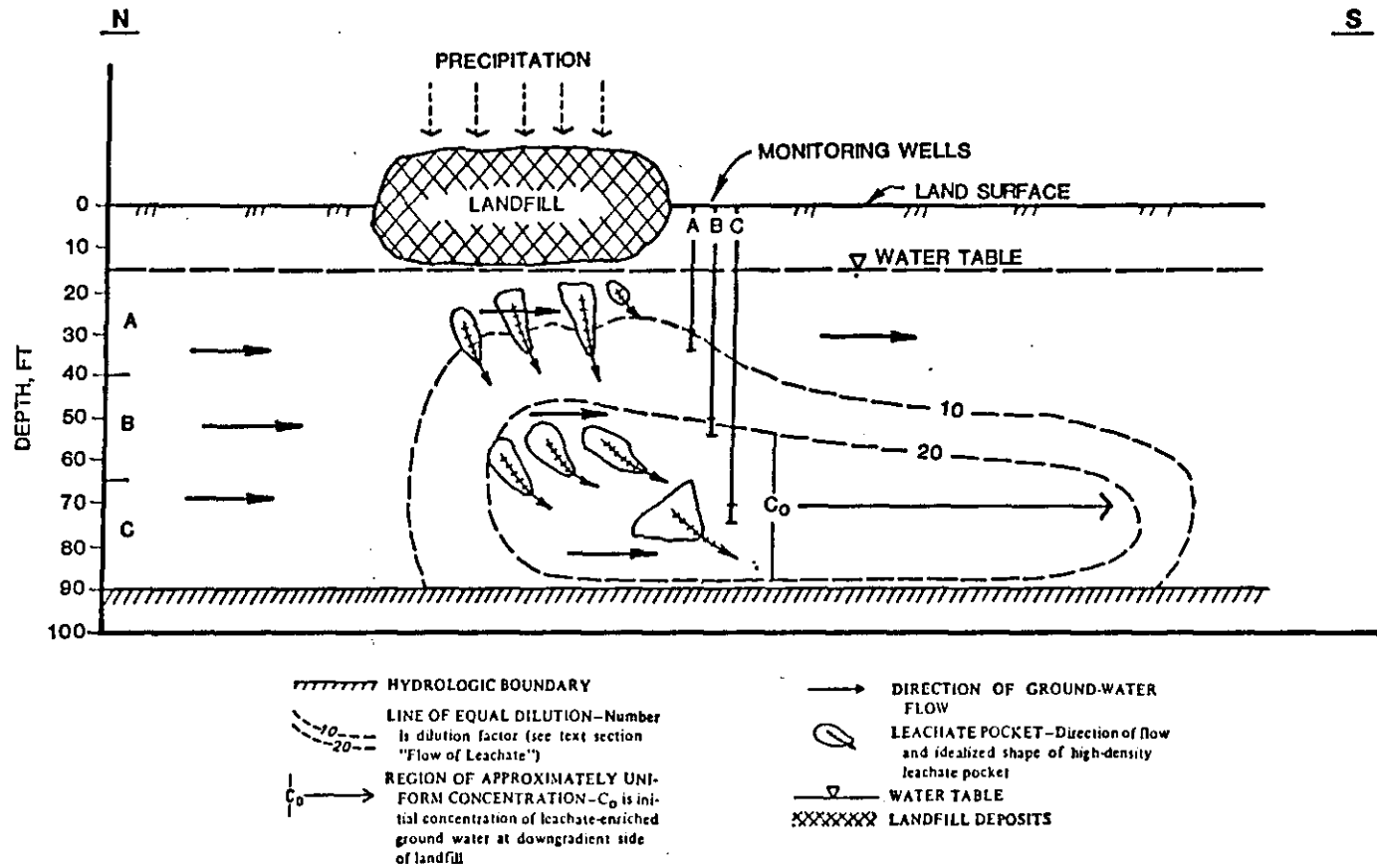


Figure 67. Leachate Movement and Dispersion in Ground Water Beneath the Babylon Landfill (After Kimmel 1980)

aquifer beneath the landfill only, and the concentration of leachate in the plume varies with depth and distance from the refuse pile. Therefore, two separate areas were considered for simulation of the Babylon site. One is the landfill and the other is the contaminated area (Figure 68). After the leachate starts to flow away from the landfill margine, the contaminants of level A, level B and level C will not intermix to any large extent due to the fact that the anisotropic transmissivity hinders the vertical movement. Thus, the concentrations of chloride at different depths in the landfill will be the initial concentrations for the correspondant depth of the contaminated area. The lower concentrations in level A are probably due in part to the surface recharge.

The boundary and initial conditions for the cross-sectional simulation are set by placing the different initial concentrations at the certain depth intervals using hypothetical injection wells, which were created for introducing flow of contaminated water and contaminants into the ground-water flow system. The B level is selected for the planar simulation due to 1) more available data and 2) ideal distribution of the locations of the monitoring wells (level B).

Source Injected Rate Calibration

The simulations of the Babylon site are based on the concentration from the wells that are located very close to

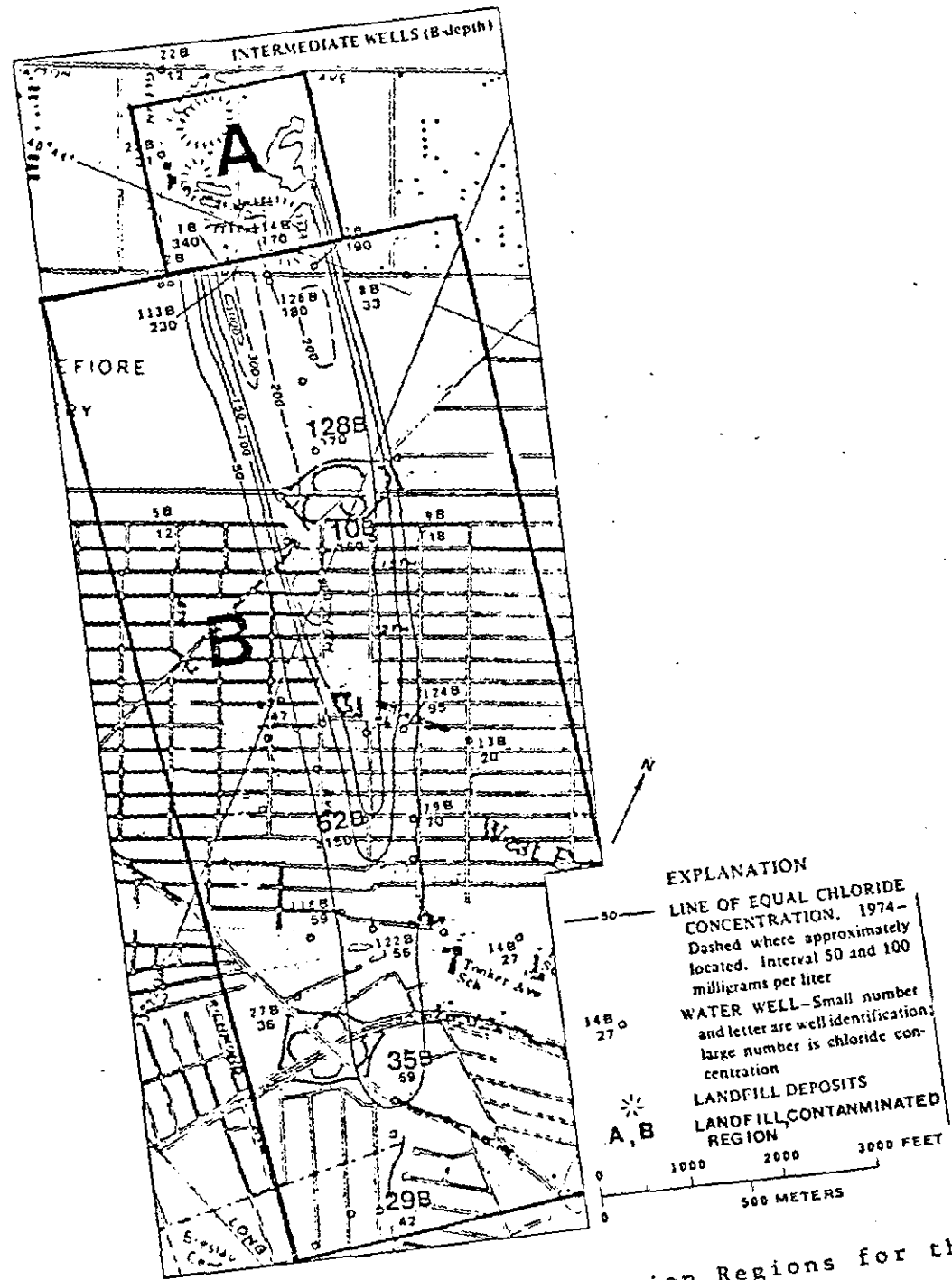


Figure 68. Two Designed Simulation Regions for the Babylon Landfill

the landfill, such as observation well # 1, #114, and #3 (Figure 68). All wells used for calibration are approximately 600 feet downgradient from the center of the landfill (Figure 68). For instance, the concentrations of these wells reflect the amount of contaminants that flowed to the observed points 600 feet downgradient from the source where the leachate was leached into the ground water over five months. Chloride is used as the indicator because it is one of the most conservative elements in ground-water flow systems. Therefore, the concentration of chloride at wells of #1, #114 and #3 can be used to back calculate the concentration of chloride of the source.

Plume Calibration

The measured chloride data of 1972 to 1974 (Kimmel and Braids, 1980), 1975 to 1977 (Cleary, 1978), and 1981 to 1982 (Geraghty and Miller, 1983) of the Babylon site were selected. It was also reported by Geraghty and Miller (1983) that the plume had been at steady state since 1972. Thus, the averaged data of chloride (1972 to 1982) can be applied as the base for updated calibrations and simulations.

The data for three levels were plotted and contoured (Figure 69). Based on the previously stated reasons, level B was used for the planar simulations. Six monitoring wells (#29, #35, #62, #10, #128 and #125) were used as control points for calibration (Figure 68) for the planar simulations. The monitoring wells on the centerline of the

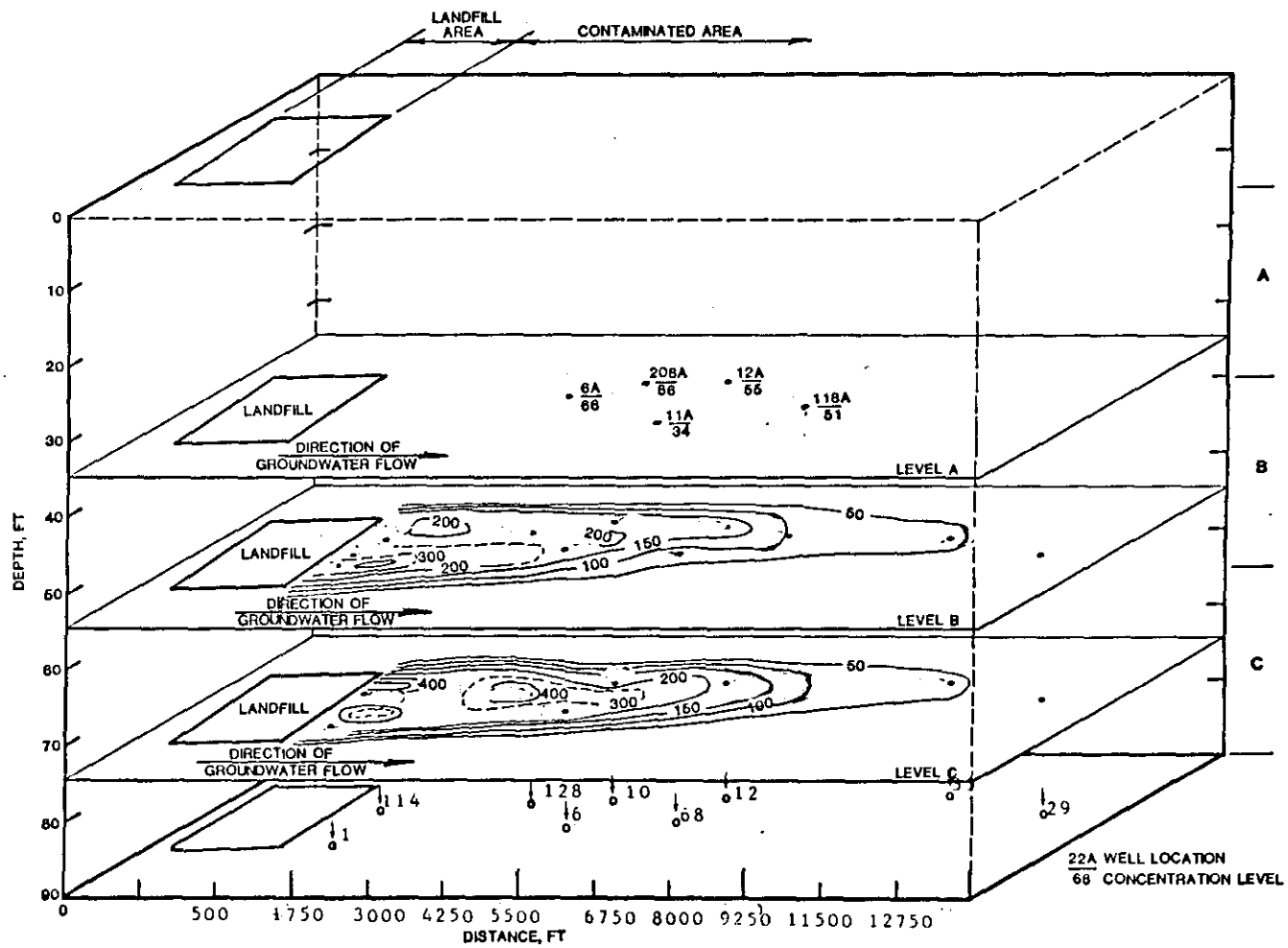


Figure 69. The Perspective View of the Babylon Plume in Three Layers

west branch were used as a calibration tool for the cross-sectional simulations. The measured chloride data were plotted and contoured in Figure 70.

Analytical Model

Cross-sectional. The region for cross-sectional simulation is defined by a 22 by 4 matrix with an x-direction from 0 to 11000 feet (500 ft interval) and a z-direction from 0 to 100 feet (25 ft interval). Three injection wells were used as the sources at different levels of depth to simulate the plume flow into the contaminated area from the landfill.

The initial concentration is unknown; the volume flow rate is calculated as (Equation VI-1):

$$\begin{aligned} Q &= K I A \\ &= (500)(\text{ft}/\text{day})(0.0018)(25)(\text{ft}^2) \\ &= 9(\text{ft}^3/\text{day}). \end{aligned}$$

As in the planar analysis, the calibration is mainly for initial concentration and the time of slug entrance times.

The input data set is listed in Table VIII.

Planar. The grid map for this analysis is set by $x=0$ to 11,000 ft with an interval of 500 ft and $y=250$ ft (left) to 2,250 ft (right) with an interval of 250 ft. The level B was applied for a forty-year period simulation with a 25 foot thickness. A dispersion coefficient of 60 square

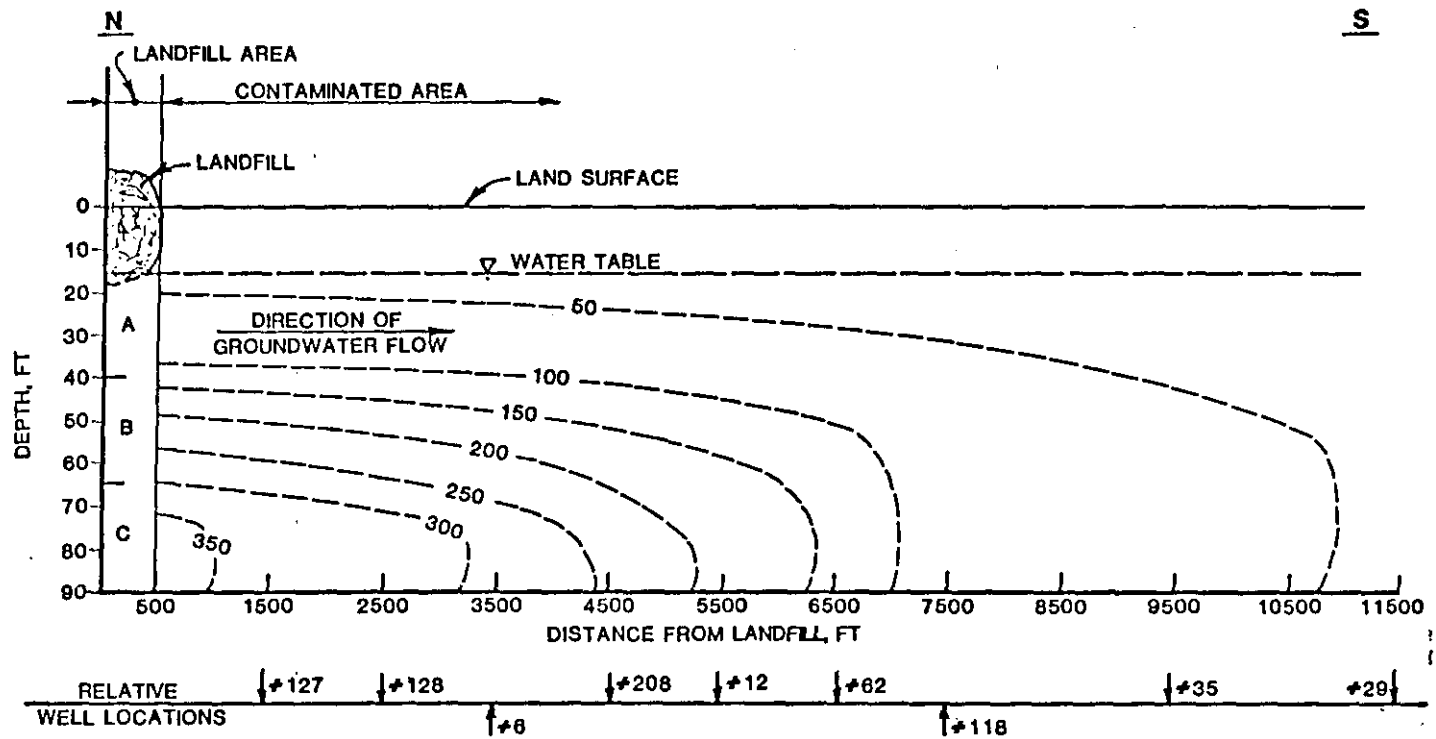


Figure 70. The Cross-sectional View of the Babylon Plume
(Base on The Averaged Measured data 1972-1982)

feet/sec for x-direction and a ratio of 5 for D_x/D_y were used. As to radioactivity and adsorption, the value for retardation is 1 and the value for decay is 0. The multiple sources, for a non-point source, are located at $x=450$ to 550 feet and $y=750$ to 1,250 feet, whereas the location for a point source is at $x=500$ and $y=1,500$ feet. There are two unknown and critical parameters for this Babylon landfill simulation: the mass flow rate and the time the slugs entered the saturated zone.

The mass flow rate (QCo) is calculated as:

$$\begin{aligned} QCo &= (Q)(Co) \\ &= (K)(I)(A)(Co) \end{aligned} \quad (VI-1)$$

in which

Q = volume flow rate	(L ³ /T)
Co = initial source concentration	(M/L ³)
K = permeability	(L ² /T)
I = gradient of ground water flow	(*)
A = cross-sectional area.	(L ²)

The initial source concentration (Co) is the only unknown parameter which affects the simulation in equation VI-1. Therefore, the calibration of the initial source concentration (Co) and the slug' entrance time is the main effort for this simulation.

The input data set is listed in Table IX.

Numerical Model

TABLE VIII
INPUT DATA SET OF THE ANALYTICAL MODEL OF
THE BABYLON SITE (PLANAR)

THE ANALYTICAL SIMULATION OF THE BABYLON LANDFILL THE INPUT DATA SET PLANAR VIEW					
THICKNESS	=	25.0000	FT		
POROSITY	=	0.250000			
VELOCITY	=	3.60000	FT/D		
X DISPERSION	=	60.0000	FT ² /D		
Y DISPERSION	=	12.0000	FT ² /D		
RETARDATION	=	1.00000			
DECAY GAMMA	=	1.00000			
X LOCATION (FT)	Y LOCATION (FT)	AREA (FT ²)	START TIME (DAYS)	VOLUME FLOW RATE (FT ³ /D)	SOURCE CONCENTR. (MG/L)
500.000	1500.00	0.000000E+00	0.000000E+00	3125.00	120.000
500.000	1500.00	0.000000E+00	9125.00	3125.00	140.000
500.000	1500.00	0.000000E+00	9855.00	3125.00	270.000
500.000	1500.00	0.000000E+00	10200.0	3125.00	180.000
500.000	1500.00	0.000000E+00	12690.0	3125.00	300.000
450.000	750.000	50000.0	0.000000E+00	12500.0	50.0000
550.000	1250.00				
450.000	750.000	50000.0	9125.00	12500.0	120.000
450.000	750.000	50000.0	9855.00	12500.0	70.0000
450.000	750.000	50000.0	10200.0	12500.0	62.0000
450.000	750.000	50000.0	12890.0	12500.0	169.000

TABLE IX
INPUT DATA SET OF THE ANALYTICAL MODEL OF THE
BABYLON SITE (CROSS-SECTIONAL)

THE BABYLON CASE FOR THE ANALYTICAL MODEL THE INPUT DATA SET CROSS-SECTIONAL VIEW					
THICKNESS	=	1.00000	FT		
POROSITY	=	0.250000			
VELOCITY	=	3.60000	FT/D		
X DISPERSION	=	60.0000	FT ² /D		
Y DISPERSION	=	1.20000	FT ² /D		
RETARDATION	=	1.00000			
DECAY GAMMA	=	1.00000			
X LOCATION (FT)	Y LOCATION (FT)	AREA (FT ²)	START TIME (DAYS)	VOLUME FLDW RATE (FT ³ /D)	SOURCE CONCENTR. (MG/L)
0.000000E+00	75.0000	0.000000E+00	0.000000E+00	22.3600	30.0000
0.000000E+00	75.0000	0.000000E+00	9130.00	22.3600	70.0000
0.000000E+00	75.0000	0.000000E+00	12415.0	22.3600	40.0000
0.000000E+00	50.0000	0.000000E+00	0.000000E+00	22.3600	60.0000
0.000000E+00	50.0000	0.000000E+00	9130.00	22.3600	320.000
0.000000E+00	50.0000	0.000000E+00	12415.0	22.3600	410.000
0.000000E+00	25.0000	0.000000E+00	0.000000E+00	22.3600	40.0000
0.000000E+00	25.0000	0.000000E+00	9130.00	22.3600	85.0000
0.000000E+00	25.0000	0.000000E+00	12415.0	22.3600	370.000

Both the planar and the cross-sectional analysis of the numerical simulation are for a forty years period with four pumping steps applied to the Babylon site. Based on the data of the water table in 1977, the gradient of ground water is 0.0018, and the seepage velocity is calculated as:

$$\begin{aligned}
 V_s &= \frac{K I}{n} && \text{(VI- 2)} \\
 &= (500)(\text{ft/day})(.0018)/(.25) \\
 &= 3.6 \text{ (ft/day)}
 \end{aligned}$$

in which

$$\begin{aligned}
 V_s &= \text{seepage velocity} && \text{(L/T)} \\
 I &= \text{gradient of ground water flow} && (*) \\
 n &= \text{effective porosity.} && (*)
 \end{aligned}$$

The dispersivity (BETA) is 17 ft which is derived from equation III-1.1 based on a value of 60 square feet/day for the dispersion coefficient at the Babylon site. The convergence criteria (TOL) is set as 0.01 for calculation.

Cross-sectional. The region for cross-sectional analysis was defined by a 27 (x-direction 500 ft/node) by 10 (z-direction 10 ft/node) matrix. The contaminated source was introduced by seven hypothetical injection wells located along column 3 at different depths (Figure 71). The injection rate for each well is derived from equation VI-1 shown as:

$$Q = K I A$$

$$\begin{aligned}
 &= (500)(\text{ft}/\text{day})(0.0018)(10 \text{ ft}^2) \\
 &= 9(\text{ft}^3/\text{day}) \\
 &= 0.000104(\text{ft}^3/\text{sec})
 \end{aligned}$$

As in the planar simulations, the initial concentration and its entrance time steps played the major role for cross-sectional simulation. In order to restrict the plume flows to follow the horizontal orientation, the ratio for transmissivity T_z/T_x and dispersivity z/x were set as 0.02 (1/50).

As to the cleanup simulation for the cross-sectional view, thirty-five wells were used as two ground-water restoration sets for this work (Figure 72).

The input data sets are listed in Appendix F.

Planar. To specify the area of the Babylon site for the Konikow model, an 18 by 31 matrix (500 ft/node) was used with a constant head boundary condition and a ground-water table matrix (Figure 73). The B level was simulated with a 25 feet thickness and the contaminated source was introduced by three injection wells located at nodes (9,4), (10,4) and (11,4); and the injection rate for each well was calculated from equation VI-1 as:

$$\begin{aligned}
 Q &= K I A \\
 &= (500)(\text{ft}/\text{day})(0.0018)(12500\text{ft}^2) \\
 &= 11250(\text{ft}^3/\text{day}) \\
 &= 0.13(\text{ft}^3/\text{sec})
 \end{aligned}$$

Because the initial concentration is unknown, the main

parameters for plume simulation are the source concentrations which were introduced into the flow system by calibrating the pumping period and time steps. The retardation constant is 1 and the dispersion ratio of D_y/D_x is 0.2.

The cleanup simulation was set by installing twenty additional injection and pumping wells as two ground-water cleanup sets (Figure 74). At the same time, the contaminant sources were shut off. The discharge and recharge rate for the cleanup wells were designed to maintain the balance of the flow system.

The input data sets are listed in Appendix F.

Results

Analytical Model

The result of the cross-sectional simulation is shown in Figure 75. The measured and simulated values from the four monitoration wells are compared in Table X.

The results of the shape and the concentration of the plume, which is from the planar simulation (Figure 76), is similar to the contour map of measured data (Figure 68). Table X also lists the comparison error between the simulated data and measured data by using six monitoring wells.

Numerical Model

The results of the cross-sectional simulation are shown in Figure 77, and Figure 70 is the comparison of the

THE LEACHATE FATE AND TRANSPORT OF THE BABYLON SITE

THE ANALYTICAL SIMULATION
THE CROSS-SECTIONAL VIEW
AT 200 YEARS

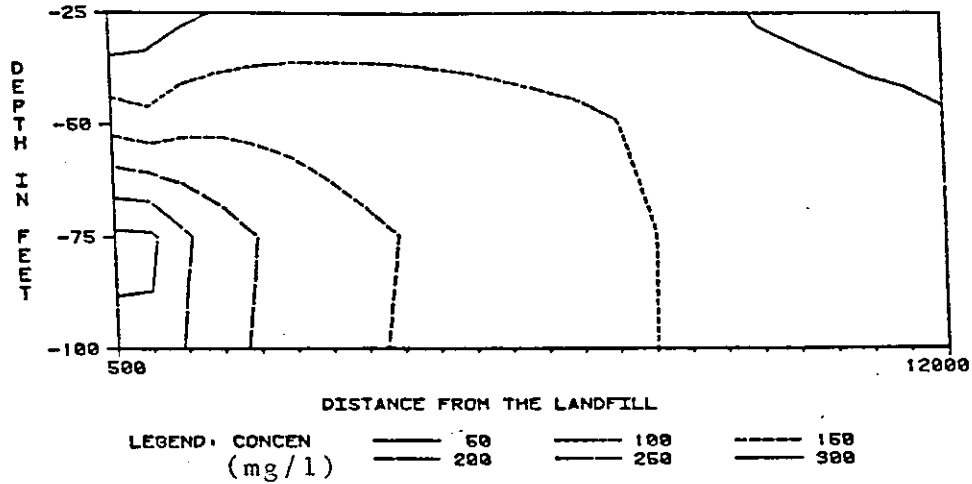


Figure 75. The Simulated Plume of the Babylon Site with a Cross-sectional View (Analytical Model)

THE LEACHATE FATE AND TRANSPORT OF BABYLON SITE

THE ANALYTICAL SIMULATION
THE PLANAR VIEW
AT 200 YEARS

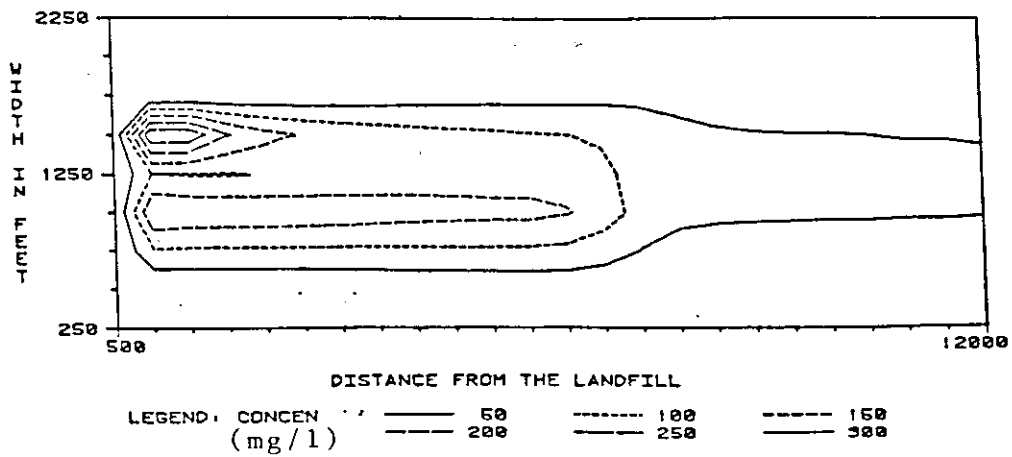


Figure 76. The Simulated Plume of the Babylon Site with a Planar View (Analytical Model)

TABLE X

THE COMPARISON BETWEEN THE MEASURED VALUES AND THE SIMULATED RESULTS

SIMULATION RESULTS Well No.	PLANAR							CROSS-SECTIONAL						
	Ave. Measurement	Analytical Simulation			Numerical Simulation			Ave. Measurement	Analytical Simulation			Numerical Simulation		
		Result	Difference	Rela. error	Result	Difference	Rela. error		Result	Difference	Rela. error	Result	Difference	Rela. error
# 128	170	146	24 ↓	0.141 ↓	177	7 ↑	0.042 ↓	-	-	-	-	-	-	-
# 10	155	123	32 ↓	0.206 ↓	148	7 ↓	0.045 ↓	-	-	-	-	-	-	-
# 6	180	177	3 ↓	0.017 ↓	185	5 ↑	0.028 ↓	180	169	11 ↓	0.060 ↓	175	5 ↓	0.028 ↓
# 62	109	124	15 ↑	0.137 ↑	95	14 ↓	0.128 ↓	109	124	15 ↑	0.138 ↑	82	27 ↓	0.247 ↓
# 35	55	54	1 ↓	0.018 ↓	57	2 ↑	0.036 ↓	55	58	3 ↑	0.055 ↑	58	3 ↑	0.055 ↑
# 29	46	52	6 ↑	0.130 ↑	52	6 ↑	0.13 ↑	46	54	8 ↑	0.174 ↑	54	8 ↑	0.174 ↑

Unit: mg/l ↑ over estimate
 ↓ under estimate

measured values and the simulated values (Table X). The probable reason for the low concentration of the bottom layer, which is lower than it should be, is that the injection wells (source wells) cause a rise of the groundwater table and this increased gradient would cause the leachate to flow out from the constant boundary at a faster rate.

Similar to the analytical simulation, the numerical simulation in a planar view (Figure 76) which represents good results when comparing the simulated values with the measured values of six monitoring wells (Table X) and the map showing the distribution of chloride concentration (Figure 68). The equalpotential lines of the Babylon site in a planar view is shown in Figure 79.

Cleanup

The cleanup simulations are presented by representing a forty-years time period for the planar and the cross-sectional simulations. Figure 80 through Figure 83 represent the cross-sectional case and Figure 83 through Figure 87 represent the planar case. The plume has been totally removed over a period of 40 years in these examples.

The comparison between the measured data simulated data, Table X, display the capabilities of the selected models that can be successfully applied to actual contaminated sites.

LEACHATE FATE AND TRANSPORT FROM THE BABYLON LANDFILL

DISTRIBUTION OVER ENTIRE AREA AFTER 40 YEARS
CROSS-SECTIONAL VIEW.

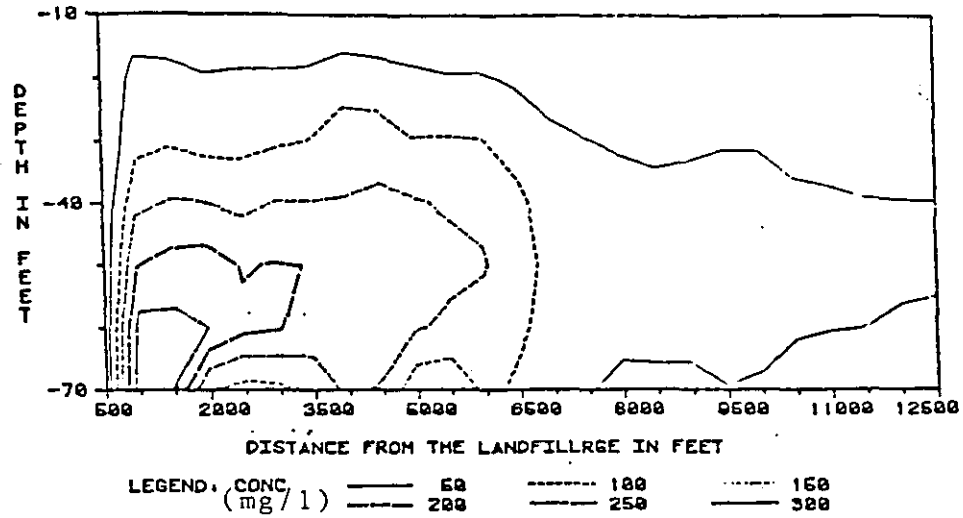


Figure 77. The Simulated Plume of the Babylon Site with Cross-sectional View (Numerical Model)

LEACHATE FATE AND TRANSPORT FROM THE BABYLON LANDFILL

DISTRIBUTION OVER ENTIRE AREA AFTER 40 YEARS
PLANAR VIEW.

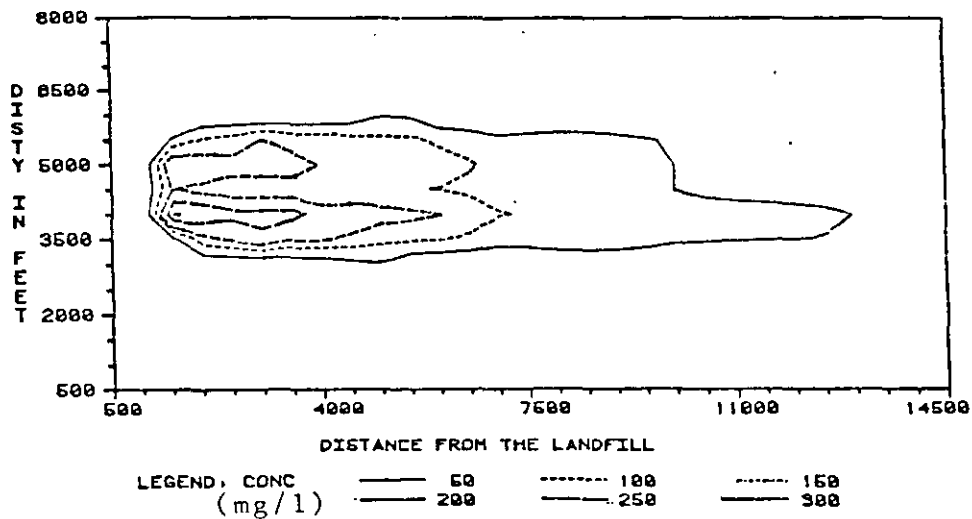


Figure 78. The Simulated Plume of the Babylon Site with Planar View (Numerical Model)

LEACHATE FATE AND TRANSPORT FROM THE BABYLON LANDFILL

EQUALPOTENTIAL DISTRIBUTION IN FEET
PLANAR VIEW

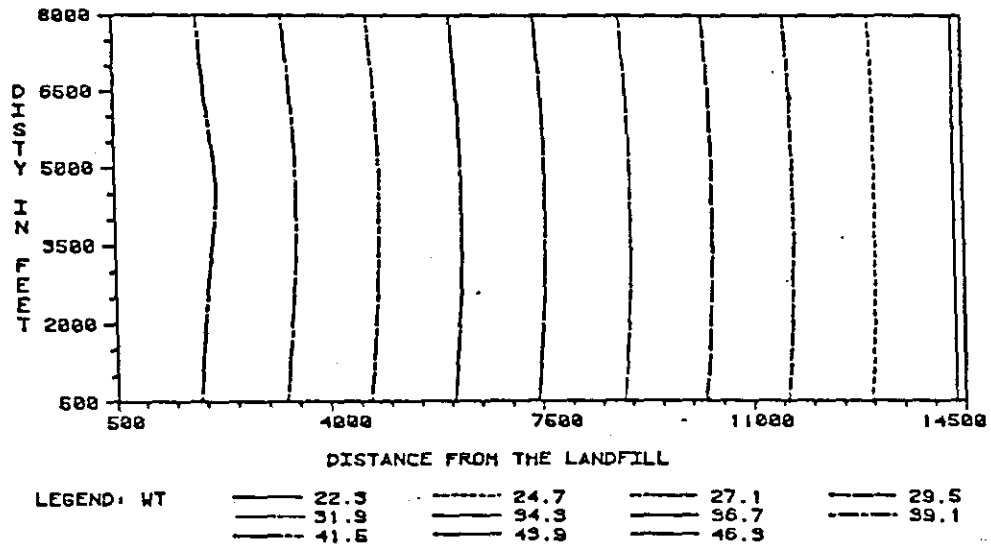


Figure 79. The Distribution of Equal-Potential Lines of the Babylon Site

LEACHATE FATE AND TRANSPORT FROM THE BABYLON LANDFILL

DISTRIBUTION OVER ENTIRE AREA AFTER 40 YEARS
CROSS-SECTIONAL VIEW.

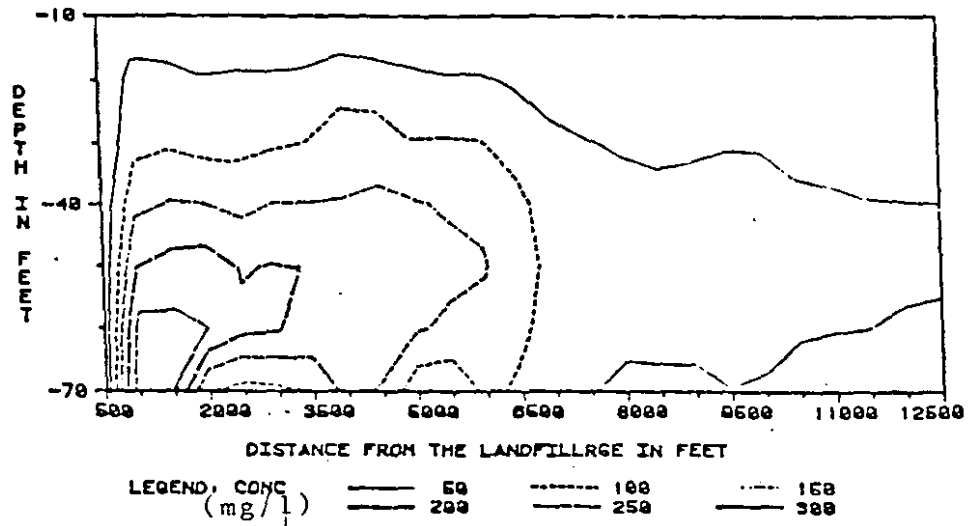


Figure 80. The Simulated Aquifer Restoration of the Babylon Site with Cross-sectional View (at Beginning)

LEACHATE FATE AND TRANSPORT FROM THE BABYLON LANDFILL

DISTRIBUTION OVER ENTIRE AREA AFTER 60 YEARS
CROSS-SECTIONAL VIEW

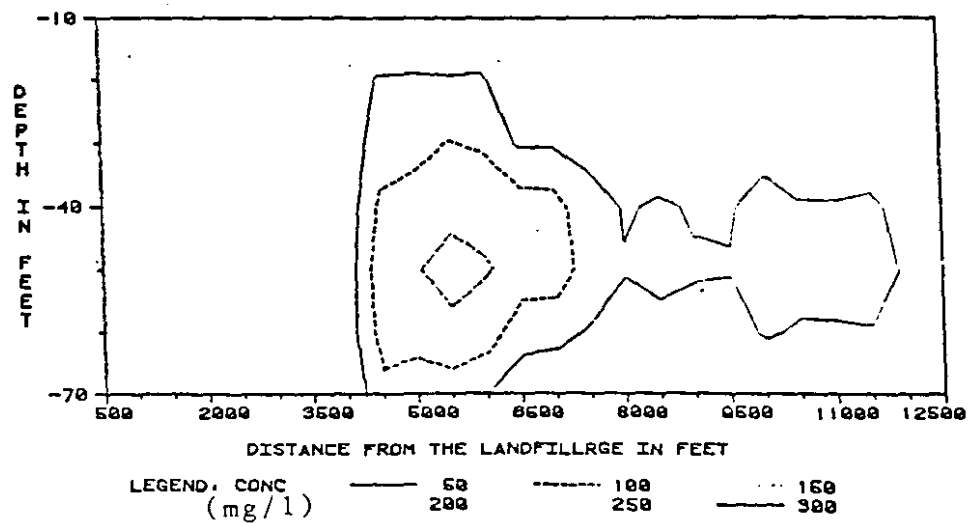


Figure 81. The Simulated Aquifer Restoration of the Babylon Site with Cross-sectional View (10 Years)

LEACHATE FATE AND TRANSPORT FROM THE BABYLON LANDFILL

DISTRIBUTION OVER ENTIRE AREA AFTER 80 YEARS
CROSS-SECTIONAL VIEW

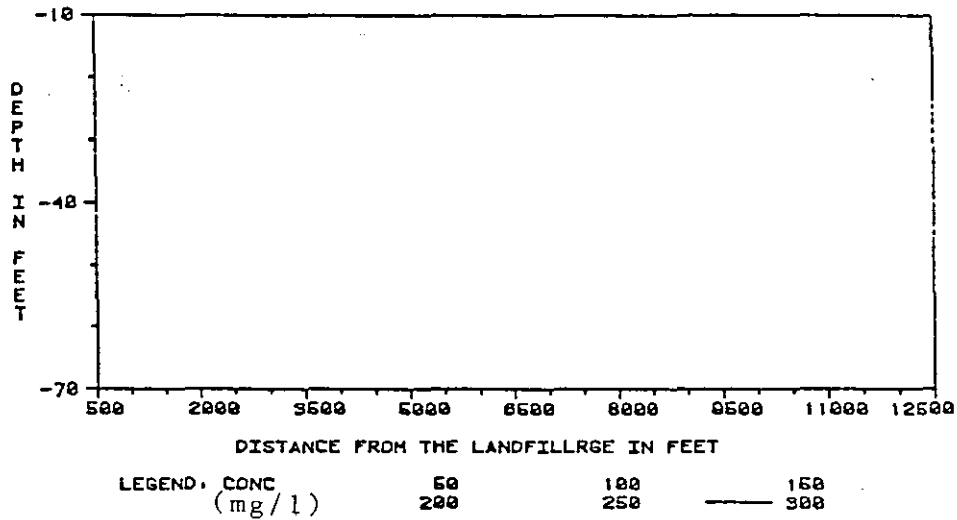


Figure 82. The Simulated Aquifer Restoration of the Babylon Site with Cross-sectional View (20 Years)

LEACHATE FATE AND TRANSPORT FROM THE BABYLON LANDFILL

DISTRIBUTION OVER ENTIRE AREA AFTER 40 YEARS
PLANAR VIEW.

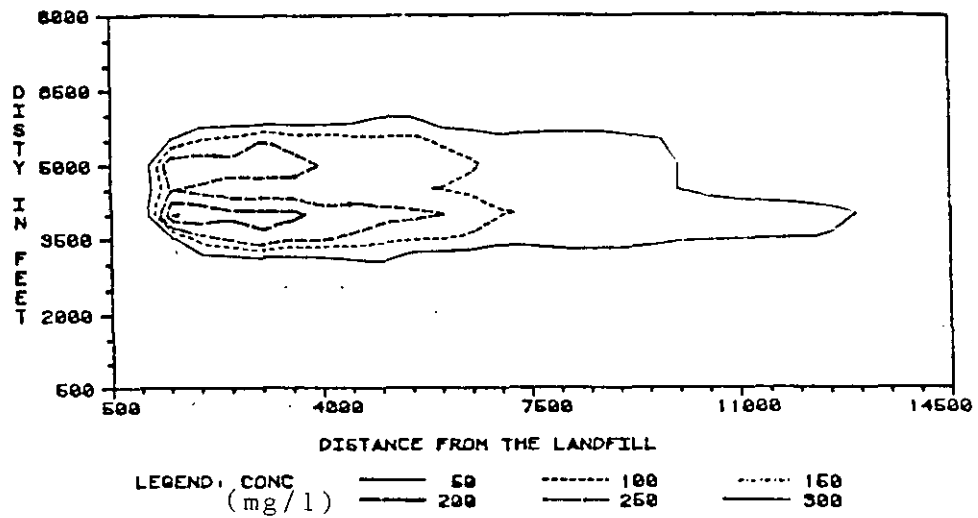


Figure 83. The Simulated Aquifer Restoration of the Babylon Site With Planar View (At Beginning).

LEACHATE FATE AND TRANSPORT FROM THE BABYLON LANDFILL

DISTRIBUTION OVER ENTIRE AREA AFTER 50 YEARS
PLANAR VIEW

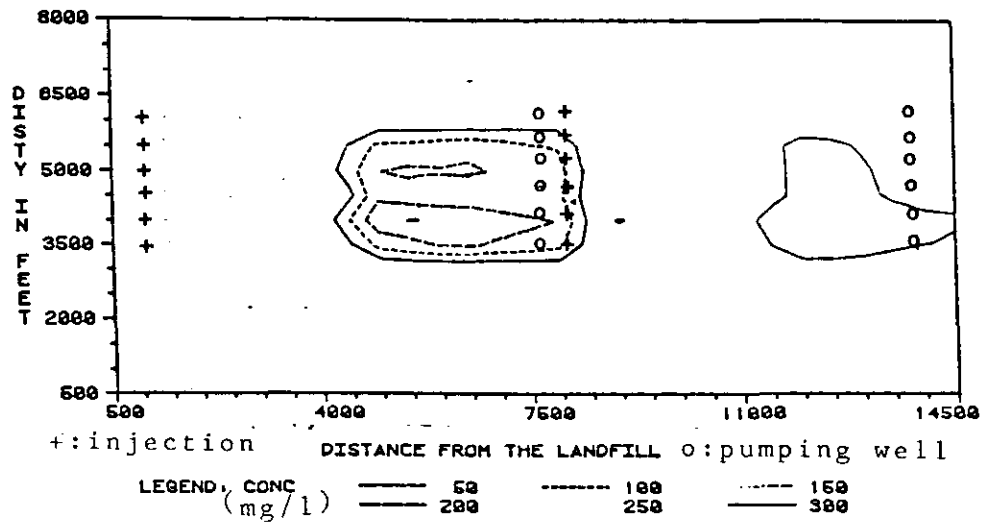


Figure 84. The Simulated Aquifer Restoration of the Babylon Site with Planar View (10 Years)

LEACHATE FATE AND TRANSPORT FROM THE BABYLON LANDFILL

DISTRIBUTION OVER ENTIRE AREA AFTER 80 YEARS
PLANAR VIEW

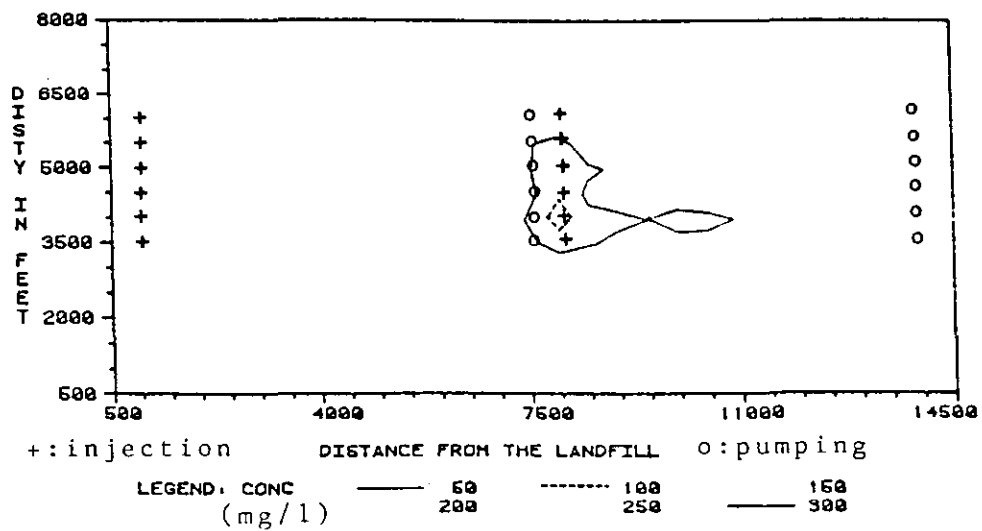


Figure 85. The Simulated Aquifer Restoration of the Babylon Site with Planar View (20 Years)

LEACHATE FATE AND TRANSPORT FROM THE BABYLON LANDFILL

DISTRIBUTION OVER ENTIRE AREA AFTER 70 YEARS
PLANAR VIEW

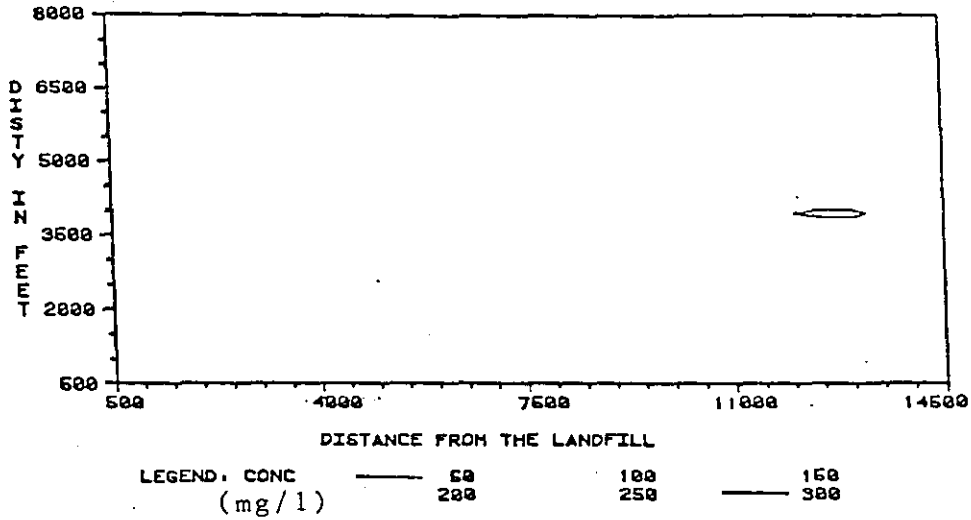


Figure 86. The Simulated Aquifer Restoration of the Babylon Site with Planar View (30 Years)

LEACHATE FATE AND TRANSPORT FROM THE BABYLON LANDFILL

DISTRIBUTION OVER ENTIRE AREA AFTER 80 YEARS
PLANAR VIEW.

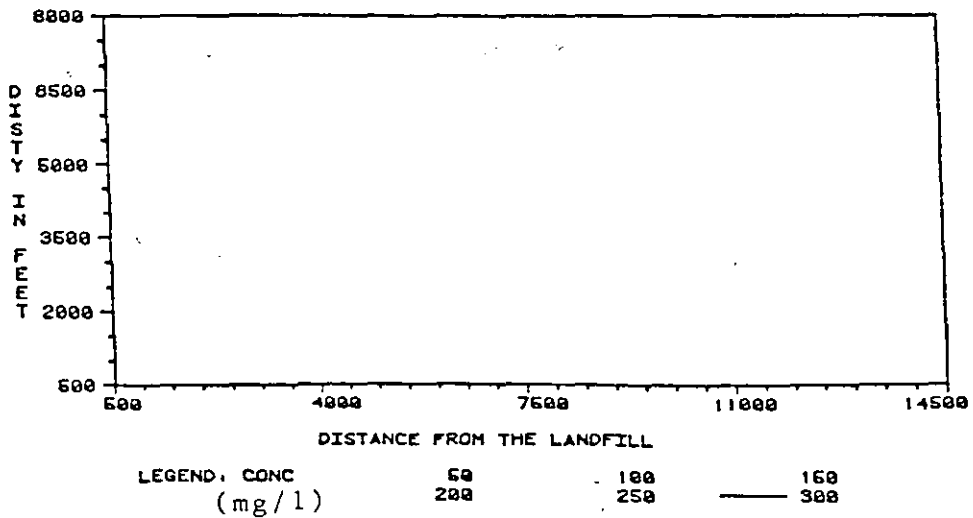


Figure 87. The Simulated Aquifer Restoration of the Babylon Site with Planar View (40 Years)

CHAPTER VII

CONCLUSION

The Analytical Model

Based on the results of the sensitivity and accuracy analysis as well as the simulations for the applied examples, the analytical model can be effectively applied to the contaminated sites which represent homogeneous aquifers. The model is not too complex for easy data processing and calibration. Base on the examples of 3W, a prediction for the development of the plume can be clearly illustrated by combining the planar and cross-sectional analyses. The simulation of the Babylon site offers a good example of reconstructing the sequence of events in tracing the movement of contaminants over time using measured data. This initial information can be used for prediction or for better understanding the hydrogeologic system.

Because most contaminated sites have anisotropic aquifers, the assumptions and the limitations of the analytical model restricts its wide application.

The Numerical Model

In this research, the numerical model was fully tested using accuracy analyses and simulation applications.

The 3W cases provided strong evidence for the capability of the numerical model for handling different geological variations. The development of a plume can also be predicted by applying the numerical model. The capability for managing the anisotropic aquifer using simulated cleanup scenarios supports the application of this model to contaminated landfills in more complex geological condition. This capability was shown using the cleanup simulations of example 3W-1C and the Babylon case. The disadvantage for this model is that it is time consuming for data processing and calibration.

Summary

The selected mathematical models were evaluated for many different aspects to represent their capability for simulating ground-water contaminant movement and analysis of possible clean up solutions. Both the analytical and numerical models were shown to be capable of successfully simulating an actual contaminated site; and both can provide a general view of the contamination in both planar and cross-sectional views.

There are several advantages and disadvantages for applying the selected models to the study sites. The analytical model offers a quick analysis, however, the numerical gives a more accurate simulation and the capability to develop clean up solution. Based on the aspects of preparing and collecting the data, the

availability of computer facilities and the time for calculation, the analytical model is faster and more economical than the numerical model.

Because the numerical model was designed to offer more functions and to be more flexible (i.e., recharge, source and sink terms, and flow boundaries), it can be applied to anisotropic simulations and to clean up scenarios, therefore, in order to accomplish the main object for many studies of ground-water pollution, only the numerical model can be applied.

The decision of using the analytical or numerical model will depend on 1) the objective (cleanup vs. plume fate), 2) degree of complexity of the study site, 3) availability of the data, and 4) the facility (computer). It is recommended that the analytical model can be applied first to obtain a general analysis; then, according to the information available and the objective, the decision whether or not to apply the numerical model may be made.

REFERENCES CITED

- Chang, C. C., 1985, Hydrogeologic Approach to the Characterization of Aquifer Contamination and Restoration Using Mathematical Models: Unpublished M.S. Thesis, Oklahoma State University, Stillwater, OK 190 p.
- Cleary, R. W., 1978a, 208 Long Island Ground-Water Pollution Study, Draft Report, Volume 2, Experimental Results: Unpublished Report, Princeton University, Princeton, N.J., 152 p.
- Cleary, R. W., 1978b, Ground-Water Quality Data, Sanitary Landfill, Babylon, Long Island: Unpublished Data, Princeton University, Princeton, N.J.
- Duckwitz, G. H., 1983, Selected Mathematical Models for Predicting Potentiometric Head and Contaminant Transport in Ground Water: Master's Thesis, Oklahoma State University, Stillwater, Oklahoma.
- Fetter, C. W., 1980, Applied Hydrogeology: Charles E. Merrill Publishing Company, Columbus, Ohio, 488 p.
- Fetter, C. W., 1981, Interstate Conflict Over Ground Water : Wisconsin-Illinois, Ground Water, Vol 19, No.2, pp 201-213.
- Franke, O. L., and McClymonds, N. E., 1972, Summary of the Hydrologic Situation on Long Island, New York, as a Guide to Water Management Alternatives: U.S. Geol. Survey Prof. Paper 627-F, 59 p.
- Freeze, R. A., and Cherry, J. A., 1980, Groundwater : Prentice Hall, Inc., Engelwood Cliffs, N.J., 604 p.
- Full, M. C., 1914, The Geology of Long Island, N.Y. : U.S. Geol. Survey Prof. Paper 82, 231 p.
- Geraghty and Miller, Inc., 1982, Babylon Landfill Monitoring Program: Unpublished Report, Geraghty and Miller, Inc., 28 p.

- Geraghty and Miller, Inc., 1983, Geologic and Hydrologic Locational Factors for Controlling Land Disposal Facility Siting: U.S. Environmental Protection Agency, Office of Solid Waste, CR 68-01-6621, Work Assignment No. 29, 115 p.
- Heath, R. C., 1982, Classification of Ground-Water Systems in the United States, Ground Water, Vol. 20, No. 9, pp. 393-401.
- Kent, D. C., LeMaster, L., and Wagner, J., 1986, Modified N.R.C. Version of the U.S.G.S. Solute Transport Model, Volume 1: Modifications: U.S. Environmental Protection Agency, CR-811142-01-0, 144 p.
- Kent, D. C., LeMaster, L., and Wagner, J., 1986, Modified N.R.C. Version of the U.S.G.S. Solute Transport Model, Volume 2: Interactive Preprocessor Program: U.S. Environmental Protection Agency, CR-811142-01-0, 299 p.
- Kent, D. C., Pettyjohn, W. A., Prickett, T. A., and Witz, F., 1982, Methods for the Prediction of Leachate Plume Migration: Proceedings of the Second National Symposium on Aquifer Restoration and Ground Water Monitoring, Columbus, Ohio, pp. 246-261.
- Kent, D. C., and Wagner, J., 1983, Mathematical Models for Transport and Transformation of Chemical Substances in Subsurface Environments: Annual Report, National Center for Ground Water Research, p.
- Kent, D. C., Wagner, J., and Witz, F. E., Two-Dimensional Analytical Model (FORTRAN) for Prediction of Contaminant Movement in Ground Water: U.S. Environmental Protection Agency, CR-811142-01-0, 44 p.
- Kimmel, G. E. and Braids, O. C., 1974, Leachate Plumes in a Highly Permeable Aquifer: Ground Water, Vol. 16, No. 2, pp. 112-118.
- Kimmel, G. E. and Braids, O. C., 1975, Preliminary Findings of Leachate Study on Two Landfills, Long Island, New York: U.S. Geol. Survey Jour. Research, Vol. 3, No. 3, pp. 273-280.
- Kimmel, G. E. and Braids, O. C., 1980, Leachate Plumes in Ground Water From Babylon and Islip Landfills, Long Island, New York: U.S. Geol. Survey Prof. Paper 1085, 38 p.
- Konikow, L. F. and Bredehoeft, J. D., 1978, Computer Model for Two-Dimensional Solute Transport and Dispersion in Ground Water: Technique of Water Resources Investigation of the U.S. Geol. Survey, Book 7, Ch. C2, 90 p.

- McClymonds, N. E., and Franke, O.L., 1972, Water-Transmitting Properties of Long Island's Aquifer: U.S. Geol. Survey Prof. Paper 677-E, 24 p.
- Naymik, T. G., 1979, The Application of a Digital Model for Evaluating Bedrock Water Resources of the Maumec River Basin, Northwestern, Ohio : Ground Water, Vol. 17, No. 5, pp 438-445.
- Ogata, Akio, and Banks, R. B., 1961, A Solution of the Differential Equation of Longitudinal Dispersion in Porous Media : U. S. Geol. Survey Prof. Paper 411-A, 4 p.
- Peaceman, D. W. and Rachford, H. H., 1953, The Numerical Solution of Parabolic and Elliptic Partial Differential Equations: SIAM Jour., 3, pp. 28-41.
- Pettyjohn, W. A., Kent, D. C., Prickett, T. A., and Witz, F., 1982, Methods for the Prediction of Leachate Plume Migration and Mixing: U.S. Environmental Protection Agency, CR-806931, 326 p.
- Pettyjohn, W. A., 1982, Cause and Effect of Cyclic Changes in Ground-Water Quality: Ground Water Monitoring Review Vol. 2, No 1, pp. 43-49.
- Pinder, G. F., 1973, A Galerkin-Finite Element Simulation of Ground Water Contamination on Long Island, N.Y. : Water Resource Research, Vol. 9, No 6, pp 1657-1669.
- Pluhowski, E. J., and Kantrowitz, I. H., 1964, Hydrology of the Babylon-Islip Area, Suffolk County, Long Island, New York: U.S. Geol. Survey Water Supply Paper 1768, 119 p.
- Remson, I., Hornberger, G. M., and Molz, F. J., 1971, Numerical Methods in Subsurface Hydrology: Wiley Interscience, New York, 389 p.
- SAS Institute Inc., 1982, SAS User's Guide, 1981 Edition: Cary, N. C., SAS Institute Inc., 126 p.
- Stone, H. L., 1968, Iterative Solutions of Implicit Approximations of Multidimensional Partial Differential Equations: SIAM Jour., Numerical Analysis 5, pp. 530-558.
- Tracy, J. V., 1982, Users Manual and Documentation of Adsorption and Decay Modifications to the U.S.G.S. Solute Transport Model: U.S. Nuclear Regulatory Commission, NUREG/Cr-2502, 136p.

- Trescott, P. C., Pinder, G. F., and Larson, S. P., 1976, Finite-Difference Model for Aquifer Simulation in Two Dimensions with Results of Numerical Experiments: Techniques of Water Resources Investigations of the U.S. Geol. Survey, Book 7, Ch. C1, 116 p.
- Wagner, J., Ruiz-Calzada, C. E., Enfield, C. G., Phan, To, and Kent, D. C., 1983, Computer Models for Two Dimensional Subterranean Flows and Pollutant Transport: U.S. Environmental Protection Agency, CR-806931, 362 p.
- Wagner, J., and Kent, D. C., 1984, Plume 3D Three-Dimensional Plumes in Uniform Ground Water Flow: U.S. Environmental Protection Agency, CR 811142-01-0, 63 p.
- Wagner, J., and Kent, D. C., 1984, Plume 2D Two-Dimensional Plumes in Uniform Ground Water Flow: U. S. Environmental Protection Agency, CR 811142-01-0, 91 p.
- Wagner, J., and Kent, D. C., 1984, Solute Transport in Uniform Ground Water Flow Mathematical Development: U.S. Environmental Protection Agency, CR 811142-01-0, 14 p.
- Wilson, J. L., and Miller, P. J., 1978, Two-Dimensional Plume in Uniform Ground-Water Flow: Jour. of the Hydraulics Div. Am. Soc. of Civil Eng., Paper No. 13665, HY4, pp. 503-514.

APPENDICES

APPENDIX A

THE MODIFICATIONS AND EFFICIENCY TESTING
OF THE ANALYTICAL MODEL

APPENDIX A

MODIFICATIONS AND EFFICIENCY TESTING OF THE ANALYTICAL MODEL

Modifications

The original Wilson and Miller (1978) solution defined $f'm$ as :

$$f'm = QCo \quad (III-A.1)$$

where

$$Q = \text{volumetric injection rate} \quad (L^2/T)$$

$$Co = \text{concentration of injected wastes.} \quad (M/L^3)$$

According to their definition for Q , it should be volumetric injection per unit length ($L^2/T/L$). Pettyjohn and Kent (1982) revised the Wilson and Miller mass injection rate to represent more accurately a two-dimensional plume.

$$f'm = \frac{QCo}{M} \quad (III-A.2)$$

where

$$M = \text{aquifer thickness.} \quad (L)$$

This analytical model would apply to an injection source which fully penetrates the saturated zone. Substitution of this term into equations III-2 and III-3 results in

equations III-A.3 and III-A.4 as below :

$$C = \left(\frac{1}{M} \right) \left[\frac{f'm \exp(x/B)}{4\pi n(DxDy)^{1/2}} W(u, r/B) \right] \quad (\text{III-A.3})$$

$$C = \left(\frac{1}{M} \right) \left[\frac{f'm \exp(x/B)}{4\pi n(DxDz)^{1/2}} W(u, r/B) \right] \quad (\text{III-A.4})$$

The Wilson model had been converted to two-dimensional planar computer programs by solving the differential equation, in a BASIC version, which can be applied on micro-computer, (Pettyjohn, Kent and Wagner, 1983) and a FORTRAN version with steady-state time calculation which can be applied on micro-computers (IBM PC, KAYPRO II and North Star) as well as in the IBM 3081D mainframe system (Kent et al, 1986).

The modified analytical model has been tested by doing the sensitivity analysis described in the following section.

Efficiency and Sensitivity Test

After the computer programs had been converted and the modifications had been done from the selected mathematical models, the accuracy and sensitivity tests were applied.

The terms in equation A.4 have been fully tested by using the TSO computer program from the modified analytical model (Pettyjohn and others, 1982; 1983). For each parameter, the concentrations were calculated for both the time of 2333.3 days and steady state at the point of X=4200 ft and y=0 ft.

The test run results for velocity (V) are from 0.015 to 5.0 ft/day (Figure 88). The concentration of steady-state is reduced with higher seepage velocity, due to increased dilution. For non-steady state, the concentration from lower velocity is negligible because the contaminant has not reached the sample point yet.

For the dispersion coefficient (Dx), from 20 to 240 sq. ft/day, and the dispersion ratios (Dx/Dy) of 1 and 5, the results are shown in Figure 89. The concentration is reduced with greater dispersion owing to the spreading of the plume over a large area; and the lower the dispersion ratio (Dx being fixed), the lower concentration that corresponds to larger y direction dispersion.

For the retardation coefficient (Rd), which is from 1.0 to 1.8, the concentration is constant for the steady state cases but is reduced with greater retardation for non-steady state. The reason for reduction is that the retardation delays the arrival of the contaminant to the sampling point.

The concentration for varying decay rate (r), from 1.0 to 2.0, shows a reduction with higher decay rate due to the loss of chemical constituents through decay.

In either case, the concentration is decreased when the aquifer thickness (M) or porosity (n) is increased for both steady state and non-steady state conditions, which accounts for the dilution. The test values are from 1 to 200 feet for aquifer thickness and from 0.26 to 0.47 for porosity.

The mass rate is another test variable (QC0), from 1 to 500 LBM/DAY. The results in Figure 90 show the concentration

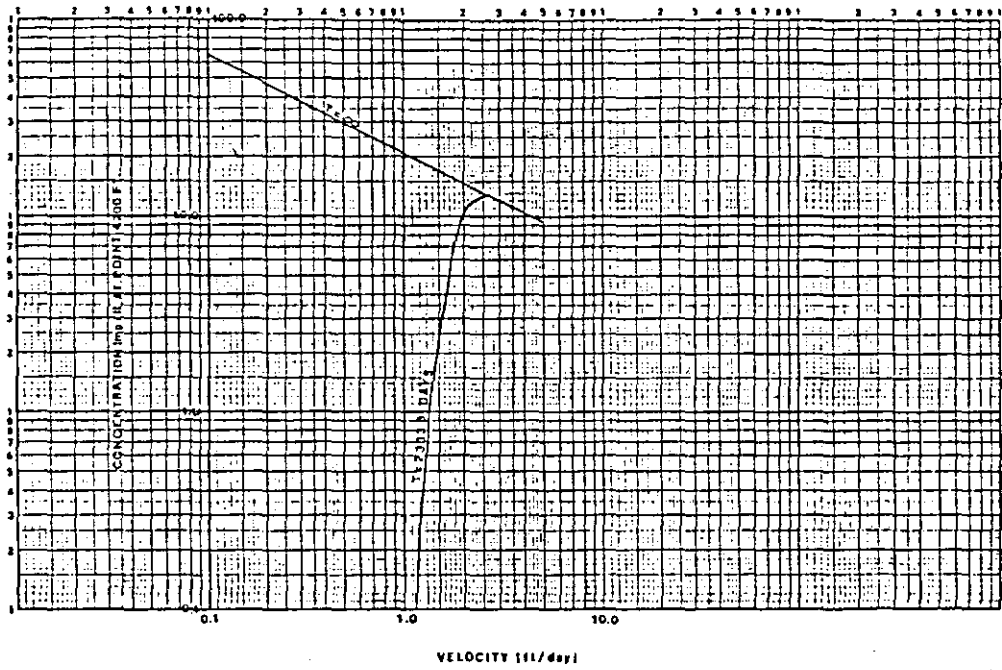


Figure 88. Concentration as a Function of Velocity

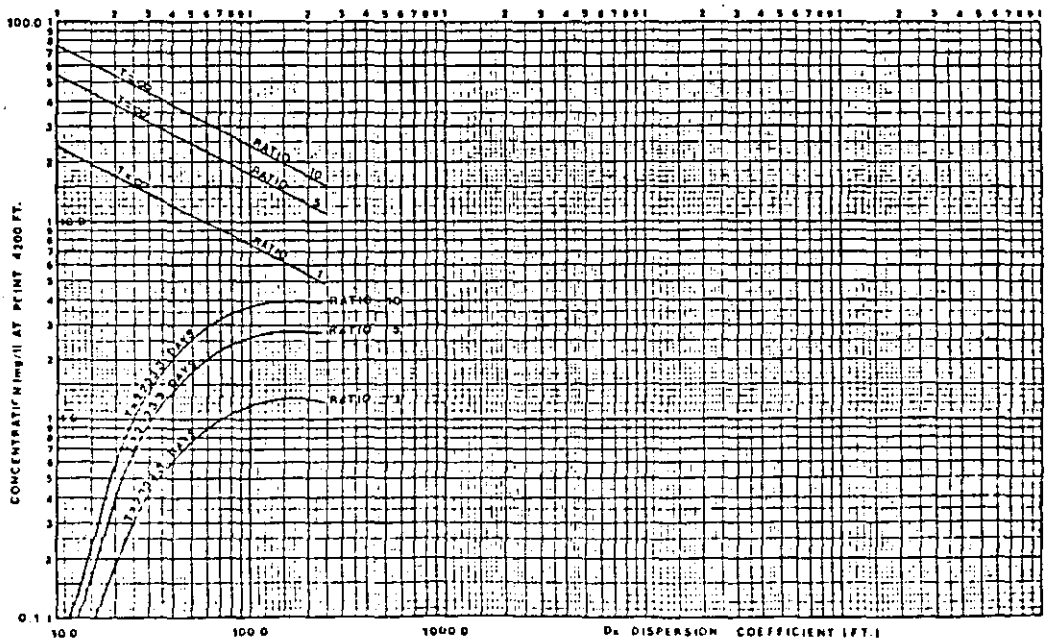


Figure 89. Concentration as a Function of Dispersion

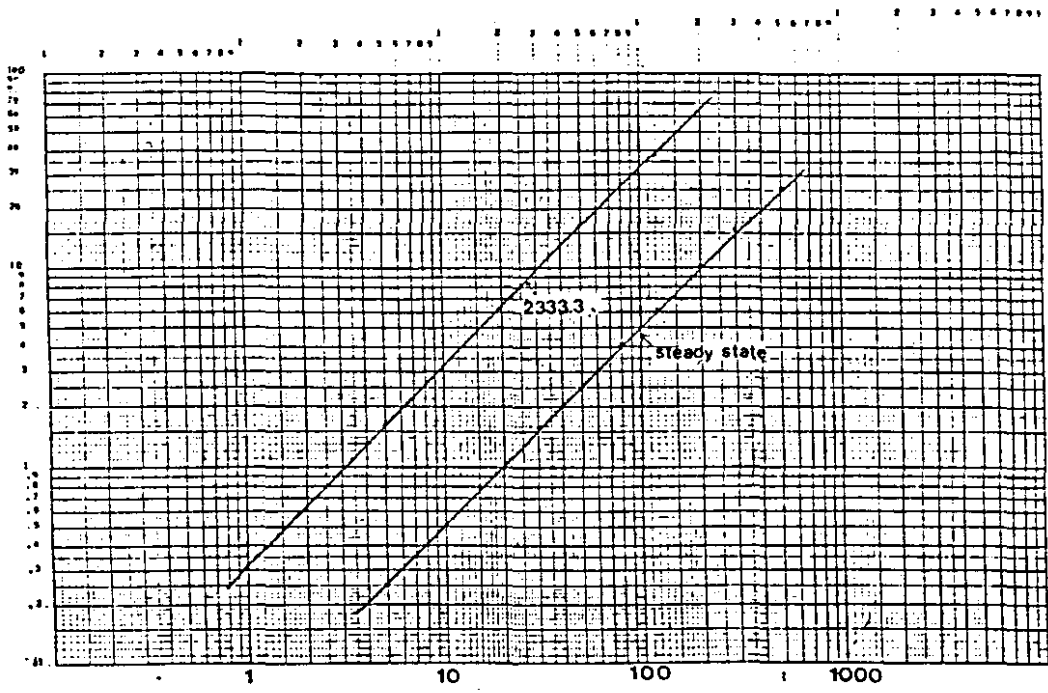


Figure 90. Concentration as a Function of Mass Rate

TABLE XI
SUMMARY OF SENSITIVITY TEST OF THE ANALYTICAL MODEL
On Concentration At Steady State

Parameter	Effect
decay coefficient (γ)	very large decrease
aquifer thickness (m)	decrease as $\frac{1}{m}$
porosity (n)	decrease as $\frac{1}{n}$
velocity (V)	decrease as $\frac{1}{\sqrt{V}}$
dispersion coefficient (D_x)	decrease as $\frac{1}{\sqrt{D_x}}$
dispersion ratio (D_x/D_y)	increase as $\sqrt{\frac{D_x}{D_y}}$
retardation factor (R_d)	no change

Not At Steady State

Parameter	Effect
Decay coefficient (γ)	very large decrease
Retardation factor (R_d)	very large decrease at leading edge
velocity (V)	large increase at leading edge
dispersion coefficient (D_x)	moderate increase at leading edge
aquifer thickness (m)	decrease as $\frac{1}{m}$
porosity (n)	decrease as $\frac{1}{n}$
dispersion ratio (D_x/D_y)	increase as $\sqrt{\frac{D_x}{D_y}}$

is increased with higher mass rate.

The summary of this sensitivity test for both steady state and non-steady state is expressed in a mathematical form in Table XI. Further discussions are found in the reports published by Kent, et al, 1982 and Pettyjohn, et al, 1982.

APPENDIX B
MODIFICATIONS AND EFFICIENCY TESTING
OF THE NUMERICAL MODEL

APPENDIX B

MODIFICATIONS AND EFFICIENCY TESTING OF THE NUMERICAL MODEL

Modifications

There are two major modifications of the Konikow-Bredheoft model which have been made by Tracy (1982) and Kent et al, (1986). The adsorption-decay modification (Tracy, 1982) as following are:

1. The decay equation

The radioactive materials in ground water will change their concentrations over a period of time. The rate of decay is directly proportional to the quantity of material. Thus, the mathematical description of radioactive decay is

$$\frac{\partial C}{\partial t} = - \lambda C \quad (\text{III-B.1})$$

in which

C = sample concentration (M/L³)

t = time (T)

λ = constant of proportionality between the quantity of sample, C, and the rate of change of the quantity of the sample. (*)

The solution for this differential equation is

$$C(t) = C_0 \text{EXP}[-\lambda (t-t_0)] \quad (\text{III-B.2})$$

in which

$$C_0 = \text{the concentration at initial time.} \quad (\text{M/L}^3)$$

The half life is the time required for the decay of one half of the quantity of the material. In solution, the term "quantity of sampled material" is replaced by "concentration".

The mathematical expression for the half life equation is

$$\frac{C_0}{2} = C_0 \text{exp}[-\lambda (t_{1/2} - t_0)] \quad (\text{III-B.3})$$

or

$$t_{1/2} = \ln 2 / \lambda \quad (\text{III-B.4})$$

in which

$$t_{1/2} = \text{the half life time.} \quad (\text{T})$$

2. The Equilibrium Sorption Equation

The mathematical expression that describes sorption is

$$Q C_{\text{sorb}}^* = M p_s (1-n) \left(\frac{S}{t} + \lambda S \right) \quad (\text{III-B.5})$$

in which

$$Q C_{\text{sorb}}^* = \text{element flux between the solute and adsorption states} \quad (\text{M/L}^2\text{T})$$

$$M = \text{saturated thickness} \quad (\text{L})$$

n	= porosity	(*)
ps	= density of solid	(M/L ³)
s	= solid concentration	(M/M)
λ	= decay constant.	(1/T)

3. The Linear Isotherm

The simplest and most widely implemented equilibrium isotherm model is described as:

$$S = K_d C \quad (\text{III-B.6})$$

and

$$K_d = \frac{\partial s}{\partial C} \quad (\text{III-B.7})$$

in which

$$S = \text{sorbed concentration} \quad (\text{M/M})$$

$$C = \text{solute concentration} \quad (\text{M/L}^3)$$

$$K_d = \text{adsorbed ratio.} \quad (*)$$

4. The Langmuir Isotherm

This isotherm was originally calculated for the sorption of gases by solids; we should consider the saturation of sites on the solid. The mathematical expression is described as:

$$K = K_1/K_2,$$

$$S = K D_s C / (1 + K C) \quad (\text{III-B.8})$$

$$dS/dC = K D_s / (1 + K C)^2 \quad (\text{III-B.9})$$

in which

$$K_1 = \text{the rate constant for adsorption} \quad (*)$$

K_2	= the desorption constant	(*)
S	= sorbed concentration	(M/M)
ρ_s	= density of the solid	(M/L ³)
C	= the solute concentration	(M/L ³)
K	= the adsorption ratio.	(*)

5. The Freundlich Isotherm

This is an experimental nonlinear isotherm on the liquid and solid. The equation for the Freundlich isotherm is:

$$S = K C^N \quad (\text{III-B.10})$$

in which

N = the power that derived from experimental data. (*)

The other major modifications to the numerical model have been done at Oklahoma State University for the E.P.A. (Kent et al, 1986) in order to provide user friendly access to the model and increase the efficiency, accuracy, flexibility, stability and capabilities of this model.

The modifications as following are

1. a preprocessor program (Kent et al, 1986) which is an interactive function that can help the user to create or edit the input data set for the model,
2. adding the Strongly Implicit Procedure (SIP) method to solve the ground-water flow equation and to make an option to use the Alternating-Direction Implicit Procedure (ADIP) or SIP method in the program,

3. broadening the size of matrices for analysis,
4. setting the option for simulating head distribution only or for solute transport also,
5. an option for simulating either a water table aquifer or a confined aquifer,
6. a revision of mass balance signs, negative for injection, or positive for discharge,
7. an option for either transmissivity or hydraulic conductivity entry,
8. and generating output datasets for use with SAS graphics programs (Appendix E).

The interactive program is designed for simplifying data entry and for helping the user to comprehend the function of the numerical model through the input of the physical and chemical parameters on the movement of plume. The preprocessor code is written in PL/I for the IBM 3081D as well as for the KAYPRO and IBM PC microcomputers. The input data managed in microcomputers can be submitted to an IBM 3081D for batch processing by using appropriate data transmission software such as PC-TALK for the IBM-PC or TERM+ for the KAYPRO.

The Strongly Implicit Procedure was developed by Stone (1968). It is a more efficient algorithm than the Alternating-Direction Implicit Procedure which was originally used in the model for solving the flow equation. Tests have been made to prove that the SIP requires only about half the number of iterations of ADIP to converge to

a desired range of error for results, therefore, the efficiency from SIP is higher than from ADIP (Table XII).

The head simulation option may be chosen over the solute transport option when the intent is to simulate the head distribution for the flow system during the early steps of calibration. This can save time because the computing time for solving the water flow equation is about one twentieth of the computing time for the solute transport equation.

The level of the ground water table is determined by the amount of water being added to or subtracted from the aquifer, assuming an unconfined aquifer. These changes cause changes in saturated thickness, which influences the transmissivity, since transmissivity is a function of hydraulic conductivity and the saturated thickness of an aquifer. Thus, the transmissivity should be updated with time, and the modification has been made to allow the user to specify whether or not an unconfined aquifer will be simulated; and the option for the input of hydraulic conductivity or transmissivity is offered, according to the necessity.

A graphics display can be more efficient than a set of matrix data in presenting plume development in an easily comprehensible and usable form. The output data format in the program has been modified to meet the form used in the SAS graphics package.

These modifications are checked by applying the revised models to a number of test examples and comparing the results

TABLE XII
 COMPUTATIONAL EFFICIENCY FOR TESTED PROBLEMS

Test Problem	Iterations and CPU Time				Mass Balance Error (%)			
	SIP		ADIP		SIP		ADIP	
	No. of Iterations	Total CPU Time (sec)	No. of Iterations	Total CPU Time (sec)	Hydraulic Mass balance error	Chemical Mass balance error	Hydraulic Mass balance error	Chemical Mass balance error
1	7	1.45	13	1.48	1.53883E-02	-7.95201E+00	1.31100E-01	-6.86250E+00
2	6	1.43	13	1.48	8.80971E-03	-3.06842E+00	1.18518E-01	-3.05039E+00
3	2	4.03	1	3.95	0.00000E+00	0.00000E+00	0.00000E+00	0.00000E+00

with those from the original models.

Efficiency and Sensitivity Test

The numerical model has been evaluated by several test problems for both the original version and the modified version. The tests for the comparison between two versions indicates the modified version has higher efficiency.

Original version. The accuracy and sensitivity of the original numerical model were evaluated by three hypothetical solute-transport problems in Konikow's report (Konikow and Bredehoeft, 1978). The criteria for these evaluations is the mass balance error which will depend on the nature of the problem and the time increments.

The first Test problem was designed to evaluate "the accuracy of simulating the processes of steady state convective transport and dispersion independent of the effects of chemical sources" (Konikow and Bredehoeft, 1978). The parameters of the model in Test Problem One are listed in Table XIII. The model was run to simulate no dispersion ($\alpha = 0.$) and moderate dispersion ($\alpha = 100.$) conditions. The averaging error for this test problem is 1.9 percent, and it is always within a range of plus or minus 8 percent; the error decreases for a higher dispersivity and minimizes the strong concentration gradients. The results are shown in Figure 91.

The second test problem was designed to apply the model to the sites in which the flow system is strongly influenced

TABLE XIII
MODEL PARAMETERS FOR TEST PROBLEM 1

Aquifer properties	Numerical parameters
$K=0.005$ ft/s (1.5×10^{-2} m/s)	$\Delta x=900$ ft (274 m)
$b=20.0$ ft (6.1 m)	$\Delta y=900$ ft (274 m)
$S=0.0$	CELDIS=0.49
$\epsilon=0.30$	NPTPND=9
$\sigma_T/\sigma_L=0.30$	

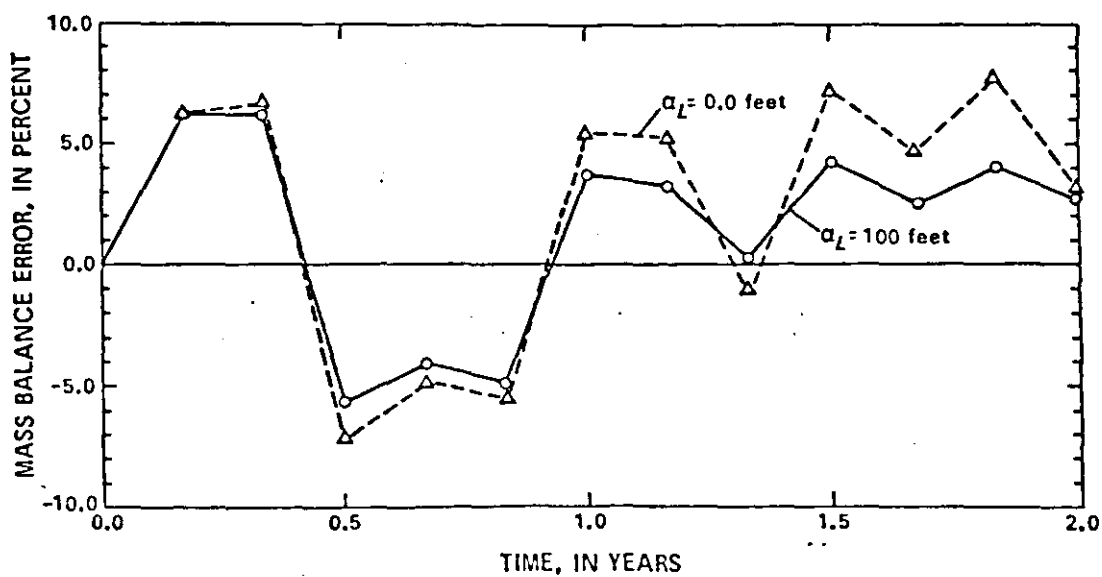


Figure 91. Mass Balance Errors for Test Problem 1

by wells. In this case, one injection well and one withdrawal well are set to influence the regional flow system controlled by two constant-head boundaries. The input parameters are listed in Table XIV, and the model was run for both no dispersion and moderate dispersion. Results are shown in Figure 92, in which the leading edge of the breakthrough curve of moderate dispersion reaches the constant-head sink just prior to 1.0 year. For no dispersion, the leading edge of the breakthrough curve still had not entered the constant-head sink after 2.4 years. "The divergence of the two curves is not caused directly by the difference in dispersion, but by the difference in arrival times at the hydraulic sinks" (Konikow and Bredhoeft, 1978). The third test applied two execution parameters to evaluate their influence on the accuracy. The parameters are the initial number of particles per node (NPTPND) and the maximum fraction of the grid dimensions that particles are allowed to move (CELDIS). In this case, the input parameters are the same as in problem two except that the NPTPND is equal to 4, 5, 8 and 9; the CELDIS is equal to 0.25, 0.50, 0.75 and 1.00. Based on the results of tests (Figure 93, 94 and Table XV, XVI). A value of 4 to 5 for NPTND and a value of 0.75 to 1.0 for CELDIS is recommended for maximum efficiency and for making frequent runs for the model calibrations during the early stages. For final runs when maximum accuracy is desired, NPTPND should be set equal to 9 and CELDIS equal to 0.5 (Konikow and Bredhoeft, 1978).

TABLE XIV
 MODEL PARAMETERS FOR TEST PROBLEM 2 AND 3

Aquifer properties and stresses	Numerical parameters
$K=0.005$ ft/s (1.5×10^{-3} m/s)	$\Delta x=900$ ft (274 m)
$b=20.0$ ft (6.1 m)	$\Delta y=900$ ft (274 m)
$S=0.0$	CELDIS=0.50
$\epsilon=0.30$	NPTPND=9
$\alpha_T/\alpha_L=0.30$	
$C'=100.0$	
$C_0=0.0$	
$q_w=1.0$ ft ³ /s (0.028 m ³ /s)	

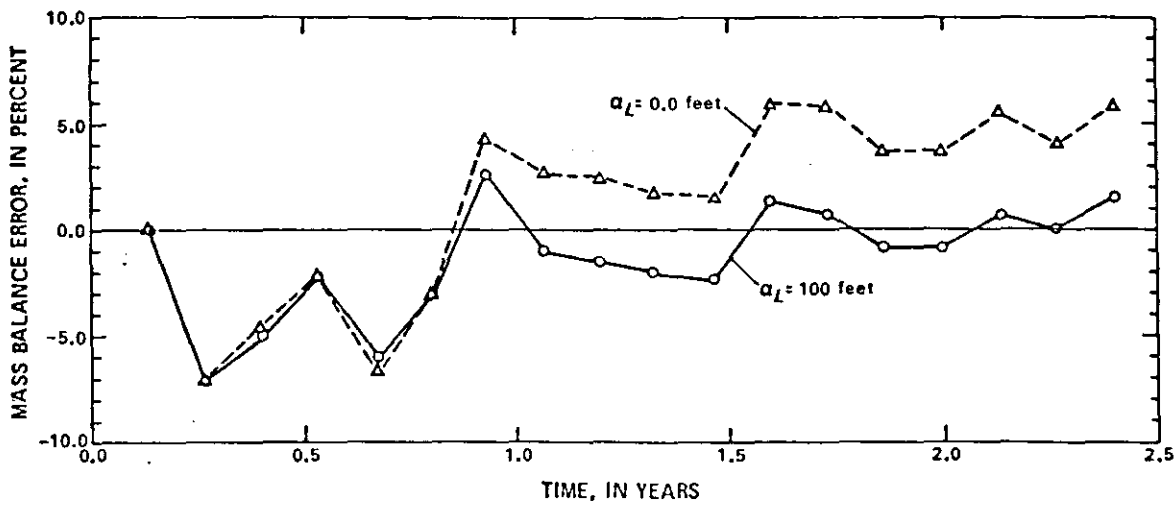


Figure 92. Mass Balance Errors for Test Problem 2

TABLE XV
EFFECT OF NPTPND ON ACCURACY AND EFFICIENCY
OF SOLUTION TO TEST PROBLEM 2

NPTPND	cpu-seconds ¹	Mass balance error (percent)	
		Mean	Standard deviation
4	12.8	1.49	5.33
5	14.0	.90	2.29
8	17.9	.48	1.53
9	19.2	.26	.69

¹The program was executed on a Honeywell 60/68 computer;
CELDIS=0.50.

(After Konikov, 1978)

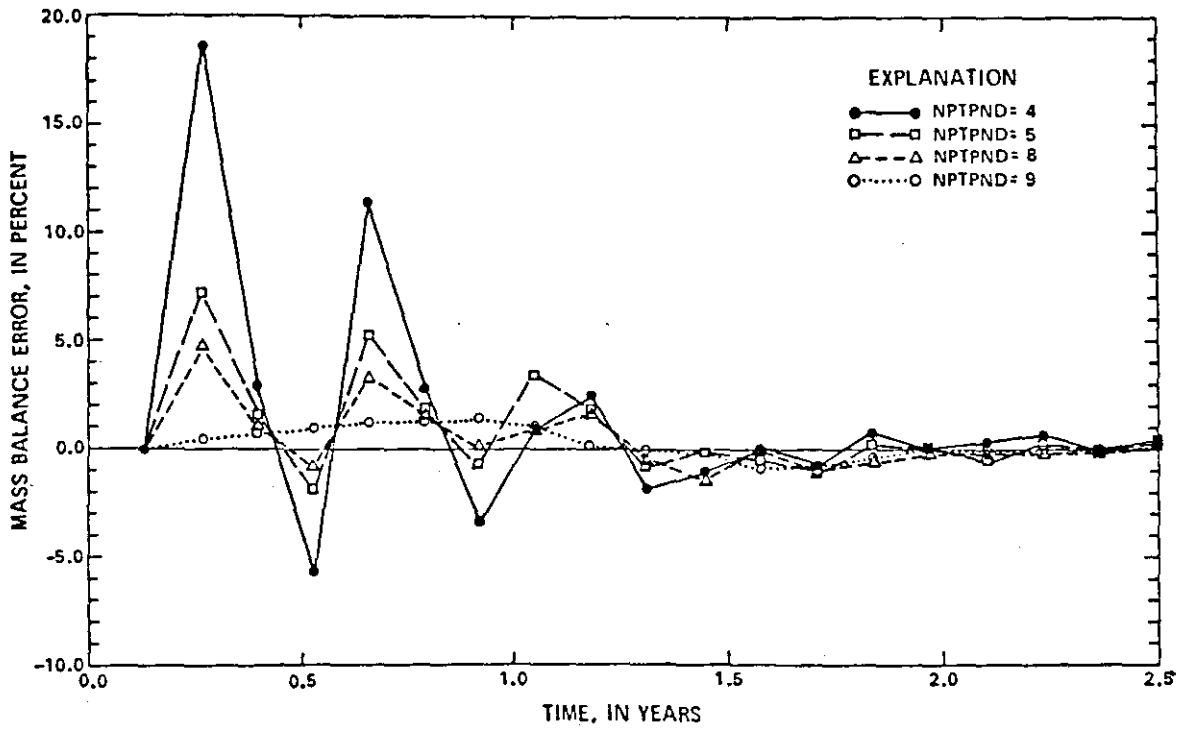


Figure 93. Effect of NPTPND on Mass Balance Error for Test Problem 3 (CELDIS=0.5)

TABLE XVI
EFFECT OF CELDIS ON ACCURACY AND EFFICIENCY
OF SOLUTION TO TEST PROBLEM 3

CELDIS	cpu-seconds ¹	Mass balance error (percent)	
		Mean	Standard deviation
0.25 -----	34.6	1.50	2.99
.50 -----	19.2	.26	.69
.75 -----	14.4	.56	.69
1.00 -----	12.1	.25	1.48

¹ The program was executed on a Honeywell 60/68 computer;
NPTND=9.

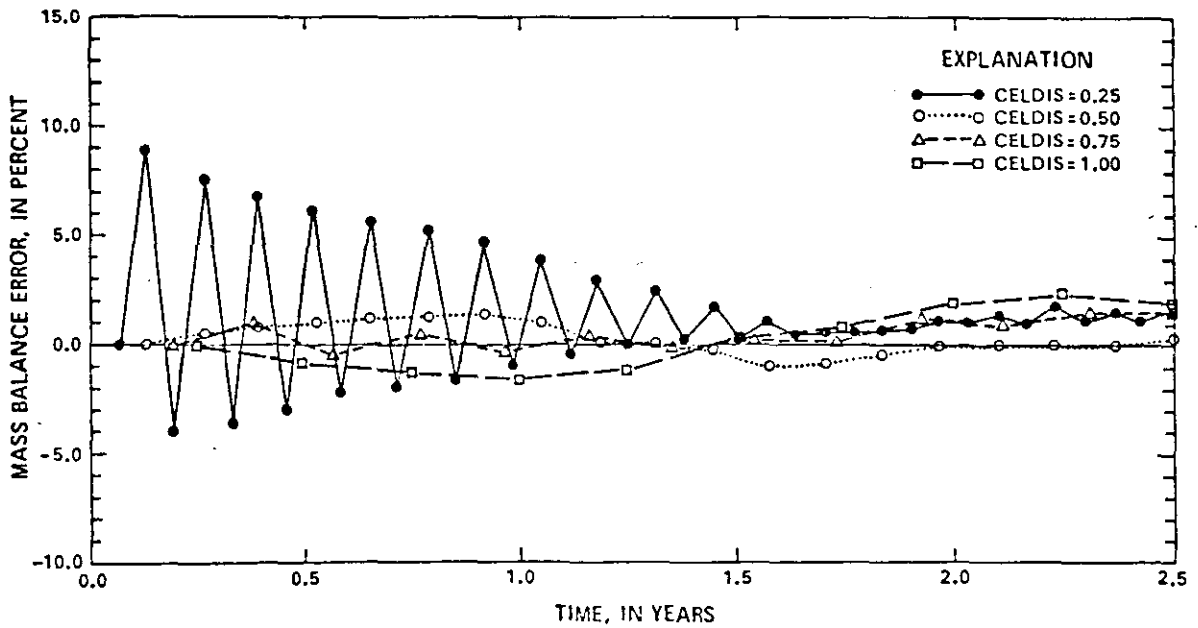


Figure 94. Effect of CELDIS on Mass Balance Error for Test Problem 3 (NPTND=9)

Modified Version. Several test examples were run to demonstrate and compare the accuracy and the efficiency of the modified version with the original version. Two of these examples were applying the same input parameters as original versions to compare the efficiency of the SIP algorithm and the ADIP algorithm. The third example was a one-dimension problem in which radioactive decay and adsorption were involved.

From the results of test problem #1 and #2 for the steady state condition, in Tables XVII and XVIII, the SIP algorithm takes only about half of the number of iterations to converge to the specified solution as the ADIP algorithm does. For test problem #3, a simple case, the rates for convergence of SIP algorithm and ADIP algorithm are similar. In the cases for transient condition, the SIP algorithm shows a significantly faster convergence rate than the ADIP algorithm during the earlier time steps. However, as the time steps proceed the convergence rates for both algorithms become insignificant (Tables XVII, XVIII). Based on these tests, the modified version (the SIP algorithm) is more efficient than the original version (the ADIP algorithm). A detailed discussion of these test examples are in the report D. C. Kent and others 1986.

TABLE XVII
 COMPUTATIONAL EFFICIENCY FOR TRANSIENT TEST
 PROBLEM 1

Time Step	Iterations and CPU Time				Mass Balance Error (%)			
	SIP		ADIP		SIP		ADIP	
	No. of Iterations	Total CPU Time (sec)	No. of Iterations	Total CPU Time (sec)	Hydraulic Mass balance error	Chemical Mass balance error	Hydraulic Mass balance error	Chemical Mass balance error
1	7	1.90	13	2.02	2.16500E-02	-2.26933E+1	1.57759E-01	-2.26953E+01
2	3		6		3.22388E-02	-2.44461E+01	1.26700E-01	-2.44459E+01
3	2		3		2.50258E-02	-7.74837E+0	7.17186E-02	-1.92833E+01
4	1		3		1.96135E-02	-1.13217E+01	5.67972E-02	-1.31429E+01
5	1		2		1.53982E-02	-5.06631E+00	4.74312E-02	-6.48212E+00
6	1		1		1.26792E-02	-2.30856E+00	4.08725E-02	-4.43758E+00
7	1		1		1.07680E-02	-3.97417E+00	3.32994E-02	-5.89064E+00
8	1		1		9.35754E-03	-3.36166E+00	3.00519E-02	-6.00104E+00
9	1		1		8.27377E-03	-3.11102E+00	2.56867E-02	-5.72208E+00
10	1		1		7.42532E-03	-2.52546E+00	2.33322E-02	-4.11365E+00

TABLE XVIII
 COMPUTATIONAL EFFICIENCY FOR TRANSIENT TEST
 PROBLEM 2

Time Step	Iterations and CPU Time				Mass Balance Error (%)			
	SIP		ADIP		SIP		ADIP	
	No. of Iterations	Total CPU Time (sec)	No. of Iterations	Total CPU Time (sec)	Hydraulic Mass balance error	Chemical Mass balance error	Hydraulic Mass balance error	Chemical Mass balance error
1	6	1.90	13	2.01	5.38178E-03	-1.13870E+01	1.33714E-01	-1.13756E+01
2	3		6		2.59461E-02	6.32174E+00	1.10818E-01	6.3452E+00
3	2		3		2.03862E-02	-7.09691E-01	6.32410E-01	-6.92257E-01
4	1		3		1.61486E-02	-3.16578E+00	5.03580E-02	-3.13439E+00
5	1		2		1.27278E-02	1.74106E+00	4.21897E-02	-1.75031E+00
6	1		1		1.04736E-02	-2.03990E+00	3.64501E-02	-2.06982E+00
7	1		1		8.89435E-03	-8.19406E+00	2.97079E-02	-8.24349E+00
8	1		1		7.71704E-03	-1.11926E+00	2.68048E-02	-1.12535E+00
9	1		1		6.81105E-03	-1.47943E+00	2.39371E-02	-1.48265E+00
10	1		1		6.12330E-03	-1.56466E+00	2.12051E-02	-1.56501E+00

APPENDIX C

THE COMPARISON OF THE MATRIX SIZES OF THE
NUMERICAL MODEL

APPENDIX C

COMPARISON OF MATRIX SIZES OF THE NUMERICAL MODEL

The major aspects in selecting the analytical matrix size for 3W cases are based not only on the accuracy but also on the time consumed for computer execution. To evaluate these two aspects, the 3w-2B case was applied to different sizes of matrices, 10 by 10 (100ft/grid), 20 by 20 (50ft/grid) and 50 by 50 (20ft/grid).

The accuracy comparison of different matrix sizes are shown in Table XIX. It implies that if the grid is finer, the results are more accurate due to a more concentrated data distribution used to more precisely cover the simulated area. The comparison of the time for calculation is shown in Table XX. The finer scale size will require more time for execution.

Using Table XIX it can be observed that the differences (within 0.067 mg/l) in simulated concentrations for 10 by 10 matrix and 50 by 50 matrix are small. Based upon Table XX, the time consumed for the 10 by 10 matrix is 1/1500 of the 50 by 50 matrix. Thus, the 10 by 10 matrix is selected for the 3W cases due to its reasonable accuracy and less time.

TABLE XIX
 CROSS-SECTIONAL COMPARISON OF DIFFERENT MATRICES (KONIKOW MODEL)
 (kd = 0.2)

Depth	Matrix Size	Time		25 years		50 years		100 years		200 years	
		Location	Concn.	at river	at 400 ft. from river	at river	at 400 ft. from river	at river	at 400 ft. from river	at river	at 400 ft. from river
100 ft.	10 x 10			0.0786	0.1932	0.1705	0.3132	0.2548	0.4130	0.3075	0.4010
	20 x 20			0.0410	0.1559	0.1366	0.3462	0.2368	0.4027	0.2500	0.5053
	50 x 50			0.0613	0.1548	0.1346	0.2628	0.1910	0.3010	0.2401	0.4434
difference between 20 x 20 and 50 x 50 (base on 50 x 50)				-0.0203	0.0011	0.0020	0.0734	0.0467	0.1011	0.0405	0.0019
difference between 10 x 10 and 50 x 50 (base on 50 x 50)				0.0173	0.0384	0.0359	0.0504	0.0647	0.0514	0.0077	0.0182

TABLE XX
C.P.U. TIME FOR DIFFERENT MATRICES SIZE

Rel. Matrix Time	10 x 10	20 x 20	50 x 50
kd = 0.2	13.32 sec	3 min 41.24 se	401 min
kd = 5	3.03 sec	25.87 sec	39 min 6.98se

In addition to the aspects discussed above, the area of the aquifer and the amount of available data are other important factors to consider when selecting the matrix size. For instance, the area of the Babylon Landfill is long and narrow in the planar view (12,000 ft long and 1,500 ft wide), where it is shallow and long in the cross-sectional view (75 ft deep and 12,000 ft long). Therefore, the matrix size 18 by 31 (500ft/grid) was chosen for the planar simulation and 10 by 27 (500ft/grid) was chosen for the cross-sectional simulation of the Babylon case.

APPENDIX D
THE INPUT DATA SETS OF 3W CASES

INPUT DATA SET FOR 3W-1A (EQUALPOTENTIAL LINES DISTRIBUTION)

```

---- TSO FOREGROUND HARDCOPY ----
DSNAME=U11834C.X103WHE9.CNTL

//C11834C JOB ( ?,TSO-TR-KONI),KONIKOWRUN.
// TIME=(0.40),CLASS=A.
// MSGCLASS=X,NOTIFY=*
/*PASSWORD ???
/*JOBPARM ROOM=C
//
//KONI EXEC PGM=KONI60G,REGION=2500K
//STEPLIB DD DISP=SHR,DSN=U11236C.KONI.LOAD
//FT06FOO1 DD DSN=U11834C.X103WHE9. OUTLIST,UNIT=STORAGE.
// SPACE=(TRK,(10,10)),DISP=(NEW,CATLG),
// DCB=(RECFM=VBA,LRECL=133,BLKSIZE=7448)
//FT10FOO1 DD DSN=U11834C.X103WHE9.GRAPH,UNIT=STORAGE,
// SPACE=(TRK,(50,10)),DISP=(NEW,CATLG),
// DCB=(RECFM=FB,LRECL=80,BLKSIZE=7440)
//FT07FOO1 DD SYSOUT=B
//FT05FOO1 DD *
CROSS-SECTION SCENARIO 3W-1 RECHARGE=13.3 IN/YR PUMP PER=50YEAR 400Y
 2 4 12 129850 1 10 0 100 10 4 2 0 0 0 0 0
100 .01 .3 75. 0 0 0 100 100 .5 .01
 0 1 0 1. .2
 1 0 0 1 0
 8 2 -3.6E-6 1.
 9 2 -3.6E-6 1.
10 2 -3.6E-6 0.0
 2 2 -3.6E-6 0.0
 3 2 -3.6E-6 0.0
 4 2 -3.6E-6 0.0
 5 2 -3.6E-6 0.0
 6 2 -3.6E-6 1.
 7 2 -3.6E-6 1.0
11 2 -3.6E-6 0.
 1 1.E-5
 0 0 0 0 0 0 0 0 0 0 0 0 0
 0 9.6 9.6 9.6 9.6 9.6 9.6 9.6 9.6 9.6 9.6 9.6 9.6 0
 0 9.6 9.6 9.6 9.6 9.6 9.6 9.6 9.6 9.6 9.6 9.6 9.6 0
 0 9.6 9.6 9.6 9.6 9.6 9.6 9.6 9.6 9.6 9.6 9.6 9.6 0
 0 9.6 9.6 9.6 9.6 9.6 9.6 9.6 9.6 9.6 9.6 9.6 9.6 0
 0 9.6 9.6 9.6 9.6 9.6 9.6 9.6 9.6 9.6 9.6 9.6 9.6 0
 0 9.6 9.6 9.6 9.6 9.6 9.6 9.6 9.6 9.6 9.6 9.6 9.6 0
 0 9.6 9.6 9.6 9.6 9.6 9.6 9.6 9.6 9.6 9.6 9.6 9.6 0
 0 9.6 9.6 9.6 9.6 9.6 9.6 9.6 9.6 9.6 9.6 9.6 9.6 0
 0 9.6 9.6 9.6 9.6 9.6 9.6 9.6 9.6 9.6 9.6 9.6 9.6 0
 0 0 0 0 0 0 0 0 0 0 0 0 0 0
 0 1
 1 .01
 0.000.000.000.000.000.000.000.000.000.000.000.000.00
 0.0010001014102810421056106910831097111111250.00
 0.0010001014102810421056106910831097111111250.00
 0.0010001014102810421056106910831097111111250.00
 0.0010001014102810421056106910831097111111250.00
 0.0010001014102810421056106910831097111111250.00
 0.0010001014102810421056106910831097111111250.00
 0.0010001014102810421056106910831097111111250.00
 0.0010001014102810421056106910831097111111250.00
 0.0010001014102810421056106910831097111111250.00
 0.0010001014102810421056106910831097111111250.00
 0.000.000.000.000.000.000.000.000.000.000.000.000.00
 0
 1
 000000000000
 020000000030

```

```

00000000030
00000000030
00000000030
00000000030
00000000030
00000000030
00000000030
00000000030
00000000030
00000000030
000000000000
 2 1. 0. 0. 0
 3 1.0 0.0 0.0
 0 0.0
 1
 2 1 10 100 10 0 0 0 0 0 100 0 0
 8 2 -3.6E-6 1.
 9 2 -3.6E-6 1.
10 2 -3.6E-6 0.0
 2 2 -3.6E-6 0.0
 3 2 -3.6E-6 0.0
 4 2 -3.6E-6 0.0
 5 2 -3.6E-6 0.0
 6 2 -3.6E-6 1.
 7 2 -3.6E-6 1.0
11 2 -3.6E-6 0.
 1
 2 1 10 100 10 0 0 0 0 0 100 0 0
 8 2 -3.6E-6 1.
 9 2 -3.6E-6 1.
10 2 -3.6E-6 0.0
 2 2 -3.6E-6 0.0
 3 2 -3.6E-6 0.0
 4 2 -3.6E-6 0.0
 5 2 -3.6E-6 0.0
 6 2 -3.6E-6 1.
 7 2 -3.6E-6 1.0
11 2 -3.6E-6 0.
 1
 2 1 10 100 10 0 0 0 0 0 100 0 0
 8 2 -3.6E-6 1.
 9 2 -3.6E-6 1.
10 2 -3.6E-6 0.0
 2 2 -3.6E-6 0.0
 3 2 -3.6E-6 0.0
 4 2 -3.6E-6 0.0
 5 2 -3.6E-6 0.0
 6 2 -3.6E-6 1.
 7 2 -3.6E-6 1.0
11 2 -3.6E-6 0.

```


INPUT DATA SET FOR 3W-5A

**** TSD FORGROUND HARDCOPY *****
DSNAME=U11834C.X103WFL1.CNTL

//C11834C JOB (7'TSD-TR-KONI),KONIKOWRUN,
// TIME=120.01,CLASS=4,
// MSGCLASS=X,NOTIFY=*,
//PASWORD=7777
//JOBPARM R00M=C
//KONI EXEC PGM=KONI102B,REGION=4000K
//STEP1B DD DISP=SHR,DSN=U11236C.KONI.LOAD
//FTOF001 DD DSN=U11834C.X103WFL4.OUTPUT,UNIT=STORAGE,
// SPACE=(TRK,(10,10)),DISP=OLD,
// DCB=(RECFM=VBA,LRCL=133,BLKSIZE=7448)
//FT10F001 DD DSN=U11834C.X103WFL4.GRAPH,UNIT=STORAGE,
// SPACE=(TRK,(50,10)),DISP=OLD,
// DCB=(RECFM=FB,LRCL=80,BLKSIZE=7440)
//FT07F001 DD SYSOUT=B
//FT05F001 DD *
CROSS-SECTION SCENARIO 3W-1 RECHARGE=13.3 IN/YR PUMP PER=50YEAR 400Y
100 .01 .3 75 .0 0 0 100 100 .5 .5 1 .2

Table with multiple columns of numerical data, including values like 0.00, 1.00, 10.00, 100.00, and scientific notation like 1E-4.

Table with multiple columns of numerical data, including values like 0.00, 1.00, 10.00, 100.00, and scientific notation like 1E-6.

INPUT DATA SET FOR SCENARIO 3W-2B

```

**** TSO FOREGROUND HARD COPY ****
DSNAME=U11834C.X10RIA.CNTL

//C11834C JOB (7,TSO-TR-KONI),KONIKOVRUM,
// TIME=(0,40),CLASS=A,
// MSGCLASS=X,NOTIFY=*,
/*PASSWORD 7777
/*JOBPARM ROOM=C
/*
//KONI EXEC PGM=KONI1028,REGION=4000K
//STEPLIB DD DISP=SMR,DSN=U11236C.KONI.LOAD
//TOGFOO1 DD DSN=U11834C.X10RIA.OUTPUT,UNIT=STORAGE,
// SPACE=(TRK,(10,10)),DISP=(NEW,CATLG),
// DCB=(RECFM=VBA,LRECL=133,BLKSIZE=7448)
//FT10FOO1 DD DSN=U11834C.X10RIA.GRAPH,UNIT=STORAGE,
// SPACE=(TRK,(50,10)),DISP=(NEW,CATLG),
// DCB=(RECFM=FB,LRECL=80,BLKSIZE=7440)
//FT07FOO1 DD SYSOUT=B
//FT05FOO1 DD *
CROSS-SECTION SCENARIO 3W-2 RECHARGE=12.3 IN/YR PUMP PER=25YEAR 10FT
  2 3 12 1289888 2 10 0 100 10 4 2 0 0 0 0
  2 .01 .3 75. 0 10 0 100 100 .5 .5 1.
  0 1 0 1. .2
  1 0 0 1 0
  8 2 -3.6E-6 0.
  9 2 -3.6E-6 0.
  10 2 -3.6E-6 0.0
  2 3 -3.6E-6 0.0
  3 2 -3.6E-6 0.0
  4 2 -3.6E-6 0.0
  5 2 -3.6E-6 0.0
  6 2 -3.6E-6 0.
  7 2 -3.6E-6 0.0
  11 2 -3.6E-6 0.
  1 1.E-5
  0 0 0 0 0 0 0 0 0 0 0 0
  0 12.812.812.812.812.812.812.812.812.8 0
  0 1.6 1.6 1.6 1.6 1.6 1.6 1.6 1.6 1.6 1.6 0
  0 1.6 1.6 1.6 1.6 1.6 1.6 1.6 1.6 1.6 1.6 0
  0 1.6 1.6 1.6 1.6 1.6 1.6 1.6 1.6 1.6 1.6 0
  0 1.6 1.6 1.6 1.6 1.6 1.6 1.6 1.6 1.6 1.6 0
  0 1.6 1.6 1.6 1.6 1.6 1.6 1.6 1.6 1.6 1.6 0
  0 1.6 1.6 1.6 1.6 1.6 1.6 1.6 1.6 1.6 1.6 0
  0 1.6 1.6 1.6 1.6 1.6 1.6 1.6 1.6 1.6 1.6 0
  0 1.6 1.6 1.6 1.6 1.6 1.6 1.6 1.6 1.6 1.6 0
  0 1.6 1.6 1.6 1.6 1.6 1.6 1.6 1.6 1.6 1.6 0
  0 0 0 0 0 0 0 0 0 0 0 0
  0 1
  0.00 0.00 0.00 0.00 0.00 0.00 0.00 0.00 0. 0.00 0.00
  0.00 0.00
  0.00 10.000 10.275 10.500 10.688 10.845 10.875 11.080 11.161 11.218
  11.250 000.00
  0.00 10.214 10.368 10.541 10.701 10.842 10.962 11.061 11.141 11.203
  11.250 000.00
  0.00 10.438 10.517 10.627 10.744 10.856 10.958 11.046 11.125 11.191
  11.250 000.00
  0.00 10.588 10.633 10.706 10.782 10.881 10.967 11.047 11.120 11.187
  11.250 000.00
  0.00 10.691 10.720 10.772 10.837 10.908 10.981 11.053 11.121 11.186
  11.250 000.00
  0.00 10.765 10.786 10.825 10.876 10.928 10.998 11.062 11.125 11.188
  11.250 000.00
  0.00 10.818 10.834 10.865 10.907 10.957 11.013 11.071 11.130 11.190
  11.250 000.00
  
```

0.00	10.854	10.868	10.894	10.930	10.975	11.025	11.078	11.135	11.192
11.250	000.00								
0.00	10.876	10.890	10.913	10.946	10.987	11.033	11.084	11.138	11.194
11.250	000.00								
0.00	10.888	10.900	10.922	10.953	10.992	11.038	11.087	11.140	11.185
11.250	000.00								
0.00	000.	000.00	0.00	0.00	0.00	0.00	0.00	0.00	0.00
0.00	0.00								
0	0								
1	1								
000000000000									
020000000030									
000000000030									
000000000030									
000000000030									
000000000030									
000000000030									
000000000030									
000000000030									
000000000030									
000000000030									
000000000030									
000000000030									
000000000030									
000000000030									
2	1								
3	1.0	0.							
0	0.0	0.0							
1									
23	23	10	100	10	0	0	0	0	0
3 2	-3.6E-6	0.							
3 2	-3.6E-6	0.							
4 2	-3.6E-6	0.							
5 2	-3.6E-6	0.							
6 2	-3.6E-6	1.							
7 2	-3.6E-6	1.							
8 2	-3.6E-6	1.							
8 2	-3.6E-6	1.							
10 2	-3.6E-6	0.							
11 2	-3.6E-6	0.							
1									
23	8	10	100	10	0	0	0	0	0
2 2	-3.6E-6	0.							
3 2	-3.6E-6	0.							
4 2	-3.6E-6	0.							
5 2	-3.6E-6	0.							
6 2	-3.6E-6	1.							
7 2	-3.6E-6	1.							
8 2	-3.6E-6	1.							
8 2	-3.6E-6	1.							
10 2	-3.6E-6	0.							
11 2	-3.6E-6	0.							

APPENDIX E
THE INFLUENCES OF SURFACE RECHARGE

LEACHATE FATE AND TRANSPORT FROM WASTE FACILITY 3W-4A

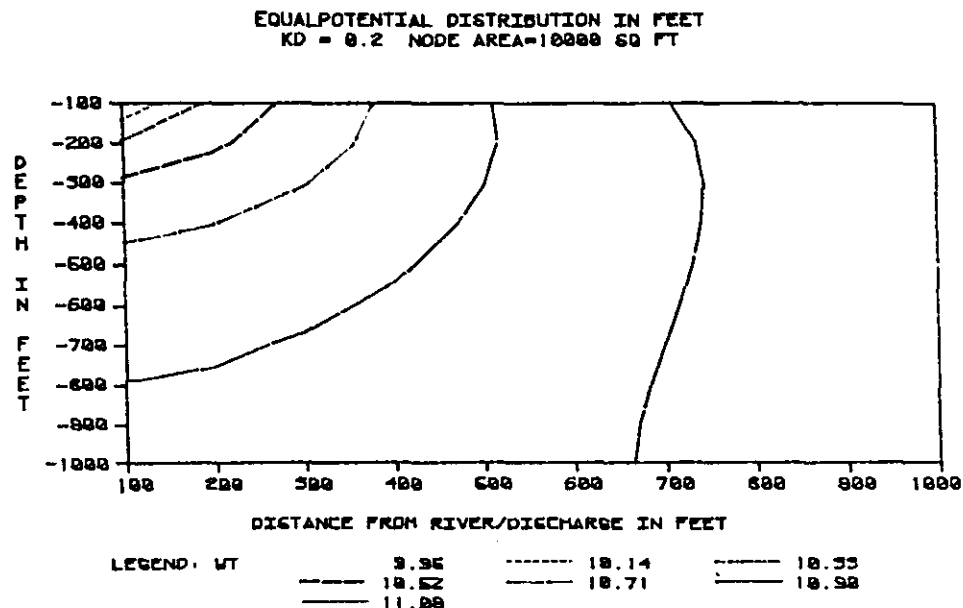


Figure 95. Equalpotential Lines of Case 3W-1A (with Surface Recharge)

LEACHATE FATE AND TRANSPORT FROM WASTE FACILITY 3W-4A

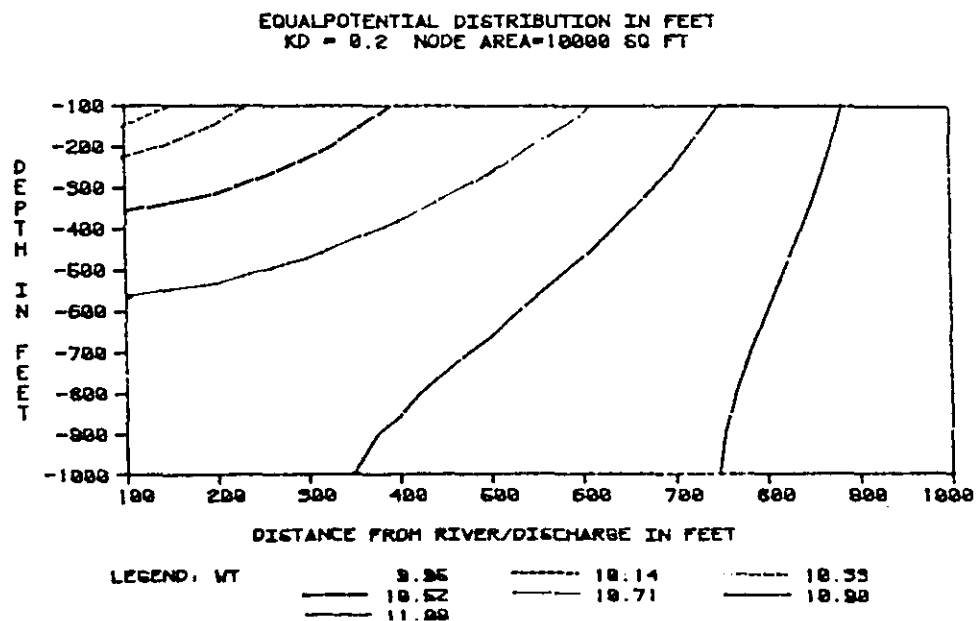


Figure 96. Equalpotential Lines of Case 3W-1A (without Surface Recharge)

TABLE XXI

GROUND-WATER FLOW VELOCITY DISTRIBUTION OF CASE 3W-1A

Time	Depth	Dist. Veloc.	DISTANCE FROM THE DISCHARGE POINT (RIVER)									
			100	200	300	400	500	600	700	800	900	1000
50	100		-3.92E-7	-1.30E-7	-3.97E-8	-3.65E-9	1.26E-8	2.05E-8	2.39E-8	2.37E-8	1.83E-8	5.71E-16
		200	-6.13E-7	-2.60E-7	-1.06E-7	-3.21E-8	5.36E-9	2.49E-8	3.41E-8	3.52E-8	2.66E-8	6.52E-16
150	100		-3.94E-7	-1.31E-7	-4.03E-8	-4.12E-9	1.22E-8	2.01E-8	2.35E-8	2.34E-8	1.81E-8	5.65E-16
		200	-6.16E-7	-2.62E-7	-1.07E-7	-3.35E-8	4.07E-9	2.38E-8	3.31E-8	3.44E-8	2.61E-8	6.41E-16
250	100		-3.95E-7	-1.32E-7	-4.06E-8	-4.38E-9	1.20E-8	1.99E-8	2.34E-8	2.33E-8	1.80E-8	5.66E-16
		200	-6.18E-7	-2.64E-7	-1.08E-7	-3.42E-8	3.54E-9	2.34E-9	3.28E-8	3.42E-8	2.59E-8	6.41E-16
350	100		-3.96E-7	-1.32E-7	-4.07E-8	-4.43E-9	1.20E-8	1.99E-8	2.34E-8	2.33E-8	1.80E-8	5.66E-16
		200	-6.19E-7	-2.64E-7	-1.08E-7	-3.43E-8	3.46E-9	3.33E-8	3.27E-8	3.42E-8	2.59E-8	6.41E-16

- : Flow to the left.

+ : Flow to the right.

APPENDIX F
THE INPUT DATA SETS OF THE BABYLON SITE

1	1	7	100	6-999	1	0	0	0	9	0	0
3 3	-1.E-4		100.								
3 4	-1.E-4		100.								
3 5	-1.E-4		320.								
3 6	-1.E-4		390.								
3 7	-1.E-4		430.								
3 8	-1.E-4		520.								
1											
1	1	7	100	6-999	1	0	0	0	6	0	0
3 3	-1.E-4		80.								
3 4	-1.E-4		80.								
3 5	-1.E-4		280.								
3 6	-1.E-4		400.								
3 7	-1.E-4		410.								
3 8	-1.E-4		490.								
1											
4	1	7	100	35-999	1	0	0	0	40	0	0
2 3	-1.E-4		0.								
2 4	-1.E-4		0.								
2 5	-1.E-4		0.								
2 6	-1.E-4		0.								
2 7	-1.E-4		0.								
2 8	-1.E-4		0.								
2 9	-1.E-4		0.								
3 3	0.E-0		0.								
3 4	0.E-0		0.								
3 5	0.E-0		0.								
3 6	0.E-0		0.								
3 7	0.E-0		0.								
3 8	0.E-0		0.								
3 9	0.E-0		0.								
14 3	1.E-4		0.								
14 4	1.E-4		0.								
14 5	1.E-4		0.								
14 6	1.E-4		0.								
14 7	1.E-4		0.								
14 8	1.E-4		0.								
14 9	1.E-4		0.								
16 3	-1.E-4		0.								
16 4	-1.E-4		0.								
16 5	-1.E-4		0.								
16 6	-1.E-4		0.								
16 7	-1.E-4		0.								
16 8	-1.E-4		0.								
16 9	-1.E-4		0.								
25 3	1.E-4		0.								
25 4	1.E-4		0.								
25 5	1.E-4		0.								
25 6	1.E-4		0.								
25 7	1.E-4		0.								
25 8	1.E-4		0.								
25 9	1.E-4		0.								

APPENDIX G

COMPARISON OF THE KONIKOW MODEL AND
THE PHAN MODEL: FIGURES

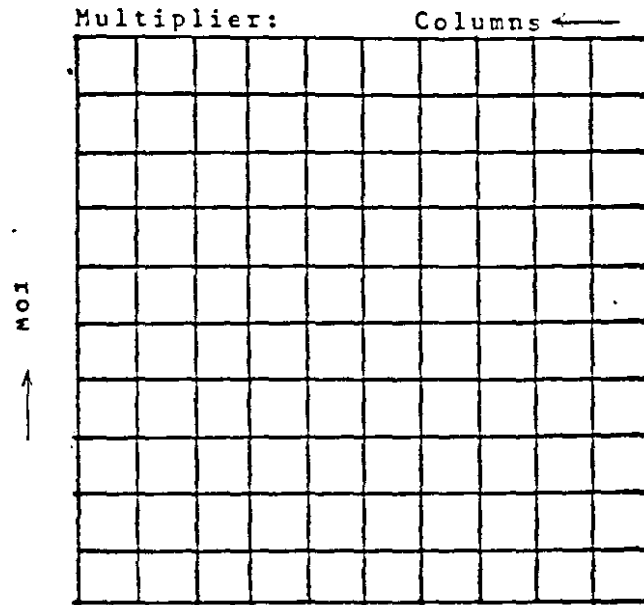


Figure 97, 10 by 10 Grid Map for the Konikow Model

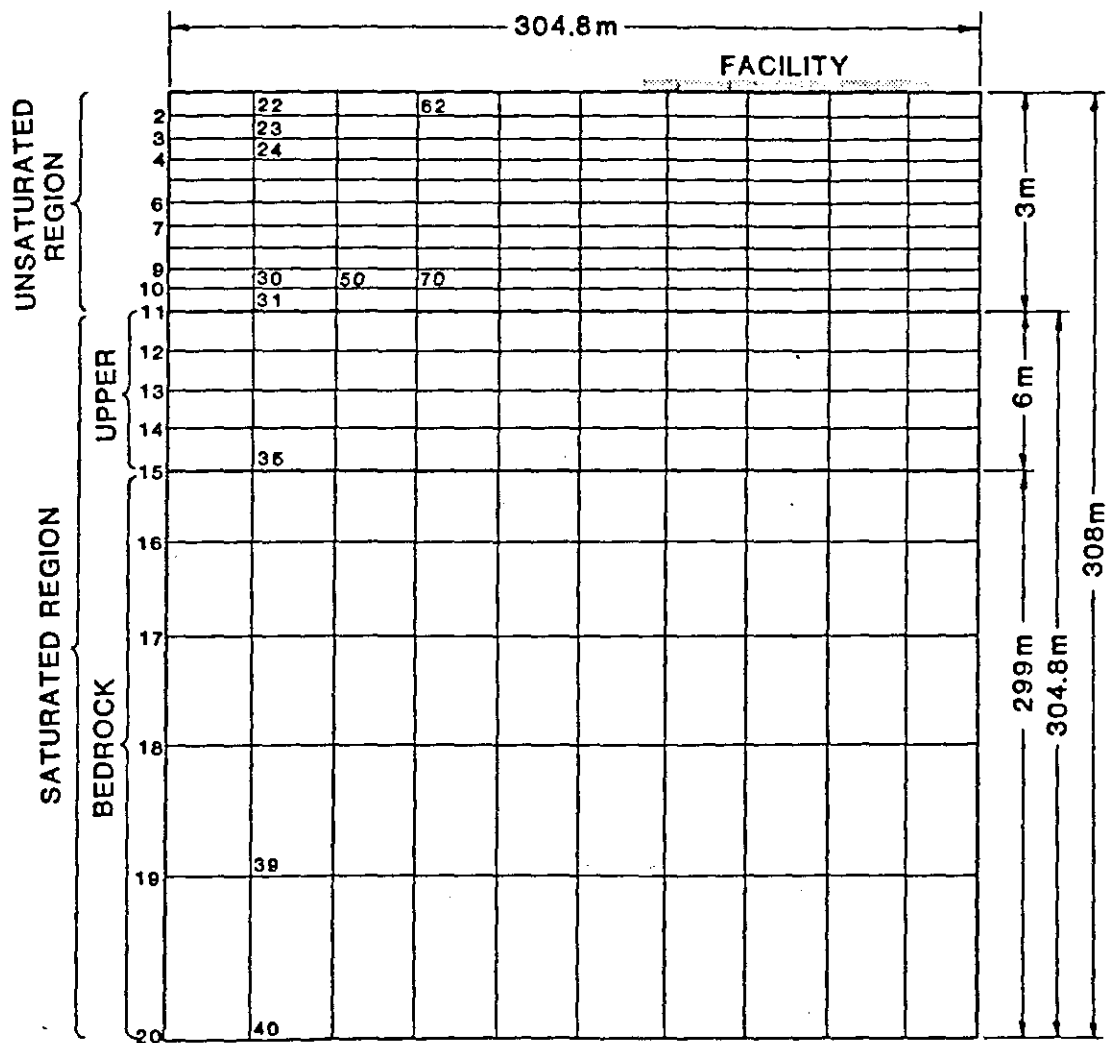


Figure 98. Grid Configuration for the Phan Model

TABLE XXII

CROSS-SECTIONAL COMPARISON OF KONIKOW MODEL (50*50) WITH PHAN MODEL.

Depth I.D.	Time Location Concn.	25 years		50 years		100 years		200 years	
		at river	at 400 ft. from river	at river	at 400 ft. from river	at river	at 400 ft. from river	at river	at 400 ft. from river
		0 20 (20 ft)	Konikow	0.1013	0.2624	0.1922	0.3406	0.2540	0.4374
	Phan	0.1725	0.3090	0.3821	0.4497	0.4143	0.4570	0.4232	0.4570
	*difference	0.0712	-0.0466	0.1899	0.1091	0.1603	0.0195	0.1167	-0.0164
20 40 (20 ft)	Konikow	0.0921	0.2611	0.1826	0.3705	0.2445	0.4424	0.2939	0.4756
	Phan	0.	0.0041	0.0074	0.0792	0.0888	0.2842	0.1440	0.3554
	*difference	-0.0921	-0.257	-0.175	-0.2913	-0.1557	-0.1562	-0.1499	-0.1202
40 80 (40 ft)	Konikow	0.0464	0.1067	0.1152	0.2374	0.1696	0.3405	0.2196	0.4429
	Phan	0.	0.	0.	0.	0.	0.0006	0.	0.0086
	*difference	-0.0464	-0.1067	-0.1152	-0.2374	-0.1696	-0.3399	-0.2196	-0.4343
80 220 (140 ft)	Konikow	0.0058	0.0074	0.0264	0.4097	0.0542	0.1137	0.0870	0.2343
	Phan	0.	0.	0.	0.	0.	0.	0.	0.
	*difference	-0.0058	-0.0074	-0.0264	-0.4097	-0.0542	-0.1137	-0.0870	-0.2343

*Base on Konikow

THE COMPARISON OF KONIKOW(400SQFT,KD=.2) WITH PHAN MODEL
 GROUP 1: AT RIVER(KONIO) 2: AT RIVER(PHANO) 3: AT 400FT FROM
 RIVER(KONIO) 4: AT 400FT FROM RIVER(PHANO)
 AT RIVER

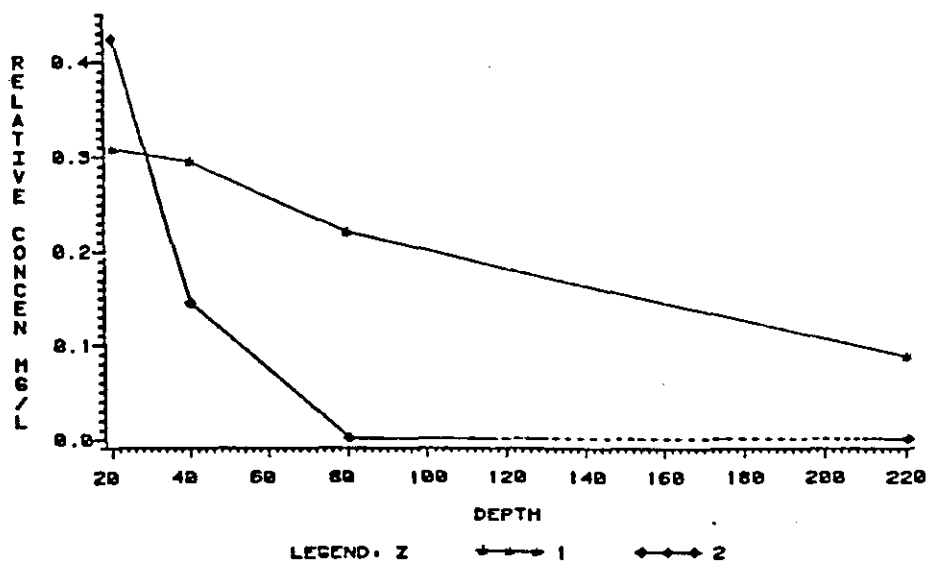


Figure 99. The Concentration Comparison the Konikow Model with Phan Model (at River)

THE COMPARISON OF KONIKOW(400SQFT,KD=.2) WITH PHAN MODEL
 GROUP 1: AT RIVER(KONIO) 2: AT RIVER(PHANO) 3: AT 400FT FROM
 RIVER(KONIO) 4: AT 400FT FROM RIVER(PHANO)
 AT 400 FT FROM FACILITY

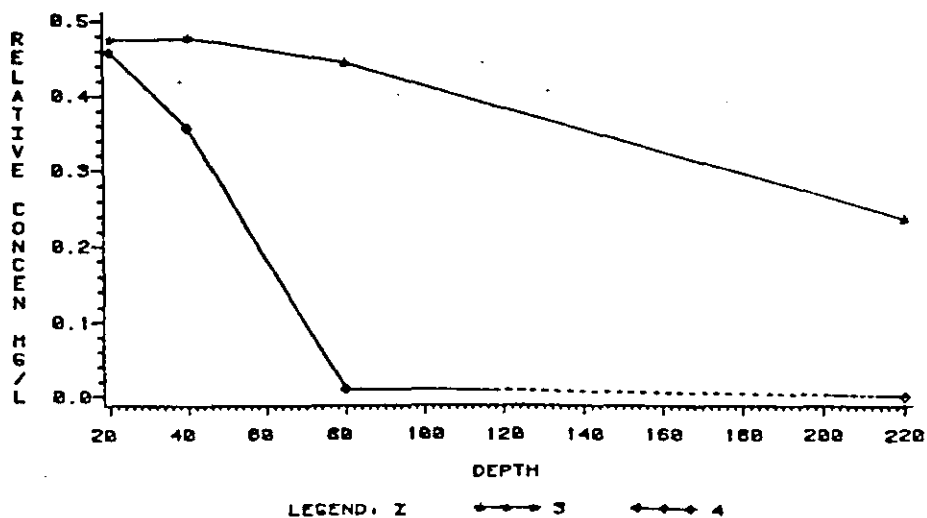


Figure 100. The Concentration Comparison of the Konikow Model with Phan Model (400 ft from River)

THE COMPARISON OF KONKOW(400SQFT,KD=.2) WITH PHAN MODEL
 GROUP 1:AT RIVER(KONI) 2:AT RIVER(PHAN) 3:AT 400FT FROM
 RIVER(KONI) 4:AT 400FT FROM RIVER(PHAN)
 AT DEPTH=20 FT

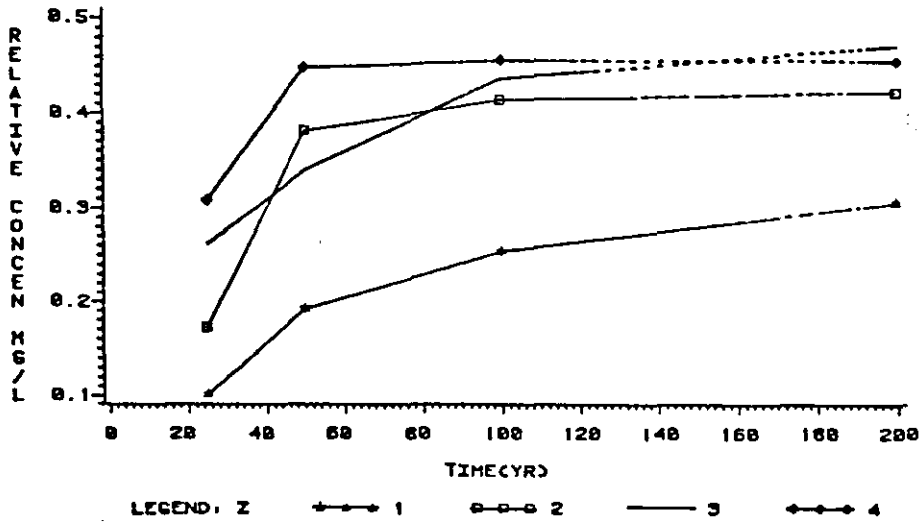


Figure 101. The Comparison of the Change of Concentration with Time (Depth=20 ft)

THE COMPARISON OF KONKOW(400SQFT,KD=.2) WITH PHAN MODEL
 GROUP 1:AT RIVER(KONI) 2:AT RIVER(PHAN) 3:AT 400FT FROM
 RIVER(KONI) 4:AT 400FT FROM RIVER(PHAN)
 AT DEPTH=220 FT

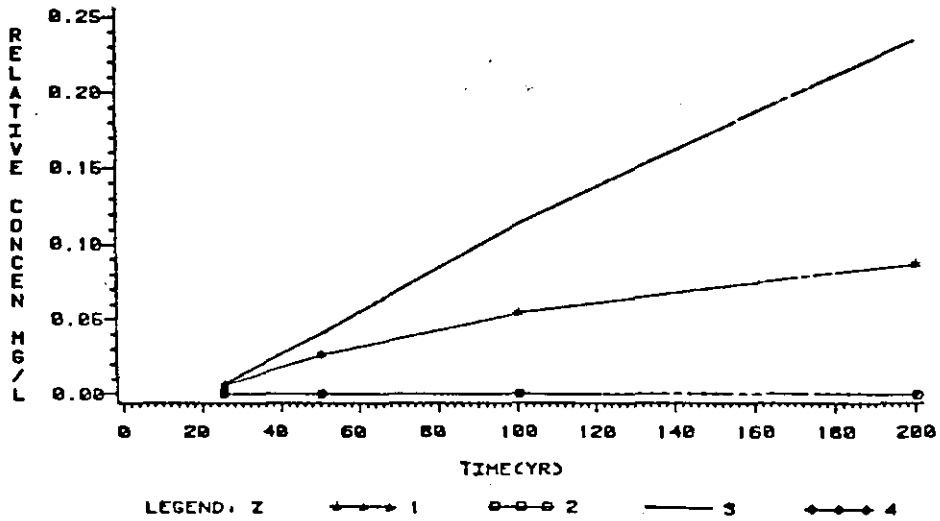


Figure 102. The Comparison of the Change of Concentration with Time (Depth=220 ft)

APPENDIX H
GRAPHICS PROGRAMS

SAS PROGRAM FOR PATTERN PLOTTING

```

**** TSD FOREGROUND HARDCOPY ****
DSNAME=U11834C.SASHADE1.CNTL

GOPTIONS DEVICE=IBM3279;
DATA INIT;
  SET LIB.ALL;
  IF INT = 0 THEN OUTPUT;
  RUN;
DATA PER1 PER2 PER3 PER4;
  SET LIB.ALL;
  IF INT = 1 THEN OUTPUT PER1;
  ELSE IF INT=2 THEN OUTPUT PER2;
  ELSE IF INT=3 THEN OUTPUT PER3;
  ELSE IF INT=4 THEN OUTPUT PER4;
  ELSE IF INT < -1 | INT > 4 THEN ERROR
    'INVALID PUMPING PERIOD: ' INT 4. ;
  RUN;
DATA ALL;
  SET PER1 PER2 PER3 PER4;
  KEEP N INT TIME DEPTH DIST CONC I J;
  IF N=1 & INT=1 THEN TIME=50;
  ELSE IF N=2 & INT=1 THEN TIME=100;
  ELSE IF N=1 & INT=2 THEN TIME=150;
  ELSE IF N=2 & INT=2 THEN TIME=200;
  ELSE IF N=1 & INT=3 THEN TIME=250;
  ELSE IF N=2 & INT=3 THEN TIME=300;
  ELSE IF N=1 & INT=4 THEN TIME=350;
  ELSE IF N=2 & INT=4 THEN TIME=400;
  ELSE TIME=.;
  IF TIME= . THEN DO;
    IF I<NX THEN DIST=(I-1)*XDEL;
    ELSE DIST=.;
    IF J<NY THEN DEPTH=(J-1)*YDEL;
    ELSE DEPTH=.;
    IF DEPTH <= 0 THEN DEPTH = .;
    IF DIST <= 0 THEN DIST = .;
  END;
  ELSE DO;
    DIST=.;
    DEPTH=.;
  END;
  LABEL CONC=RELATIVE CONCENTRATION IN MG/L
    DEPTH=DEPTH IN FEET
    DIST=DISTANCE FROM RIVER/DISCHARGE IN FEET
    TIME=TIME (YR);
  TITLE LEACHATE FATE AND TRANSPORT FROM WASTE FACILITY 3W-3B ;
  TITLE2 ;
  /* */
DATA RIVER;
  SET ALL;
  IF DEPTH > 0 & I = 2 THEN OUTPUT;
  /* */
DATA FACILITY;
  SET ALL;
  IF DEPTH > 0 & DIST = 600 THEN OUTPUT;
  /* */
DATA R50 R100 R150 R200 R250 R300 R350 R400;
  SET RIVER;
  IF TIME=50 THEN OUTPUT R50 ;
  ELSE IF TIME=100 THEN OUTPUT R100;
  ELSE IF TIME=150 THEN OUTPUT R150;
  ELSE IF TIME=200 THEN OUTPUT R200;
  ELSE IF TIME=250 THEN OUTPUT R250;
  ELSE IF TIME=300 THEN OUTPUT R300;
  ELSE IF TIME=350 THEN OUTPUT R350;

```

```

00000100
00000200
00000300
00000400
00000500
00000600
00000700
00000800
00000900
00001000
00001010
00001100
00001200
00001300
00001400
00001500
00001600
00001700
00001800
00001900
00001910
00002000
00002010
00002020
00002030
00002100
00002200
00002300
00002400
00002500
00002600
00002700
00002800
00002900
00003000
00003100
00003200
00003300
00003400
00003500
00003600
00003700
00003800
00003900
00004200
00004300
00004400
00004500
00004600
00004700
00004800
00004900
00005000
00005100
00005200
00005300
00005400
00005500
00005600
00005610
00005620
00005630

```

```

ELSE IF TIME=400 THEN OUTPUT R400;
/* */
DATA F50 F100 F150 F200 F250 F300 F350 F400;
SET FACILITY;
IF TIME=50 THEN OUTPUT F50 ;
ELSE IF TIME=100 THEN OUTPUT F100;
ELSE IF TIME=150 THEN OUTPUT F150;
ELSE IF TIME=200 THEN OUTPUT F200;
ELSE IF TIME=250 THEN OUTPUT F250;
ELSE IF TIME=300 THEN OUTPUT F300;
ELSE IF TIME=350 THEN OUTPUT F350;
ELSE IF TIME=400 THEN OUTPUT F400;
/* */
DATA BIGLTL;
SET ALL;
RETAIN BIG LTL DIFF 0;
BIG = MAX(BIG,CONC);
LTL = MIN(LTL,CONC);
IF DEPTH=1000 & DIST=1000 & TIME=400 THEN DO;
DIFF =(BIG - LTL)/5;
KEEP BIG LTL DIFF TIME;
DD TIME = 50 TO 400 BY 50;
OUTPUT;
END;
/* */
PROC SORT DATA=ALL;
BY TIME;
DATA PLUMES;
MERGE BIGLTL ALL;
BY TIME;
/* */
DATA PLUM50 PLUM100 PLUM150 PLUM200 PLUM250 PLUM300 PLUM350 PLUM400;
SET PLUMES;
IF CONC <= .001 THEN CONC = .001;
ELSE IF CONC <= (LTL+(DIFF*1)) THEN CONC = LTL+(DIFF*1);
ELSE IF CONC <= (LTL+(DIFF*2)) THEN CONC = LTL+(DIFF*2);
ELSE IF CONC <= (LTL+(DIFF*3)) THEN CONC = LTL+(DIFF*3);
ELSE IF CONC <= (LTL+(DIFF*4)) THEN CONC = LTL+(DIFF*4);
ELSE CONC = BIG;
IF TIME= 50 THEN OUTPUT PLUM50;
ELSE IF TIME=100 THEN OUTPUT PLUM100;
ELSE IF TIME=150 THEN OUTPUT PLUM150;
ELSE IF TIME=200 THEN OUTPUT PLUM200;
ELSE IF TIME=250 THEN OUTPUT PLUM250;
ELSE IF TIME=300 THEN OUTPUT PLUM300;
ELSE IF TIME=350 THEN OUTPUT PLUM350;
ELSE IF TIME=400 THEN OUTPUT PLUM400;
/* */
PROC GPLDT DATA=RIVER;
PLDT DEPTH*CONC=TIME/VREVERSE;
SYMBOL1 C=BLUE I=JOIN;
SYMBOL2 C=RED I=JOIN;
SYMBOL3 C=GREEN I=JOIN;
SYMBOL4 C=PURPLE I=JOIN;
TITLE3 DISTRIBUTION AT RIVER/DISCHARGE POINT;
TITLE4 KD = 0.2 NODE AREA=10000 SQUARE FEET;
/* */
PROC GPLDT DATA=FACILITY;
PLDT DEPTH*CONC=TIME/VREVERSE;
SYMBOL1 C=BLUE I=JOIN;
SYMBOL2 C=RED I=JOIN;
SYMBOL3 C=GREEN I=JOIN;
SYMBOL4 C=PURPLE I=JOIN;
TITLE3 DISTRIBUTION AT 300 FEET FROM THE FACILITY;
TITLE4 KD = 0.2 NODE AREA=10000 SQUARE FEET;

```

```

00005640
00005700
00005800
00005900
00006000
00006100
00006200
00006300
00006310
00006320
00006330
00006340
00006400
00006500
00006600
00006700
00006800
00006900
00007000
00007100
00007200
00007300
00007400
00007500
00007600
00007700
00007800
00007900
00008000
00008100
00008200
00008300
00008400
00008500
00008600
00008700
00008800
00008900
00009000
00009100
00009200
00009300
00009400
00009500
00009510
00009520
00009530
00009540
00009600
00009700
00009800
00009900
00010000
00010100
00010200
00010300
00010310
00010400
00010500
00010600
00010700
00010800
00010900
00011000
00011100
00011110

```

```

*/
PROC GPLOT DATA=PLUM100;                                00011200
PLOT DEPTH*DIST=CONC/VREVERSE;                          00012300
SYMBOL1 V=PAW      C=BLUE I=NONE;                       00012301
SYMBOL2 V=X        C=GREEN I=NONE;                     00012302
SYMBOL3 V=PLUS     C=ORANGE I=NONE;                    00012303
SYMBOL4 V=DIAMOND  C=BROWN I=NONE;                    00012304
SYMBOL5 V=STAR     C=RED I=NONE;                      00012305
SYMBOL6 V=%        C=PURPLE I=NONE;                   00012306
TITLE3 DISTRIBUTION OVER ENTIRE AREA AFTER 100 YEARS;  00012307
TITLE4 KD = 0.2   NODE AREA=10000 SQUARE FEET;        00013100
/* */                                                    00013110
/* */                                                    00013200
PROC GPLOT DATA=PLUM200;                                00014210
PLOT DEPTH*DIST=CONC/VREVERSE;                          00014220
SYMBOL1 V=PAW      C=BLUE I=NONE;                       00014221
SYMBOL2 V=X        C=GREEN I=NONE;                     00014222
SYMBOL3 V=PLUS     C=ORANGE I=NONE;                    00014223
SYMBOL4 V=DIAMOND  C=BROWN I=NONE;                    00014224
SYMBOL5 V=STAR     C=RED I=NONE;                      00014225
SYMBOL6 V=%        C=PURPLE I=NONE;                   00014226
TITLE3 DISTRIBUTION OVER ENTIRE AREA AFTER 200 YEARS;  00014290
TITLE4 KD = 0.2   NODE AREA=10000 SQUARE FEET;        00014291
/* */                                                    00014292
/* */                                                    00014310
PROC GPLOT DATA=PLUM300;                                00014400
PLOT DEPTH*DIST=CONC/VREVERSE;                          00014401
SYMBOL1 V=PAW      C=BLUE I=NONE;                       00014402
SYMBOL2 V=X        C=GREEN I=NONE;                     00014403
SYMBOL3 V=PLUS     C=ORANGE I=NONE;                    00014404
SYMBOL4 V=DIAMOND  C=BROWN I=NONE;                    00014405
SYMBOL5 V=STAR     C=RED I=NONE;                      00014406
SYMBOL6 V=%        C=PURPLE I=NONE;                   00015100
TITLE3 DISTRIBUTION OVER ENTIRE AREA AFTER 300 YEARS;  00015110
TITLE4 KD = 0.2   NODE AREA=10000 SQUARE FEET;        00016100
/* */                                                    00016200
/* */                                                    00016201
PROC GPLOT DATA=PLUM400;                                00016202
PLOT DEPTH*DIST=CONC/VREVERSE;                          00016203
SYMBOL1 V=PAW      C=BLUE I=NONE;                       00016204
SYMBOL2 V=X        C=GREEN I=NONE;                     00016205
SYMBOL3 V=PLUS     C=ORANGE I=NONE;                    00016206
SYMBOL4 V=DIAMOND  C=BROWN I=NONE;                    00016207
SYMBOL5 V=STAR     C=RED I=NONE;                      00017000
SYMBOL6 V=%        C=PURPLE I=NONE;                   00017010
TITLE3 DISTRIBUTION OVER ENTIRE AREA AFTER 400 YEARS;  00017100
TITLE4 KD = 0.2   NODE AREA=10000 SQUARE FEET;
/* */

```

PROGRAM FOR CONTOURING (SAS)

```

**** TSD FOREGROUND HARDCOPY ****
DSNAME=U11834C.SASG2H.CNTL

GOPTIONS DEVICE=IBM3279:
DATA INIT;
  SET LIB.ALL;
  IF INT = 0 THEN OUTPUT;
  RUN;
DATA PER1 PER2 PER3 PER4;
  SET LIB.ALL;
  IF INT = 1 THEN OUTPUT PER1;
  ELSE IF INT=2 THEN OUTPUT PER2;
  ELSE IF INT=3 THEN OUTPUT PER3;
  ELSE IF INT=4 THEN OUTPUT PER4;
  ELSE IF INT < -1 | INT > 4 THEN ERROR
  'INVALID PUMPING PERIOD: ' INT 4.
  RUN;
DATA ALL;
  SET PER1 PER2 PER3 PER4;
  IF N= 1 & INT=1 THEN TIME=50;
  ELSE IF N=2 & INT=1 THEN TIME=100;
  ELSE IF N=1 & INT=2 THEN TIME=150;
  ELSE IF N=2 & INT=2 THEN TIME=200;
  ELSE IF N=1 & INT=3 THEN TIME=250;
  ELSE IF N=2 & INT=3 THEN TIME=300;
  ELSE IF N=1 & INT=4 THEN TIME=350;
  ELSE IF N=2 & INT=4 THEN TIME=400;
  ELSE TIME=.;
  IF TIME=.= THEN DO;
    IF I<NX THEN DIST=(I-1)*XDDEL;
    ELSE DIST=.;
    IF J<NY THEN DEPTH=(J-1)*YDEL;
    ELSE DEPTH=.;
    IF DEPTH <= 0 THEN DEPTH = .;
    IF DIST <= 0 THEN DIST = .;
  END;
  ELSE DO;
    DIST=.;
    DEPTH=.;
  END;
  LABEL CONC=RELATIVE CONCENTRATION IN MG/L
  DEPTH=DEPTH IN FEET
  DIST=DISTANCE FROM RIVER/DISCHARGE IN FEET
  TIME=TIME (YR)
  WT= EQUIPOTENTIAL VALUES IN FEET;
  TITLE LEACHATE FATE AND TRANSPORT FROM WASTE FACILITY 3W-4A;
  TITLE2 ;
  /* */
DATA CONT50 CONT100 CONT150 CONT200 CONT250 CONT300 CONT350 CONT400;
  SET ALL;
  IF DEPTH =.= THEN DEPTH=-DEPTH;
  IF TIME= 50 THEN OUTPUT CONT50 ;
  ELSE IF TIME=100 THEN OUTPUT CONT100;
  ELSE IF TIME=150 THEN OUTPUT CONT150 ;
  ELSE IF TIME=250 THEN OUTPUT CONT250;
  ELSE IF TIME=200 THEN OUTPUT CONT200;
  ELSE IF TIME=300 THEN OUTPUT CONT300;
  ELSE IF TIME=350 THEN OUTPUT CONT350 ;
  ELSE IF TIME=400 THEN OUTPUT CONT400;
  /* */
PROC GCONTOUR DATA=CONT300 ;
  PLOT DEPTH=DIST=WT/CLEVELS='BLUE' 'GREEN' 'BROWN' 'RED' 'PURPLE'
  LLEVELS=1 LEVELS=9.95 TO 11.25 BY .19;
  TITLE4 EQUALPOTENTIAL DISTRIBUTION IN FEET;
  TITLES KD = 0.2 NDDE AREA=10000 SQ FT;

```

```

00000100
00000110
00000115
00000120
00000125
00000130
00000135
00000140
00000145
00000150
00000151
00000155
00000160
00000165
00000200
00000300
00000400
00000500
00000600
00000610
00000700
00000701
00000710
00000720
00000800
00000900
00001000
00001100
00001200
00001300
00001400
00001500
00001600
00001700
00001800
00001800
00002000
00002100
00002200
00002300
00002400
00002500
00002600
00002700
00003000
00003100
00003200
00003300
00003400
00003500
00003600
00003610
00003700
00003710
00003720
00003730
00003800
00003900
00004000
00004100
00004210
00004220

```